THESIS

HYDRAULIC MODELING ANALYSIS OF THE MIDDLE RIO GRANDE RIVER FROM COCHITI DAM TO GALISTEO CREEK, NEW MEXICO

Submitted by

Susan J. Novak

Department of Civil Engineering

In partial fulfillment of the requirements

For the degree of Master of Science

Colorado State University

Fort Collins, Colorado

Spring 2006

COLORADO STATE UNIVERSITY

October 24, 2005

WE HEREBY RECOMMEND THAT THE THESIS PREPARED UNDER OUR SUPERVISION BY **SUSAN JOY NOVAK** ENTITLED **HYDRAULIC MODELING ANALYSIS OF THE MIDDLE RIO GRANDE RIVER FROM COCHITI DAM TO GALISTEO CREEK, NEW MEXICO** BE ACCEPTED AS FULFILLING IN PART REQUIREMENTS FOR THE DEGREE OF MASTER OF SCIENCE.

Committee on Graduate Work

_____

_____

_____
Adviser

_____
Department Head

ABSTRACT OF THESIS

HYDRAULIC MODELING ANALYSIS OF THE MIDDLE RIO GRANDE FROM COCHITI DAM TO GALISTEO CREEK, NEW MEXICO

Sedimentation problems with the Middle Rio Grande have made it a subject of study for several decades for many government agencies involved in its management and maintenance. Since severe bed aggradation in the river began in the late 1800's, causing severe flooding and destroying farmland, several programs have been developed to restore the river while maintaining water quantity and quality for use downstream. Channelization works, levees, and dams were built in the early 1900's to reduce flooding, to control sediment concentrations in the river and to promote degradation of the bed. Cochiti Dam, which began operation in 1973, was constructed primarily for flood control and sediment detention. The implementation of these channel structures also had negative effects, including the deterioration of the critical habitats of some endangered species.

The reach under analysis stretches 8.2 miles from Cochiti Dam to Galisteo Creek. This study quantifies spatial and temporal trends in channel geometry, discharge, and sediment in the reach, and estimates future potential conditions of the Cochiti Dam reach. This will help various management agencies identify areas of the Middle Rio Grande that are more conducive to restoration efforts for these endangered species.

This study focuses on post-dam trends in the Cochiti Dam reach. The existing Middle Rio Grande database was updated and completed for facilitation of this analysis. The highly controlled dam reduced peak annual flow rates to less than 10,000 cfs. Decreasing trends in width, width/depth ratio, and cross-sectional area were noted. Thalweg degradation averaged 2 feet over the entire reach. Median bed sediment sizes increased from an average of 0.1 mm in 1962 to an average of 24 mm in 1998. This was due to the 98% decrease in suspended sediment

after the dam construction. The clearwater discharge from the dam scoured the bed and has narrowed the channel slightly. The bed degradation and bed material coarsening seen in this reach is consistent with previous studies on the Middle Rio Grande River. The planform has changed from a braided to single thread meandering channel from 1918 to 2004.

The sediment transport capacity of the river is very high at the outlet of Cochiti Dam due to the release of clear, sediment starved water. The capacity has decreased since 1972, however, because the bed has coarsened. The upstream bed has armored and the sediment-starved water may soon begin eroding the banks and increasing lateral motion.

Susan J. Novak
Department of Civil Engineering
Colorado State University
Fort Collins, CO 80523
Spring 2006

ACKNOWLEDGEMENTS

I would like to thank the USBR in Denver and Albuquerque for the opportunity to work on this project. I would like to especially thank Chris Holmquist-Johnson, Jan Oliver, and Suzanne DeVergie for sending me so much data and then taking the time to explain it to me. Thanks to Drew Baird and my advisor Dr. Pierre Julien for overseeing the project and keeping me on track.

I am grateful to Mark Velleux for helping me with my project and with schoolwork and to the rest of the group, Forrest, Seema, Chad, James, Un, and Max. Thanks to my friends Erin, Tessa, Esther, and Paul for their support and to my parents for taking care of my dog when I had working marathons. Thanks to my dog Millie for never complaining and sleeping quietly in my office when I had to work late at night.

Finally, thanks to my committee members, Dr. Bill Fairbank of the Physics Department and Dr. Jose Salas of the Civil Engineering Department.

TABLE OF CONTENTS

LIST OF FIGURES

LIST OF TABLES

Chapter 1: Introduction

The Middle Rio Grande has historically been the most documented river in the United States. The Embudo gaging station, located 27 miles upstream of Otowi, New Mexico, was installed in 1889, making it the longest-running measurement site in the U.S. In the past, the Middle Rio Grande in New Mexico has been a wide, shallow, aggrading sand bed river with extensive lateral mobility. The bed began aggrading in the mid 1800s due to drought conditions and increasing sediment input from tributaries. To prevent flooding and other problems, the U.S. Army Corps of Engineers (USACE) and the US Bureau of Reclamation (USBR) built dams and began channelizing the river in the 1920s. This changed the hydrologic and sediment regime of the river, resulting in the deterioration of the habitat of the Rio Grande silvery minnow (*Hybognathus amarus*) and the southwestern willow flycatcher (*Empidonax traillii extimus)*.

Since the implementation of diversion dams and channelization throughout the Middle Rio Grande River over the last century, the hydrologic regime has changed from a shallow, silt and sand-bed river, which the silvery minnow prefers, to a narrow, deep, sand and gravel-bed river. The minnow now occupies less than 10% of its original range and does not occupy water upstream of Cochiti Dam. The remaining population has continued to dwindle due to the lack of warm, slow-moving silt-sand substrate pools, dewatering of the river, and abundance of non-native and exotic fish species. The US Fish and Wildlife Service (USFWS) placed the minnow in the endangered species list in July 1999 due to the extreme changes to the minnow's habitat.

In addition, the habitat of the southwestern willow flycatcher has been affected. This bird generally prefers southwestern cottonwood-willows and arrowweed for foraging and nesting. These plants were native and plentiful in the riparian corridor, but have since deteriorated. For this reason, the southwestern willow flycatcher was put on the endangered species list in February 1995 by the USFWS.

The Cochiti Dam reach of the middle Rio Grande is located in north-central New Mexico and is included as the upstream boundary of the critical habitat designations of both the Rio Grande silvery minnow and the southwestern willow flycatcher. The objective of this study is to analyze historical data and estimate potential future conditions of this reach. This will help to identify those areas that are most conducive to efforts to restore the habitat of these endangered species.

To achieve this objective, the Middle Rio Grande Database was updated to include the most recent possible Environmental Protection Agency (EPA), USGS, and USBR data. Also added were the most recent studies and analyses performed by members of Colorado State University's hydraulic research group under Dr. P. Y. Julien. In addition, an analysis of spatial and temporal trends in discharge, sediment, and channel geometry data were performed. Finally, equilibrium state predictors were used to estimate potential future conditions in the channel. A quantitative approach was used and is outlined below:

- Temporal trends in discharge were analyzed using data from US Geological Survey (USGS) gage data.
- Spatial and temporal trends in channel geometry were evaluated using cross-sectional surveys
- Spatial and temporal trends in bed material were identified though the evaluation of particle size distributions.
- Planform classifications were assessed through the analysis of aerial photos and channel geometry data

- The applications of hydraulic geometry methods, empirical width-time relationships, stable channel design, and sediment transport analyses to the Cochiti Dam reach yielded potential equilibrium conditions.

This thesis has been developed in five chapters. Chapter 1 contains an introduction to the project, including objectives and motives for the study. Chapter 2 contains a literature review of relevant studies regarding the morphology of the Middle Rio Grande River. It also describes the historical background of the river, including the climate, hydrology, and geology of the Middle Rio Grande Valley. Chapter 3 contains the analysis and results of the historical Cochiti Dam reach data. In Chapter 4, the equilibrium state predictors used are described, along with the results from the analysis. Chapter 5 contains a summary of all results and conclusions. Appendices A through E contain a summary of tables of data, cross-section plots, bed material gradations, and model outputs. Appendix F is a summary of the updating of the Middle Rio Grande Database.

Chapter 2: Literature Review

2.1 Reach Description

The Rio Grande River stretches 2000 miles from its headwaters along the Continental Divide in the San Juan Mountains of southwestern Colorado, through New Mexico, and to its outlet at the Gulf of Mexico near Brownsville, Texas and Matamoros, Mexico. The middle section of the river, or the Middle Rio Grande, is the 143-mile portion of the river that stretches from White Rock Canyon, through Albuquerque, NM, to the San Marcial Constriction at Elephant Butte Reservoir (Lagasse 1994).

The Middle Rio Grande valley includes four New Mexico counties and six Indian pueblos. In addition, the land is managed and maintained by several agencies including the Middle Rio Grande Conservancy District, Bureau of Reclamation, Army Corps of Engineers, New Mexico Department of Game and Fish, U.S. Fish and Wildlife Service, New Mexico State Parks, the City of Albuquerque Parks and Recreation Division, and private landowners

The part of the river analyzed in this study, the Cochiti Dam reach, is an 8.2-mile long stretch of river that begins at the outlet of Cochiti Dam, 40 miles upstream of Albuquerque, and ends at the confluence of the Middle Rio Grande River with Galisteo Creek. This reach was analyzed for geomorphic and sedimentologic changes since the installation of Cochiti Dam. Figure 2-1 contains a map of the location of the Cochiti Dam reach.

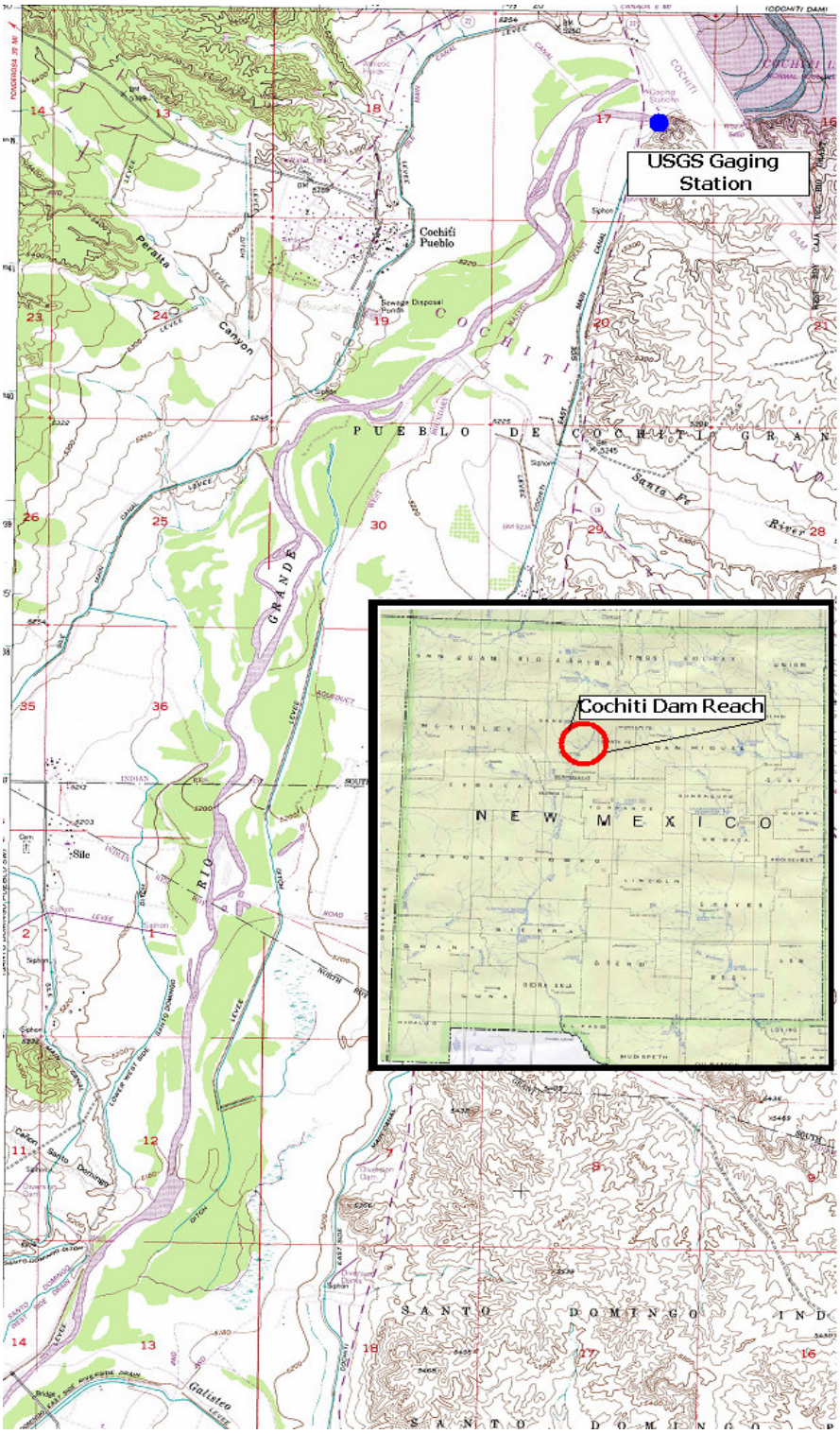

Figure 2-1 Cochiti Dam reach topographical map and location map

2.2 Middle Rio Grande History

The Middle Rio Grande valley has been cultivated for hundreds of years. The earliest Pueblo (Anasazi) Indian villages date back to the 1300's (Scurlock 1998) and consisted of over 25,000 acres of farmland with hand-dug irrigation ditches from the Rio Grande. Spanish explorers conquered the land in the early 1500's, led by Coronado (Burkholder 1929, Crawford et al. 1993). In the 1800's, white settlers began to farm the area as well. Irrigated lands reached a maximum area of 124,000 acres of land by 1880 (Lagasse 1980). The agricultural area was reduced thereafter due to the rising water table and strains on water supply.

The heavy agricultural use by farmers and ranchers in Colorado reduced the water quality received by New Mexico farmers. The overall flow was reduced and became laden with agricultural pollutants and erosion-induced sediment. In addition, arroyo cutting began in the late 1800's, increasing upland erosion (Hereford 1984). The sediment transport capacity of the river was reduced with the decreasing flow, and the bed began to aggrade. Aggradation of the bed caused seepage and an increase in water table elevation. The river became very shallow and wide with a high susceptibility to flooding (Burkholder 1929). The agricultural lands along the river experienced flooding, waterlogged land, and failed irrigation systems (Scurlock 1998). By 1925, irrigated agricultural area still in use was reduced to 40,000 acres (Leon 1998).

During the early 1900's, the US Congress commissioned a series of dams, levees, diversion structures, and channelization works during the Rio Grande Reclamation Project. A component of this project, Elephant Butte Dam, was completed in 1915. This dam is the principal storage facility for the Rio Grande-Chama Project, which delivers water for downstream use under contract between the USBR and the Elephant Butte Irrigation District in New Mexico and the El Paso County Water Improvement District #1 in Texas. It is operated to ensure that 60,000 acre-feet per year of water is delivered to the Aceuia Madre headgate in Mexico, in accordance with the U.S. 1906 Treaty with Mexico (USACE 2005).

The Middle Rio Grande Conservancy District (MRGCD) was organized in 1925 to improve drainage, irrigation, and flood control for 128,000 acres of land, including urban areas, in the Middle Rio Grande region. Flood control and sediment detention works were established in the early 1930's. The Middle Rio Grande Floodway was constructed in 1935 (Woodson 1961). It was designed with an average width of 1500 feet (between levees), and 8-foot-high levees. Design flow for the floodway was 40,000 cfs. The floodway levee heights were increased in Albuquerque to accommodate a passing design flow of 75,000 cfs (Woodson and Martin 1962).

In addition to the numerous drainage canals, main irrigation canals, and two canal headings, the MRGCD is responsible for the building, operation, and maintenance of the El Vado Dam on the Rio Chama, Angostura Dam, Isleta Dam, San Acacia Dam, and Cochiti Dam (Lagasse 1980).

In 1948, as the result of a highly damaging flood, the USACE and the USBR together with various other Federal, State, and local agencies proposed the Comprehensive Plan of Improvement for the Rio Grande in New Mexico (Pemberton 1964). Aggradation and seepage leading to floodway deterioration indicated the need for the regulation of floodflows, sediment retention, and channel stabilization (Woodson and Martin 1963). The Comprehensive Plan included plans for a system of reservoirs (Abiquiu, Jemez, Cochiti, Galisteo) on the Rio Grande and its tributaries, along with floodway rehabilitation (Woodson and Martin 1962). This reduced the floodway capacity to 20,000 cfs with a reduction to 42,000 cfs in Albuquerque (Leon 1998). The reservoirs were built by the USACE and the floodway rehabilitation was done by the USACE and the USBR (Woodson and Martin 1963).

Cochiti Dam on the Middle Rio Grande and Galisteo Dam on Galisteo Creek were both authorized in 1960 by the USACE (Woodson and Martin 1963). Cochiti Dam was built chiefly for flood and sediment control. An initial 50,000 acre-feet of San Juan-Chama Project water was released for the original filling of a pool of 1200 acres of surface area in Cochiti Reservoir

USACE 2005) and continues to maintain an average of 50,000 acre-feet behind Cochiti Dam for recreational purposes. Trap efficiency for Cochiti Reservoir is estimated at 87% by the USACE (USACE 2005). Trapping of the sediment prevented continued aggradation of the reach and began clearwater scour (Lagasse 1980). Bed material coarsening was expected as far downstream as the Rio Puerco confluence, preventing excessive degradation (Sixta 2004).

Since the closure of Cochiti Dam, there has been very little suspended sediment recorded at the USGS gage located just below the dam outlet (Figure 2-2) and Cochiti gage data is available only from 1974 to 1988. Suspended sediment in Albuquerque is much higher than that at the outlet of Cochiti Dam. This is due to bank and bed erosion and sediment influx from the various arroyos, the Jemez River, the Santa Fe River, Arroyo Tonque, and Galisteo Creek (Albert et al. 2003).

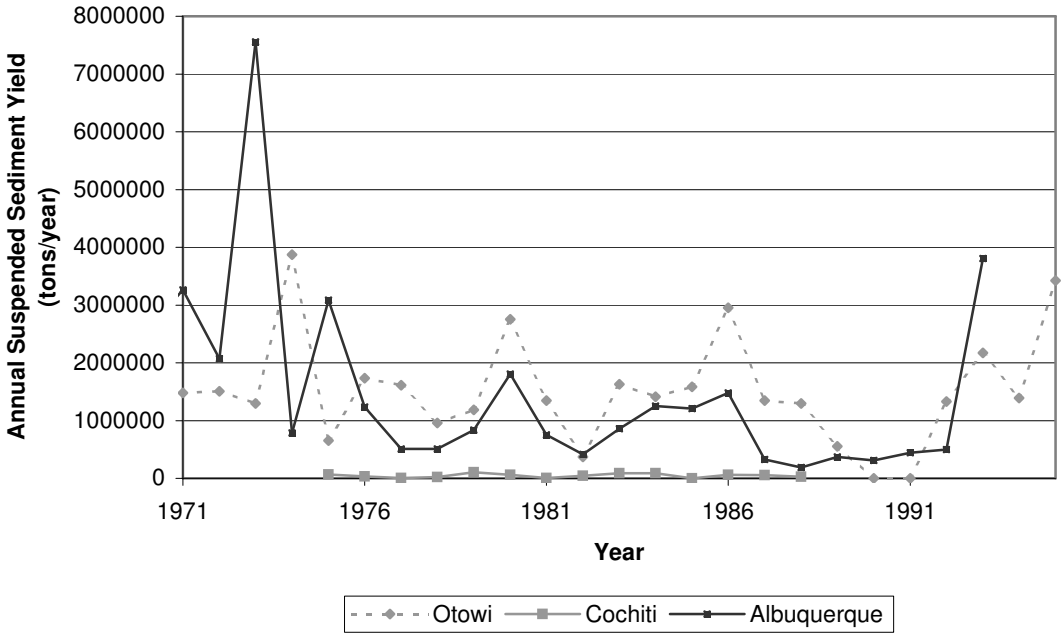

Figure 2-2 Annual suspended sediment Yield on the Middle Rio Grande at the USGS gages at Otowi, below Cochiti Dam, and at Albuquerque.

Cochiti Reservoir is located within the boundaries of the Pueblo de Cochiti Nation. The native peoples living in the Cochiti Dam reach did not welcome the plans for Cochiti Dam because of the potential damage to their cultural, agricultural, economical, and political life. As a result of the dam's construction, the Pueblo people endured structural testing that led to the flood of their agricultural land and a resulting twenty year loss of farming and way of life. In 2001, after lengthy lawsuits and victories for the Pueblo people, the USACE gave a public apology and cooperative efforts have been maintained since (Pueblo de Cochiti Web site 2005). Data on the Pueblo de Cochiti Nation, however, is very difficult to obtain and was sometimes not taken at all.

2.3 Hydrology, Geology, and Climate of the Middle Rio Grande

Cochiti Dam was under construction from 1965 to 1975 and was originally built for flood and sediment control (Lagasse 1980). The peak flows through this reach as a result of the dam have been reduced and regulated. Figure 2-3 shows a typical yearly hydrograph in the Middle Rio Grande. The Cochiti gage is located at the upstream end of the study reach, the Otowi gage is located approximately 17 miles upstream of the study reach, and the San Felipe gage is located approximately 12 miles downstream of Galisteo Creek, the lower boundary of the study reach.

Floods have plagued the Middle Rio Grande for centuries. In the late 1800's, maximum flood discharges ranged from 45,000 cfs to 125,000 cfs. In the 1920's, floods were reduced to 20 to 30,000 cfs. Since the installation of Cochiti Dam, no flows over 10,000 cfs have been recorded at the Cochiti Dam gage.

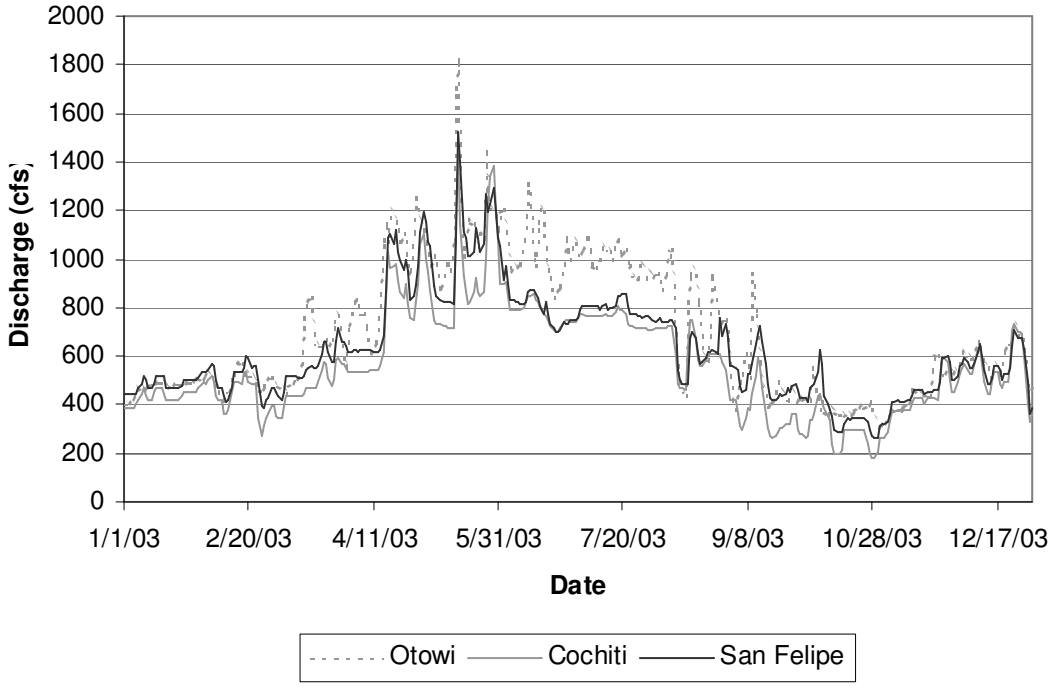

Figure 2-3 2003 Middle Rio Grande hydrograph

The geology of the Middle Rio Grande region is diverse. Several mountain ranges, including the Jemez, Sandia, and Manzano, create the topography. Underground aquifers affect the hydrology of the Middle Rio Grande region as well.

The Jemez range was created by intense volcanic activity. The volcanic ash may help replenish the nearby aquifers, affecting the hydrology of the Rio Grande and its tributaries. The Sandia and Manzano ranges were created by crust uplift and are composed of limestone and shale near the surface, and granite deeper in the earth (New Mexico Culture Web site 2005).

Sediment in the valley has entrapped a large amount of water in underground aquifers, including the Santa Fe aquifer system that is used by Albuquerque municipalities (USGS 2005). As of 2002, water for municipal and domestic supply is almost completely derived from groundwater storage.

The climate of the Middle Rio Grande region is moderate. The Cochiti Dam reach is classified as a semi-arid region. Annual precipitation averages 8.88 inches with record maximum

(1988) of 13.11 inches and record minimum (1989) of 4.99 inches. Mean annual temperature is 56.4 degrees Fahrenheit with a daily maximum (6/26/1994) of 107 and a daily minimum (1/07/1971) of -17 degrees. More than 90 percent of New Mexico's precipitation returns to the atmosphere through evapotranspiration due to the warm, dry climate and high winds (USBR 2005).

The hot dry climate makes loss rates for the Middle Rio Grande fairly high. From Otowi to Cochiti Dam, 0.33 % of water is lost to evaporation, storage, and seepage into the banks. Flow takes three days to travel from Cochiti Dam to Elephant Butte Reservoir and can have water loss of anywhere from 3.3% in the winter to 7.2% in the summer (USACE 2005).

2.4 Previous Studies of the Middle Rio Grande

The Middle Rio Grande is one of the most historically documented rivers in the US (Graf 1994). Numerous studies on the changes to the Middle Rio Grande have been done to estimate river bed and planform configurations, geometry patterns, bed material characteristics, and future conditions. Research has been done on the changes to the river as a result of agriculture, channelization, levees, dams and restoration techniques. Figure 2-4 outlines the locations of reaches and tributaries in the Middle Rio Grande.

Nordin and Beverage (1965) describe the pre-Cochiti Dam river below Cochiti Pueblo to be a wide, unconfined, braided channel with many coarse gravel and cobble islands. During low-flow, the riverbed was mostly sand, and during high flows the bed was mostly gravel. Below the mouth of the Jemez River the Rio Grande was a sand bed river. Lane and Borland (1953) had a similar assessment of the dam, noting that the river did not have the bends and crossings that are generally found in other large alluvial rivers.

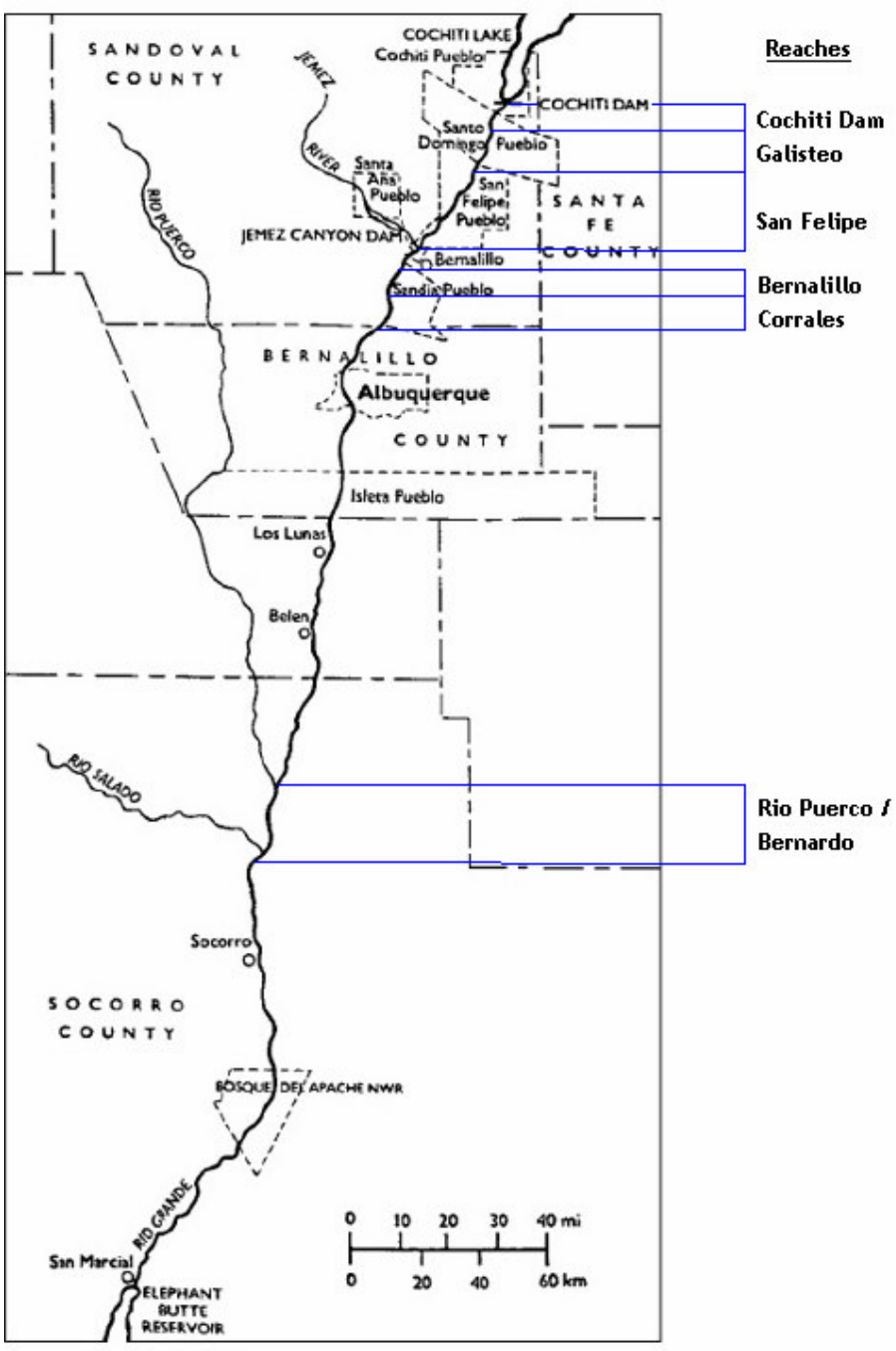

Figure 2-4 Map of Middle Rio Grande with counties, pueblos, and reaches outlined

Lane and Borland (1953) also found that the narrow sections of the river were scoured during high flows while the wider sections experienced aggradation. Since USGS gaging stations are located in narrow portions of the river where local scouring occurred, the appearance of degradation was given (Bauer 2000).

Studies were done to estimate aggradational and degradational trends to the river after the construction of the dams. Woodson and Martin (1962) estimated that the system of reservoirs (Abiquiu, Jemez, Galisteo, and Cochti) would reduce the sediment inflow into Bernalillo by 75 percent after 20 years. They also expected degradation to begin at Cochiti Dam and to progress downstream as far as the Rio Puerco. Due to bed armoring, this degradation was not expected to exceed 3 feet. The USBR also estimated that degradation would begin by 1965 and the river would experience no more than 1 foot of aggradation by 1985 (Schembera 1962).

Within two months after the Cochiti Dam closure in 1973, observers noted that the first three miles below the dam were lacking bed material sizes smaller than 1 mm. Gravel bars began appearing as far downstream as Albuquerque (Dewey et al. 1979). Bed material surveys taken in the early 1970's indicated the median grain size for much of the reach was less than 1 mm. By 1995, the median grain size had increased to over 10 mm. The coarsening of the bed had progressed downstream over 28 miles below Cochiti Dam (Dewey et al. 1979, Bauer 2000).

Lagasse (1980) performed a geomorphic analysis of the Middle Rio Grande from Cochiti Dam to the Isleta Diversion Dam for the time period from 1971 to 1975. This study concluded that the water and sediment influx from arroyos and tributaries have dominated the river's response to the dam construction (Leon 1998). After the dam closure, Lagasse calculated a zone of channel incision and bed coarsening, which migrated rapidly downstream at a rate of 5 km/year. After 1980, it slowed to an average of 0.7 km/year (Ortiz and Meyer 2005). Stable conditions were approached sooner above the confluence of the middle Rio Grande with the Jemez River than downstream due to armoring and stable tributary base levels (Leon 1998). Just upstream of the Isleta Diversion Dam, Lagasse (1980) found the bed had aggraded, indicating large amounts of sediment load transport from upstream in the reach (Bauer 2000). Lagasse's analysis was documented through a qualitatative analysis of planform, profile, cross-section and sediment data (Leon 1998). Lagasse's methodology has been used as a guide for this study.

Leon's 1998 study of the river from Cochiti Dam to Bernalillo Bridge found similar results to Lagasse's (1980) report. A degradational trend was noted with the maximum degradation occurring at the downstream end of the reach. Degradation of up to 8 feet was observed between 1971 and 1995.

Graf (1998) studied plutonium transport into the Northern Rio Grande. He documented channel changes based on 1940 to 1980 aerial photos and topographical maps. The photos indicated that the river had a shallow, wide, braided planform before 1940. After implementation of the Comprehensive Plan of Improvement, flows decreased and the channel narrowed throughout most of the Middle Rio Grande reach. The floodplain increased and the river transitioned from a braided planform to a single-thread channel (Bauer 2000). This transition may be due to dam closures or regional hydroclimatic influences since the river upstream of Cochiti Dam has also narrowed and tended towards a single thread channel since the 1940s. With the narrowing of the channel came instability and higher rates of lateral migration. The main channel of the Middle Rio Grande changed position by as much as 1 km (0.6 miles) between 1940 and 1980. These changes occurred during high flows when sediment blocked the main flow path and forced channel avulsions (Graf 1994).

The reduced peak flows have also complicated the hydraulics at the tributary confluences to the Rio Grande (Bauer 2000). The sediment transported by these tributaries frequently exceeds the rivers capacity to transport the sediment (Crawford et al. 1993). Complications from occurrence can be seen at the mouth of the Rio Puerco. The Rio Puerco is not as stable as the Rio Grande due to constant aggradation and channel cutting that has occurred over the past 3000 years, cutting and filling at least three major channels. This process is a result of varying sediment fluxes to the Rio Grande (Crawford et al. 1993). The sediment transported through the Rio Grande due to bed degradation is estimated to be 65% of the total sediment passing the Albuquerque and Bernardo gages. However, downstream at the San Acacia and San Marcial

gages, the majority of the transported sediment passing the gage is supplied by the Rio Puerco with the degradation of the bed contributing less than 8% of the sediment downstream of the Rio Puerco (Albert 2004). The Rio Puerco currently contributes twice the sediment through its channel than what is carried through the Rio Grande in Albuquerque. This sediment is deposited upstream of the San Marcial gaging station (Bauer 2000).

Sanchez and Baird (1997) studied morphologic changes to the river since 1918. A narrowing trend was observed that did not accelerate after the completion of Cochiti Dam. The sinuosity of the river increased after dam construction, but did not reach the peak value observed in 1949. The historical bankfull discharge of 11,166 cfs has never been released from Cochiti Dam. Due to flow regulation at the dam, the two-year return flow has been reduced to 5650 cfs. According to Sanchez and Baird's study, the channelization works, dam construction, and regulated flows together account for the overall channel narrowing that has occurred since the 1940's.

Mosley and Boelman (1998) studied the Santa Ana, located between the Angostura Diversion Dam and the Highway 44 Bridge in Bernalillo. Their study concluded that the reach altered its planform from braided to a meandering riffle/pool pattern, the bed material size increased to gravel, and the width to depth ratio decreased since dam construction (Sixta 2004).

Similar findings were reported by Ortiz and Meyer (2005), who studied changes to the river just downstream of Bernalillo Bridge. They characterized the pre-dam channel as having a multi-thalweg, shallow, bar-braided planform, with uniform channel width due to bank stabilization structures and associated dense vegetation. Post-dam conditions included an increase in vegetated island surface area, widespread thalweg incision, and a disconnected floodplain throughout the reach, due to the regime of reduced peak discharges.

Several other studies have been funded by the USBR on the morphology of the Middle Rio Grande. The research conducted for these reports was performed at Colorado State

University under the guidance of Dr. P. Y. Julien. The following reaches have been investigated as of 2005:

Rio Puerco (Richard et al. 2001). This is the downstream-most reach studied, spanning 10 miles from the mouth of the Rio Puerco (agg/deg 1101, river mile 126) to the San Acacia Diversion Dam (agg/deg 1206, river mile 116.2).

Corrales (Leon and Julien, 2001a), updated by Albert et al. (2003). This reach spans 10.3 miles from the Corrales Flood Channel (agg/deg 351, river mile 196) to the Montano Bridge (agg/deg 462, river mile 188)

- Bernalillo Bridge (Leon and Julien 2001b), updated by Sixta et al. (2003a). This reach spans 5.1 miles from New Mexico Highway 44 (agg/deg 298, river mile 203.8) to cross-section CO-33 (agg/deg351, river mile 198.2).
- San Felipe (Sixta et al. 2003b). This reach spans 6.2 miles from the mouth of Arroyo Tonque (agg/deg 174, river mile 217) to the Angostura Diversion Dam (agg/deg 236, river mile 209.7).
- Cochiti Dam (Novak 2005 draft). This reach spans 8.2 miles from the outlet of Cochiti Dam (agg/deg 17, river mile 232.6) to the mouth of Galisteo Creek (agg/deg 97, river mile 224.4).

The vast research done on the Middle Rio Grande at CSU under Dr. P. Y. Julien over the past several years has prompted the creation of the Middle Rio Grande Database. The database includes all data, analysis and literature pertaining to these studies. The database was updated in 2004 to include all theses and dissertations, as well as all USBR reports for completeness. Appendix G contains a summary of the updating of the Middle Rio Grande Database.

Chapter 3: Geomorphic Characterization

Understanding the historical spatial and temporal trends in the Cochiti Dam reach is a crucial step in developing habitat restoration plans for the Rio Grande silvery minnow and the southwestern willow flycatcher. The objective of this chapter was to identify and quantify changes and trends in the channel geometry, discharge, and sediment characteristics.

To achieve this objective, the following tasks will be addressed:

- Analysis of spatial and temporal trends in channel geometry through inspection of cross-section survey data.
- Channel planform classification through analysis of aerial photos, topographic maps, and digitized planforms.
- Identification of spatial and temporal trends in water and sediment discharge and concentration using USGS gaging station data.

3.1 Site Description and Background

The 8.2-mile-long Cochiti Dam Reach of the middle Rio Grande stretches from Cochiti Dam (river mile 232.6) to the confluence with Galisteo Creek (river mile 224.6). The reach meanders slightly with an average sinuosity between 1.1 and 1.2. The reach has an average valley slope of 0.0016. The median bed material in the channel reach is coarse gravel, with a sediment distribution ranging from fine sand to small cobbles.

The Santa Fe River joins the Rio Grande from the east just 2 miles downstream of Cochiti Dam, and Peralta Canyon joins the river from the west after an additional mile. Galisteo Creek joins the Rio Grande at the downstream end of the 8.2-mile long study reach. Peralta Canyon has a noticeable sediment input at confluence with the Rio Grande in the form of a large sediment bar. The locations of these tributaries are labeled in Figures 3-1, 3-2, and 3-3. Note the presence of split flow and the heavily vegetated floodplain along the entire reach.

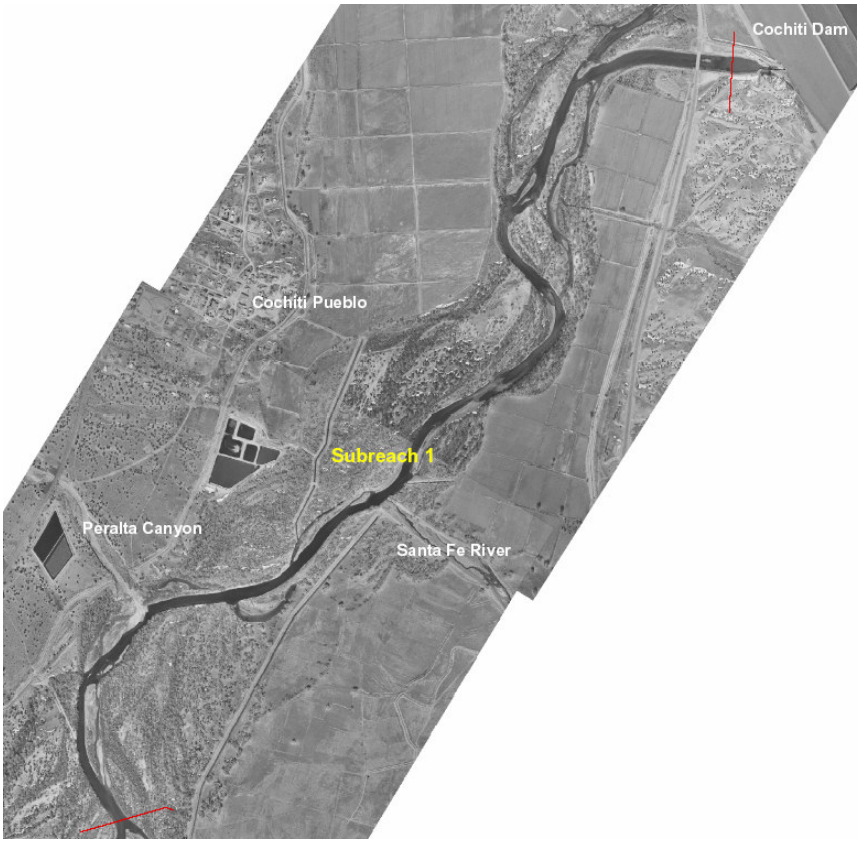

Figure 3-1 Aerial photo of subreach 1. Year: 2004

Figure 3-2 Aerial photo of subreach 2. Year: 2004

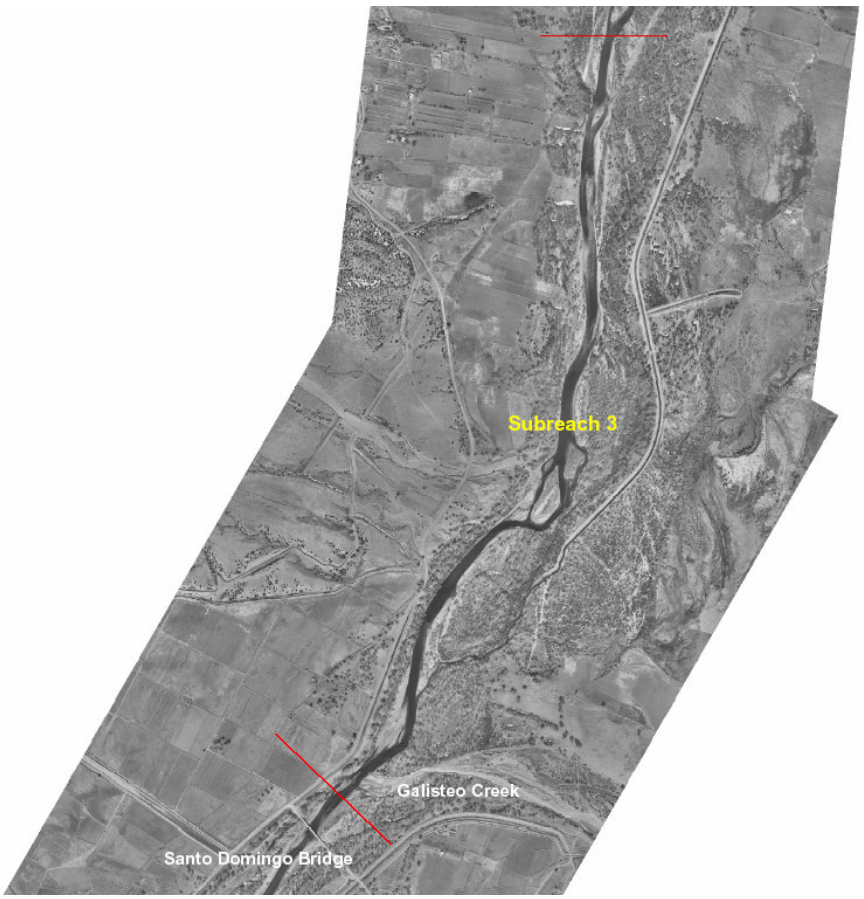

Figure 3-3 Aerial photo of subreach 3. Year: 2004

Along the Middle Rio Grande, surveys and data are taken at range-lines (Figure 3-4). In the figure, Agg/Deg lines are in blue and CO lines 2 through 8 are in red. CI-lines are in grey and all lines progress downstream. CO (Cochiti) lines, Agg/Deg (aggradation/degradation) lines, and CI (Cochiti Pueblo) lines provide survey and sediment data. In the Cochiti Dam reach, 80 agg/deg-lines are available (agg/deg 17 through agg/deg 97), seven CO-lines are available (CO-2 through CO-8), and four CI-lines are available (CI 27, CI-28, CI-28.1, CI-29.1).

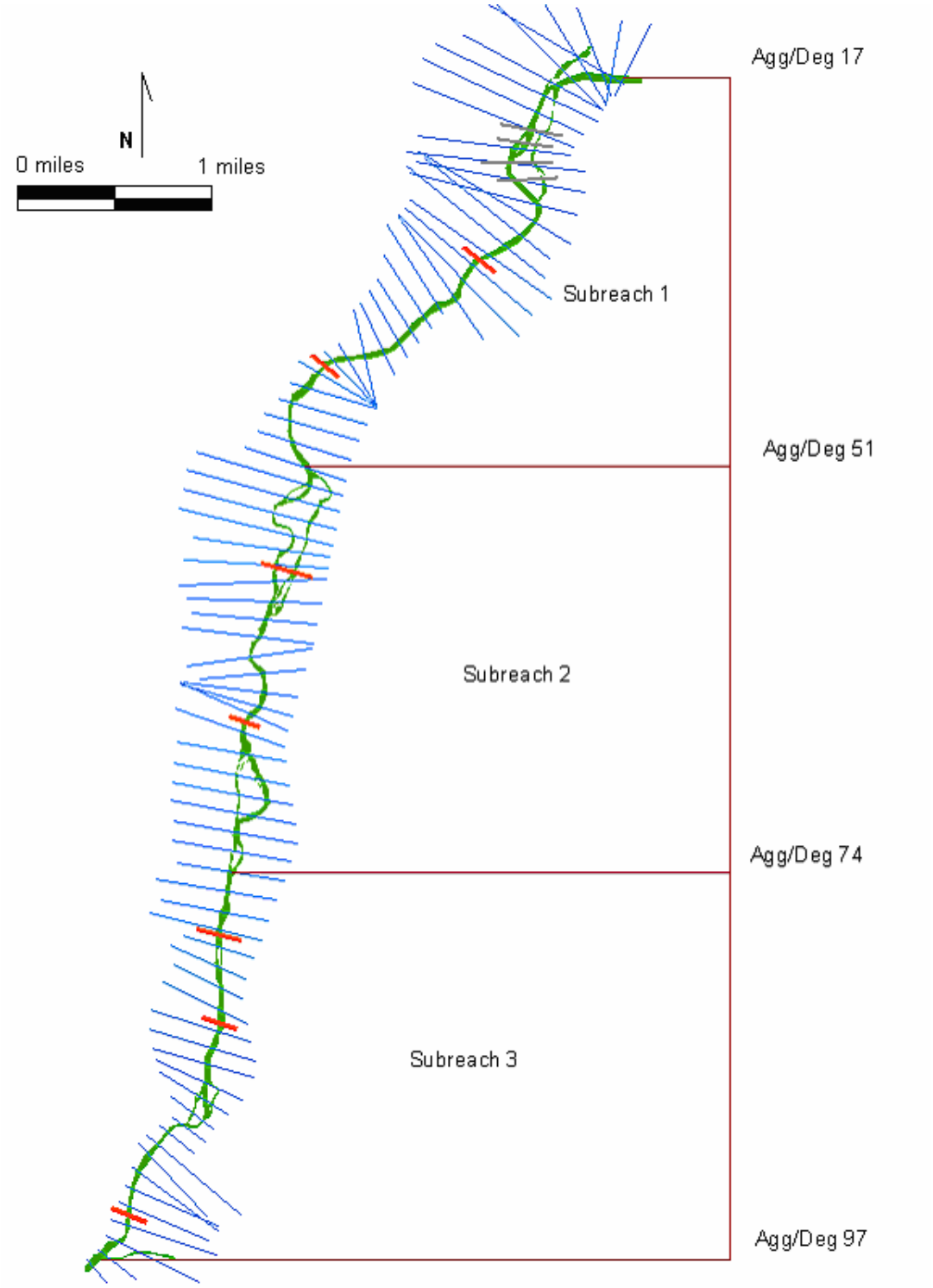

Figure 3-4 Cochiti Dam reach subreach definitions. The channel flows north to south.

3.1.1 Subreach Definition

The Cochiti Dam reach of the middle Rio Grande was subdivided into three subreaches to facilitate geomorphic and sedimentologic analysis. The subreaches were chosen based on characteristic similarities such as planform, width, and sinuosity. Subreach 1 is 2.54 miles long and stretches from agg/deg line 17 to 51; subreach 2 is 2.14 miles long and runs from agg/deg line 51 to 74, and subreach 3, 2.11 miles long, runs from agg/deg line 74 to 95. Agg/deg line 95 is located immediately at the mouth of Galisteo Creek, just upstream of Santo Domingo Bridge. The subreaches are defined in Figure 3-4.

3.1.2 Available Data

Data was collected from both USGS gaging stations and range-lines. One USGS gaging station exists just downstream of Cochiti Dam (Rio Grande below Cochiti Dam, NM, 08317400), and another one is located approximately 8 miles downstream of the study reach in San Felipe (Rio Grande at San Felipe, NM, 08319000). In addition, there is a USGS gaging station located on Galisteo Creek (Galisteo Creek at Domingo, NM, 08318000), and one downstream in Albuquerque (Rio Grande at Albuquerque, NM, 08330000). Before the Cochiti Dam, the Cochiti gage was located just upstream (Rio Grande at Cochiti, NM, 08314500). Adjustments were not made in this analysis for the transition of this gage. Available dates for gages used in this analysis are shown in Table 3-1.

USGS Gaging Station	Dates
RG at Otowi	1895-2004
RG at Cochiti	1926-1970
RG below Cochiti Dam	1970-2004
RG at San Felipe	1930-2004
RG at Albuquerque	1942-2004

Table 3-1 Periods of record for discharge at USGS gages.

Survey data was collected along CO range lines 2 through 8, and agg/deg lines 17 through 97 (see Table 3-2). This data was obtained through the USBR offices in Denver and Albuquerque. CO-lines 2-4 were available until 1998. No CO-lines in the Pueblo de Cochiti Nation (CO-lines 5-8) were surveyed after 1998. For many sets of data, agg/deg-lines 17, 18, 96 and 97 had sporadic or missing data, and were left out of the analysis. Agg/deg lines are photogrammetrically surveyed and have inherent errors. The channel-bottoms are estimated mean bed elevations based on normal depth calculations and do not contain any additional underwater definition of the bed (Holmquist-Johnson personal communication 2005).

Suspended sediment and bed material data was limited in this reach (Table 3-3). Suspended sediment data is available for the Otowi gaging station since the 1950s, but suspended sediment data was not taken at the Cochiti gage until after the dam closure in 1973, and was not taken at all after 1988. Bed material data is available along range lines CO-2 through CO-8, but was only taken consistently at CO-3, CO-5, and CO-8. All data was collected through USGS, USBR, or EPA's STORET database.

	CO-lines		Agg/Deg lines	CI-lines
Years	2-4	5-8	19-97	27.1-29.1
1962			X	
1970	X	X		
1971	X	X		
1972	X	X	X	
1973	X	X		
1974	X	X		
1975	X	X		
1979	X	X		
1980	X	X		
1990				X
1992	X	X	X	
1993				X
1995	X	X		
1998	X	X		X
2002			X	
2004	X			X

Table 3-2 Periods of record for cross-sectional surveys collected by the USBR

Station	Suspended	Bed Material
RG at Otowi	1956-1995	1960-1961
RG below Cochiti Dam	1974-1988	---
RG at Albuquerque	1969-1999	1969-2001
CO-lines 2-8	---	1970-1998

Table 3-3 Periods of record for suspended sediment and bed material collected by the USGS, USBR, and EPA.

Digitized aerial photos were collected from USBR's GIS and Remote Sensing group in Denver, CO. Digitized aerial photos and/or topographic surveys were available for 1918, 1935, 1949, 1962, 1972, 1992, 2001, and 2004. The dates, scales, and mean daily discharges for the aerial photos are available in Appendix A.

3.1.3 Channel Forming Discharge

The USBR's Albuquerque office has performed a detailed analysis to determine channel-forming discharge. Based on analyses of maximum sediment capacity and maximum flows in the Rio Grande, the two-year instantaneous peak discharge (Q_{2y}=5000 cfs) is used as the effective discharge. This value was used in the Santa Ana Geomorphic Analysis (Mosley and Boelman 1998).

Figure 3-5 displays the annual peak mean daily discharges recorded at USGS gaging station 08317400, located just downstream of Cochiti Dam. Pre-Cochiti Dam discharge data was taken from the Rio Grande at Cochiti Dam gage, 08314500. According to the figure, there have not been any flows above 10,000 cfs recorded at the Cochiti gage since 1958. Since the 1940s, the average yearly peak flow has decreased and fewer extreme events have occurred.

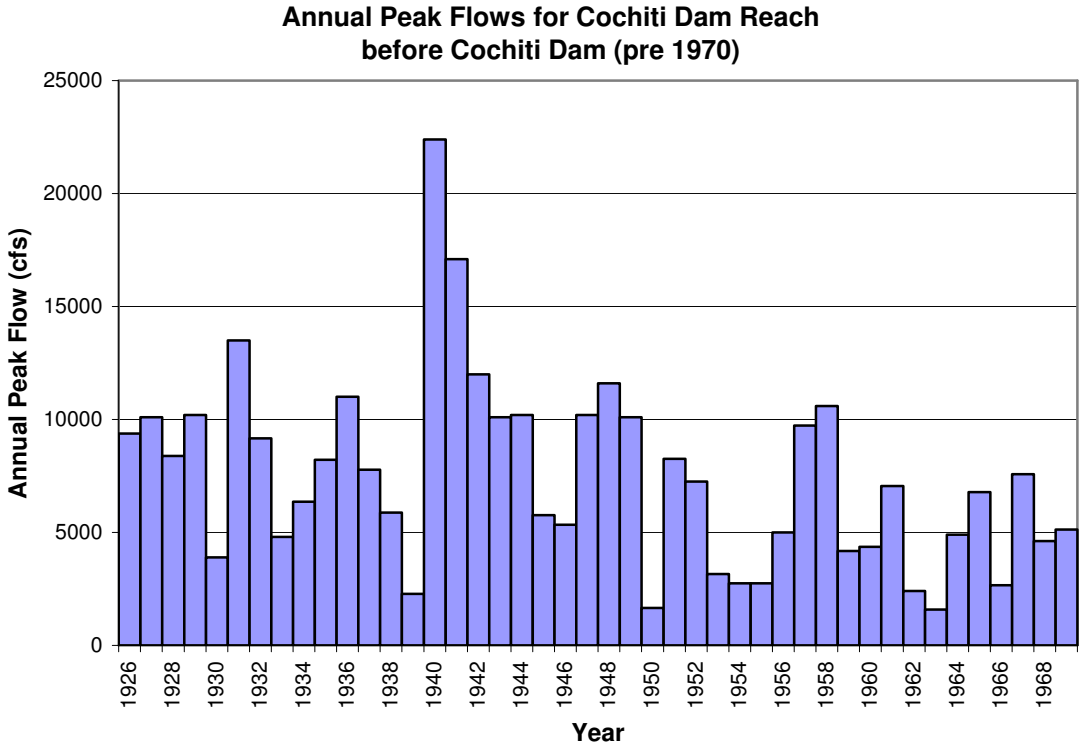

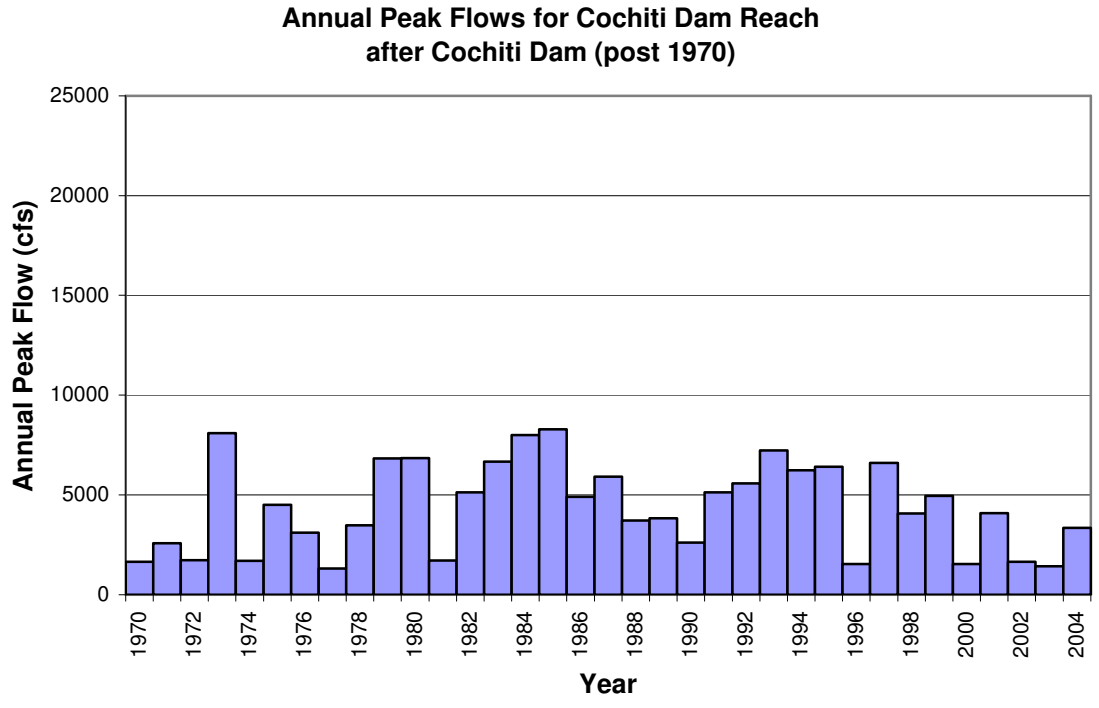

Fig. 3-5 Annual peak mean daily discharges for the Rio Grande at Cochiti Dam 1926 through 2002.

3.2 Methods

3.2.1 Channel Classification

The channel reach was classified using aerial photos from 2002. Geographic Information System (GIS) coverages ranging from 1918 to 2004 of the historical active channel were used to qualitatively describe the non-vegetated channel planform. The determination of channel classification for the Cochiti Dam reach was done using several different methods, discussed below:

Slope-discharge relationships were applied using methods devised by Leopold and Wolman (1957), Lane (1957, from Richardson et al. 1990), Henderson (1963, from Henderson 1966), Ackers and Charlton (1970, from Ackers 1982) and Schumm and Kahn (1972). Channel morphology methods were implemented from Rosgen (1994).

In addition, channel classifications based on stream-power were calculated using methods by Chang (1979), Van den Berg (1995), Knighton and Nanson (1993), and Nanson and Croke (1992). Finally, Parker's (1976) method of stream classification was used, which employs slope/Froude number and flow depth/flow width.

Slope-Discharge methods:

Leopold and Wolman (1957) classify channel planforms as meandering, braided, or straight. Slope-discharge relationships provide the criterion upon which these classifications are based. Braided and meandering channels are separated by the following equation:

$$S_o = 0.06 Q^{-0.44},$$

where Q is the bankfull discharge in cfs and S_o is the channel bedslope in ft/ft. Leopold and Wolman refer to meandering rivers as those with a sinuosity greater than 1.5. Channels with relatively stable alluvial islands are refered to as braided. All units are English.

Lane (1957, from Richardson et al. 1990) proposed a relationship for sand bed channels based on a dimensionless parameter, K:

$$S_o Q^{0.25} = K,$$

where S_o is in ft/ft and Q is in cfs. The channel classification is then determined using the following criteria:

$K \leq 0.0017$ meandering

$0.0017 < K < 0.010$ intermediate (transitional)

$K \geq 0.010$ *braided*

All units are English.

Henderson (1963, from Henderson 1966) began with Leopold and Wolman's slope-discharge relationship, and added a bed material factor, *d*, which describes the median grain size in feet. Plotting $S_o/0.06Q^{-0.44}$ against d empirically derived the following relationship:

$$S_o = 0.64 d^{1.14} Q^{-0.44}$$

According to Henderson, two-thirds of the channels with meandering or straight patterns had values of *S* that fall close to this line. Braided channels had values of *S* that were much higher than the line. *Q* is in cfs and S_o is in ft/ft. All units are English.

Ackers and Charlton (1979, Ackers 1982) developed a relationship that would distinguish a meandering channel from a straight channel or straight channel with alternating bars.

- $S_w < 0.001Q^{-0.12}$ straight channel
- $0.001Q^{-0.12} < S_w < 0.0014Q^{-0.12}$ straight channel with alternating bars
- $S_v > 0.0014Q^{-0.12}$ meandering channel

S_w represents the water surface slope along a straight channel's axial line in m/m, and S_v represents the straight-line slope for meandering channels in m/m. Q is in cfs. Ackers also found that the equation,

$$S_v=0.0008Q^{-0.21},$$

can be used to distinguish between meandering and straight channels in sand-bed rivers. All units are SI.

Schumm and Khan (1972) suggested the following valley slope thresholds to determine channel type.

- S < 0.0026 straight channel
- 0.0026< S < 0.016 meandering channel (meandering thalweg)
- S > 0.016 braided channel

These relationships were empirically derived from flume experiments.

Channel Morphology Methods:

Rosgen (1994) used slope, entrenchment, sinuosity, and bed material characteristics to classify channels into seven major stream types. The table shown in Figure 3-6 is widely used to classify rivers and channels.

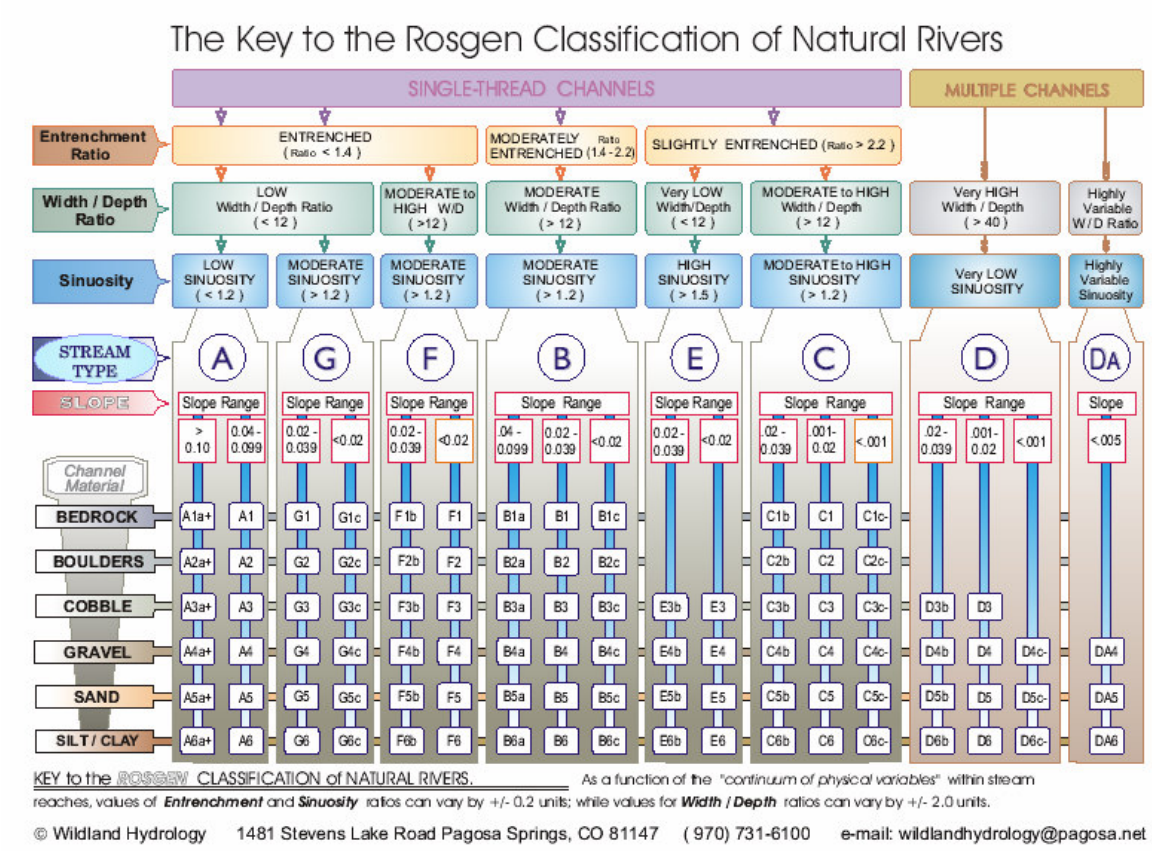

Figure 3-6 Rosgen classification system key (Rosgen 1996).

Parker (1976) does not factor in sediment transport when classifying rivers. His method delineated meandering from braided streams independently of sediment transport by examining width-depth ratios and slopes. If slope and width-depth ratios are high, braided systems are favored. If slope and width-depth ratios are low, meandering planform is likely.

- $S_o/Fr << d/b$ meandering channel
- $S_o/Fr \sim d/b$ transitional channel
- $S_o/Fr >> d/b$ braided channel

In these criteria, S_o/Fr represents the ratio of the bedslope to the Froude number, and d/b represents the width-depth ratio.

Stream Power Methods:

Van den Berg (1995) proposed an equation based on potential stream power, grain size, and valley slope. This discriminator is compared to the potential specific stream power to determine the stream's stream power and channel pattern.

- $\omega_{v,t} = 900\ D_{50}^{0.42}$ *discriminator*
- $\omega_{v,bf} = 2.1 * S_v\ Q_{bf}^{1/2}$ (kW/m^2) *potential specific stream power for sand-bed channels*
- $\omega_{v,bf} = 3.3 * S_v\ Q_{bf}^{1/2}$ (kW/m^2) *potential specific stream power for gravel-bed channels*

In these equations, D_{50} represents the median grain size in mm, Q is discharge in m^3/s and S_v is the valley slope in m/m. All units are in SI. Using these equations and Figure 3-7, the following criteria were established:

- If $\omega_{v,bf}/\omega_{v,t} > 1$, the channel corresponds to a low sinuosity single-thread and multi-thread channel.
- If $\omega_{v,bf}/\omega_{v,t} < 1$, the channel is a single-thread channel.
- If measure to reference width ratio > 1, the river is a high-energy wide channel.
- If measure to reference width ratio < 1, the river is a low-energy narrow channel.

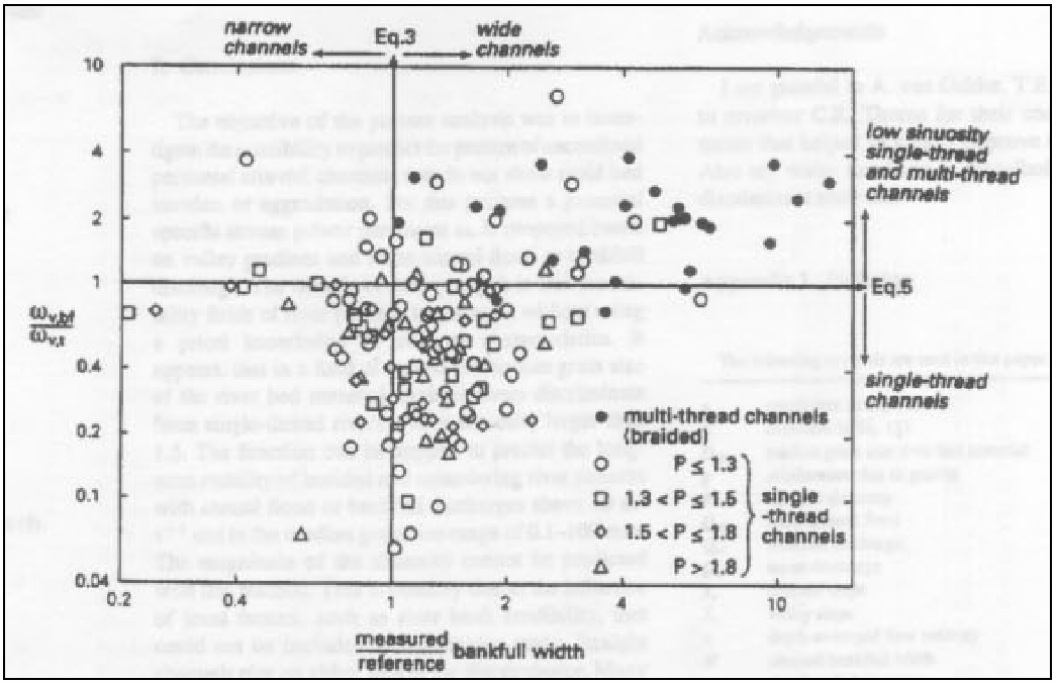

Figure 3-7 Channel pattern, width/depth ratio and potential specific stream power relative to defined reference values (after van den Berg 1995)

Knighton and Nanson (1993) used flow strength, bank erodibility, and relative sediment supply to describe channel patterns. The relative sediment supply is defined here as the rate at which material is supplied from either bank erosion or from upstream relative to the rate it is transported downstream.

According to their method, straight channels correspond to low values of flow strength, bank erodibility, and relative sediment supply rate. Braided channels correspond to high values of flow strength, bank erodibility, and relative sediment supply rate. Meandering channels correspond to median values. No specific threshold values are specified, but rather a relative scale is assumed.

Chang (1979) discriminates between stream planforms using a method based on stream power and slope-discharge relationships. For a given input of water and sediment discharge, a stable geometry and slope corresponds to a minimum stream power per unit length of the channel. Based on the number of stream power minimums, different planform configurations can be

estimated, as shown in Figure 3-8. Higher sinuosity rivers occur at lower valley slopes, but will narrow and deepen into meandering or straight rivers with increasing valley slope (Chang 1979).

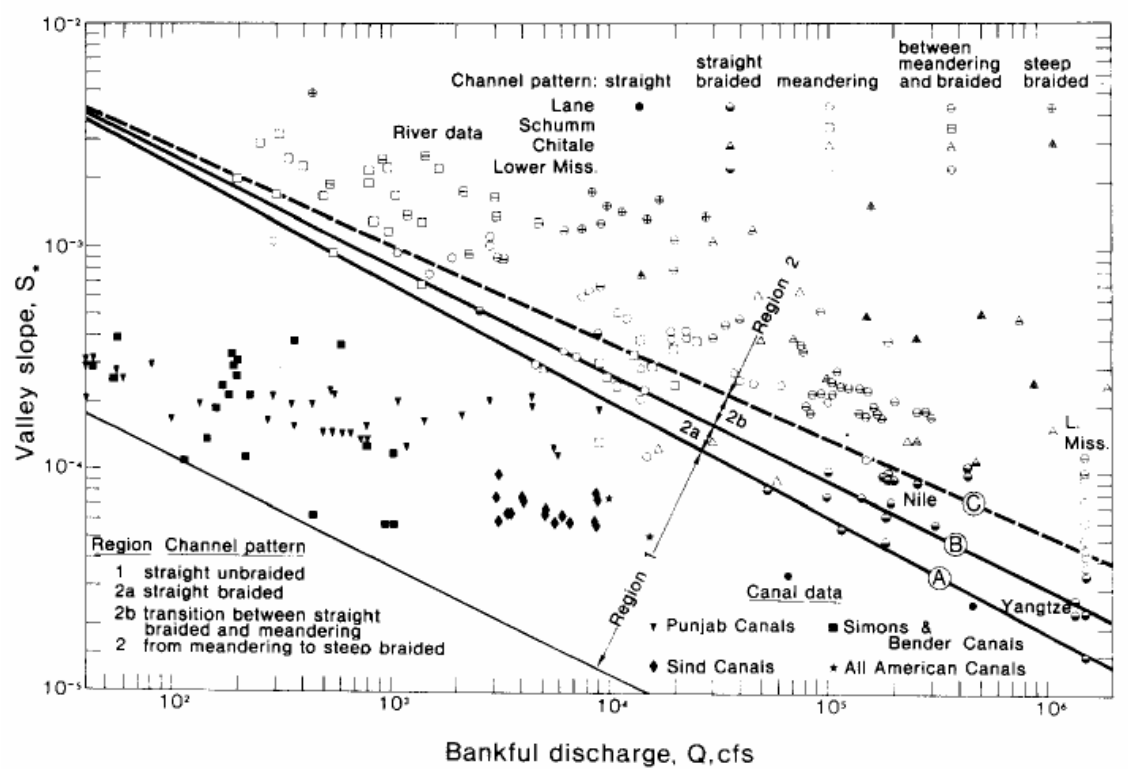

Figure 3-8 Channel patterns of sand streams (after Chang 1979)

3.2.2 Sinuosity

The sinuosity of the study reach was estimated as the ratio of the channel thalweg length to the valley length. The GIS data containing channel thalweg length was obtained from the USBR's Albuquerque office. Also provided were aerial photos, topographic maps, and measured valley lengths. The thalweg location was estimated and used as the active channel length.

Identification of the channel length and thalweg location was subject to several factors, such as water depth, survey date, and photo quality variability.

3.2.3 Valley Slope

The valley slope of the study reach was estimated using the agg/deg survey data. The valley slope was computed as the ratio of valley elevation differences to the valley length. The valley lengths were measured using GIS coverages obtained from the USBR's GIS and Remote Sensing Group in Denver, CO. The valley elevations were computed averages at each agg/deg range line. Agg/deg lines are generally 400 to 600 feet apart, measuring from center to center. The variances in this rule of thumb were taken into account throughout the analysis of this report.

3.2.4 Longitudinal Profile

Thalweg Elevation

The lowest point in each CO-line cross-section was taken to be the thalweg elevation of the channel in that location. For the Cochiti Dam reach, thalweg data was available for CO-lines 2 through 4 from 1973 through 2004. For CO-lines 5 though 9, data was available only until 1998. CO-line surveys have not been taken in land residing in this part of the Pueblo de Cochiti Nation since 1998. Agg/deg surveys have been taken since 1998; however, these surveys are not detailed and give only a mean bed elevation for the channel. The changes in thalweg elevation were plotted to show temporal trends at each location. Each CO-line cross-section for every available date is plotted in Appendix B.

Mean Bed Elevation

The agg/deg surveys use an average bed elevation in the survey data. The cross-section itself is not surveyed in detail. Agg/deg surveys were available for 1962, 1972, 1992, and 2002 for the 80 cross-sections in the Cochiti Dam reach. Longitudinal profiles were plotted for each subreach, as well as for the entire reach. In addition, the subreach-averaged mean bed elevations were calculated. Bed slope changes were measured using the differences in the average mean bed elevation.

Friction and Water Slopes

The friction slopes were estimated at each CO-line cross-section at the channel forming discharge mentioned in section 2.2 of 5,000 cfs. The slopes were modeled using HEC-RAS 3.1.3. The slopes were averaged over each subreach using a weighting factor. The weighting factor was calculated as the sum of one-half of the distances to each neighboring cross-section. An overall average slope for the entire study reach was also calculated.

3.2.5 Channel Geometry

Hydraulic Geometry

HEC-RAS 3.1.3 was used to describe the channel geometry of this reach using agg/deg line surveys. The available 1962, 1972, 1992, and 2002 agg/deg data was modeled using the channel forming discharge of 5,000 cfs. Seventy-six cross-sections were used in the modeling, utilizing Agg/Deg lines 19 through 95. The cross-sections were generally spaced between 400 and 600 feet apart. These distances were measured using the digitized aerial photos in ArcGIS 9. The same channel forming discharge of 5,000 cfs was routed through the model. The Manning's *n* values used in HEC-RAS are shown in Table 3-4. The Manning *n* in the channel bed increased over time due to the increasing median grain size (d_{50}) in the bed.

The Manning *n* on the floodplain was determined by inspection of aerial photographs. This value did not change significantly over time. The value of Manning *n* was also fairly constant over the length of the entire reach. HEC-RAS results are displayed in Appendix C.

	Manning *n*	
	channel	**floodplain**
1962	0.02	0.1
1972	0.02	0.1
1992	0.028	0.1
2002	0.032	0.1

Table 3-4 Manning's *n* values for the study reach.

Digitized photos were also used for channel geometry interpretation. Channels were delineated from aerial photographs for determination of the width of the active channel at each agg/deg line. This was done using ArcGIS 9.

Channel geometry parameters were computed and averaged using the same weighting scheme used for slope. Wetted perimeter, P, wetted cross-sectional area, A, mean flow velocity, V, top width, W, Mean depth, h, and Froude number, Fr, were all calculated using these means. Numerical results are available in Appendix C.

Overbank Flow/Channel Capacity

HEC-RAS results contain both main channel flow and overbank flow. The main channel flow, where most sediment transport occurs, was used for the bulk of this hydraulic modeling analysis.

3.2.6 Sediment

Bed Material

Characterization of spatial and temporal trends in bed material size was performed for each subreach in the Cochiti Dam reach. Median grain sizes, d_{50}, were computed for the available dates. Suspended sediment data was available for CO-lines from 1970 through 1998. Data since 1998 has not been taken in the Pueblo de Cochiti Nation. Table 3-5 lists the available bed material data for this analysis.

Sporadic bed material data was available for CO-lines 2 through 8. CO-3, CO-5, and CO-8 had the most complete data over time, and were chosen to represent subreaches 1, 2, and 3, respectively. Using this data, temporal changes in the median grain size, d_{50}, were examined, and temporal and spatial particle size distributions over the entire reach were generated.

	Subreach 1		Subreach 2		Subreach 3							
	CO-2	CO-3	CO-4	CO-5	CO-6	CO-7	CO-8	CO-9	CI-28	CI-29.1	Cochiti Gage	San Felipe Gage
1970	X	X	X	X	X	X	X					X
1971	X	X	X	X	X	X	X	X				X
1972	X	X	X	X	X	X	X	X				X
1973	X	X	X	X							X	X
1974		X		X		X	X	X				X
1975		X		X	X		X	X				
1979		X		X	X	X	X	X				
1980		X		X	X	X	X	X				
1992		X		X			X	X				
1995		X		X			X	X				
1998		X		X			X	X	X	X		

Table 3-5 Bed material data availability for study reach

3.3 Results

3.3.1 Channel Classification

The Middle Rio Grande has been characterized in the past as an aggrading, braided, sandbed river (Baird 1996). As a result of this trend, measures were taken, as described in Chapter 2, to control aggradation and flooding in this region.

The current channel pattern description is from 2004 aerial photos, shown in Figures 3-1, 3-2, and 3-3. At low flow, several sections of the channel exhibit braiding and mild anastomosing in some short sections of subreach 2. Vegetated bars lateral to the flow and within the channel are apparent sporadically along the reach. A large, sandy sediment fan is apparent at the mouth of Peralta Canyon in Figure 2-1.

GIS coverages were obtained from the USBR to show the planform changes to the river over time. Planform geometries were available for 1918, 1935, 1949, 1962, 1972, 1985, 1992, and 2004. Figure 3-9 was produced from these coverages. Note the extensive braiding and wide channel in 1935.

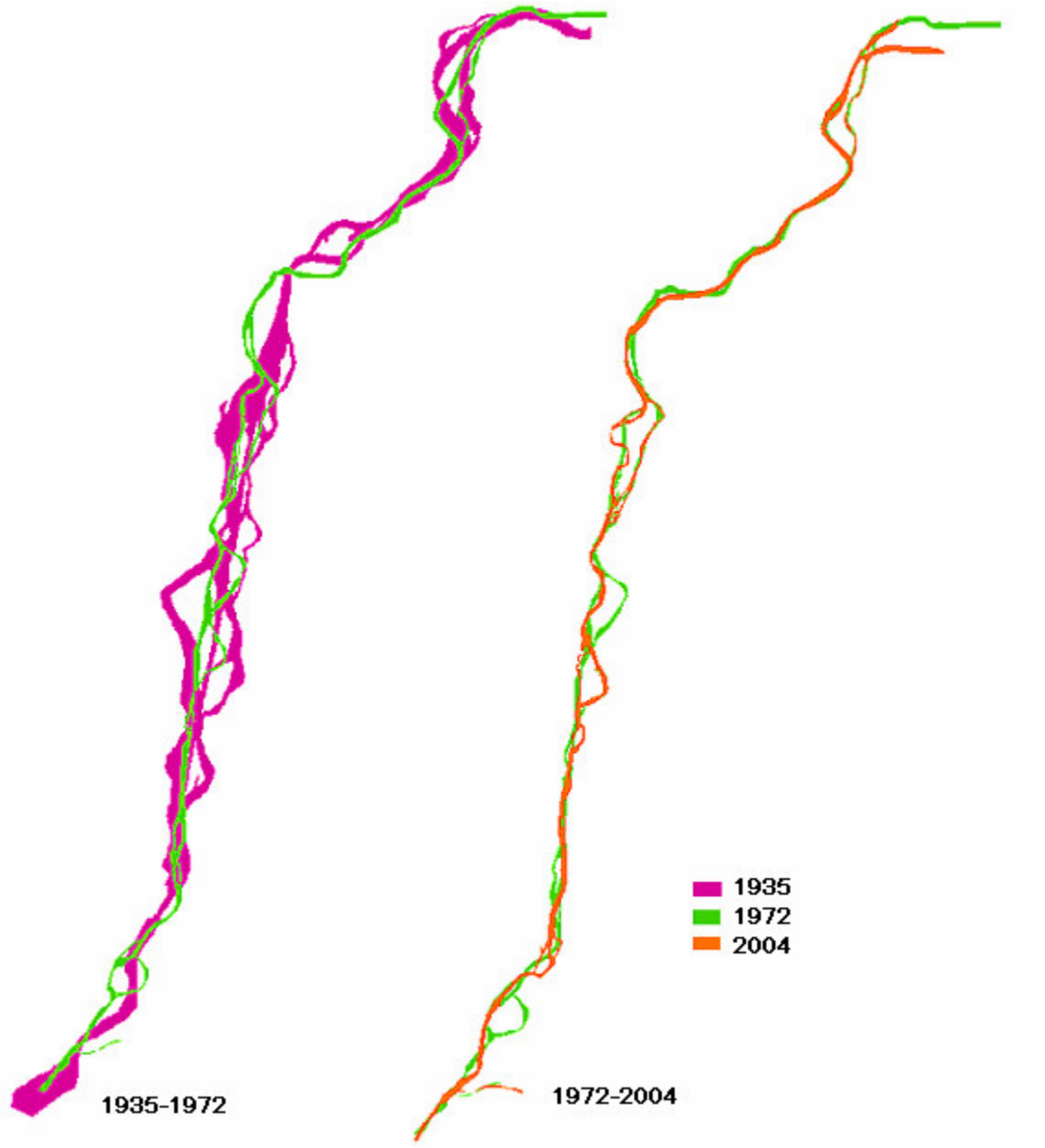

Figure 3-9 Non-vegetated active channel changes to the Cochiti Dam Reach. Cochiti Dam is located at the upstream-most point of the 2004 planform. Planforms are from aerial photos.

A HEC-RAS model of this reach was run at a channel forming discharge of 5,000 cfs and the output values were used in the channel classification section. These methods produce planform descriptions of the channel that range from straight to meandering and braided. Table 3-6 displays the input parameters used.

	Subreach	Q (cfs)	Channel Slope (ft/ft)	Valley Slope (ft/ft)	d50 (mm)	d50 (ft)	Width (ft) from	Depth (ft)	Velocity (ft/s)	Froude No.	EG Slope (ft/ft)
1962	1	5,000	0.0014	0.0019	0.21	0.00069	361	2.80	5.47	0.58	0.0015
	2	5,000	0.0017	0.0018	0.21	0.00069	538	2.59	4.77	0.59	0.0017
	3	5,000	0.0015	0.0013	0.21	0.00069	469	3.72	4.47	0.47	0.0012
	Total	5,000	0.0016	0.0017	0.21	0.00069	444	2.99	4.98	0.55	0.0015
1972	1	5,000	0.0013	0.0016	0.31	0.00100	300	3.17	5.70	0.57	0.0014
	2	5,000	0.0018	0.0019	0.18	0.00058	392	2.79	5.28	0.60	0.0017
	3	5,000	0.0013	0.0011	0.29	0.00094	389	2.94	5.16	0.55	0.0014
	Total	5,000	0.0014	0.0016	0.26	0.00084	352	2.97	5.43	0.58	0.0015
1992	1	5,000	0.0015	0.0017	32.18	0.10558	349	3.10	5.45	0.58	0.0016
	2	5,000	0.0016	0.0019	14.85	0.04873	422	2.89	5.23	0.61	0.0018
	3	5,000	0.0015	0.0012	51.10	0.16763	351	2.94	5.50	0.59	0.0016
	Total	5,000	0.0015	0.0016	32.71	0.10732	372	2.99	5.40	0.59	0.0017
2001	1	5,000	0.0015	0.0017	16.01	0.05252	301	3.54	5.50	0.56	0.0021
	2	5,000	0.0019	0.0019	32.04	0.10512	394	2.68	5.54	0.64	0.0024
	3	5,000	0.0015	0.0012	24.58	0.08064	290	3.30	6.03	0.62	0.0017
	Total	5,000	0.0016	0.0016	24.21	0.07943	326	3.17	5.66	0.60	0.0021

Table 3-6 Input parameters for Channel Classification Methods

The methods used had varying results. Ackers & Charloton (1970, from Ackers 1982) and Parker (1976) both calculated the Cochiti Reach to be a meandering channel, not varying over space or time. Both Lane (1957, from Richardson et al. 1990) and Henderson (1963, from Henderson 1966) described the reach as a braided channel with no temporal or spatial variation. Leopold & Wolman (1957) and Schumm & Khan (1972) agree that the Cochiti Dam reach is straight over space and time. Chang's (1979) method, when plotted on Figure 3-8, finds the reach transitioning from meandering to steep braided with no temporal or spatial change. With a valley slope that remains between 0.0011 and 0.0019, and an assumed channel forming discharge of 5,000 cfs, Figure 3-3 shows the channel as remaining in "region 2" for the entire length of the channel and span of the study.

Rosgen (1996) and Parker (1976) both have classification methods based on channel morphology variables. According to Rosgen's method, the Cochiti Dam reach best fits the D5 class for 1962 and 1972, and D4 for 1992 and 2002 (see Figure 3-6). D5 is described as a multiple channel stream with very high (>40) width-to-depth ratio, very low sinuosity sand bed river with slopes between 0.001 ft/ft and 0.02 ft/ft. A D5 class river is the same, but for gravel beds. These streams are typically characterized by braids, a channel slope that is approximately

equivalent to the valley slope, and high bank erosion rates. Parker's method describes the stream to be meandering for all years, since the slope-to-Froude number ratio is much smaller than the depth to width ratio.

Van de Berg's (1995) method described the entire channel as a low sinuosity single thread and multi thread channel in 1962 with no spatial variability. In 1972, the subreach remained the same, with the exception of subreach 3, which is now classified as simply a single thread channel. In 1992 and 2002, the entire length of the reach was reclassified as a single thread channel. After the dam, the reach changed to a gravel bed river, and the potential specific stream power for gravel bed rivers began to exceed the discriminator, as described in the methods section.

Knighton and Nanson (1993) did not quantify threshold values for flow strength, bank erodibility, and sediment supply. It is possible, however, to interpret the change in these variables in the Cochiti Dam reach qualitatively. Just downstream of the dam, the discharge peaks have decreased, and the sediment supply has been all but starved. Thus, the sediment capacity has increased while the bank erodibility is high. Thus, the bed and banks of the previously braided river have been eroded by the sediment starved clear water discharge from the dam. This would suggest that the river has narrowed and deepened, transforming it from a braided to a meandering planform.

The different channel classification methods employed varying parameters to estimate the planform of the Cochiti Dam reach. Ackers and Charlton, Parker, Rosgen, and van den Berg seemed to produce results that made physical sense (See Table 3-7).

Year	Subreach	D_{50} type	Slope-discharge						Channel Morphology		Stream Power	
			Leopold and Wolman	Lane	Henderson	Ackers & Charlton		Schumm & Khan	Rosgen	Parker	van den Berg	Chang
						using S_o	*using* S_v					
1962	1	sand	Straight	Braided	Braided	Meandering	Meandering	Straight	D5	Meandering	low sinuosity single thread and multi thread channel	from meandering to steep braided
	2	sand	Straight	Braided	Braided	Meandering	Meandering	Straight	D5	Meandering	low sinuosity single thread and multi thread channel	from meandering to steep braided
	3	sand	Straight	Braided	Braided	Meandering	Meandering	Straight	D5	Meandering	low sinuosity single thread and multi thread channel	from meandering to steep braided
	Total	sand	Straight	Braided	Braided	Meandering	Meandering	Straight	D5	Meandering	low sinuosity single thread and multi thread channel	from meandering to steep braided
1972	1	sand	Straight	Braided	Braided	Meandering	Meandering	Straight	D5	Meandering	low sinuosity single thread and multi thread channel	from meandering to steep braided
	2	sand	Straight	Braided	Braided	Meandering	Meandering	Straight	D5	Meandering	low sinuosity single thread and multi thread channel	from meandering to steep braided
	3	sand	Straight	Braided	Braided	Meandering	Meandering	Straight	D5	Meandering	single thread channel	from meandering to steep braided
	Total	sand	Straight	Braided	Braided	Meandering	Meandering	Straight	D5	Meandering	low sinuosity single thread and multi thread channel	from meandering to steep braided
1992	1	gravel	Straight	Braided	Braided	Meandering	Meandering	Straight	D4	Meandering	single thread channel	from meandering to steep braided
	2	gravel	Straight	Braided	Braided	Meandering	Meandering	Straight	D4	Meandering	single thread channel	from meandering to steep braided
	3	gravel	Straight	Braided	Braided	Meandering	Meandering	Straight	D4	Meandering	single thread channel	from meandering to steep braided
	Total	gravel	Straight	Braided	Braided	Meandering	Meandering	Straight	D4	Meandering	single thread channel	from meandering to steep braided
2002	1	gravel	straight	Braided	Braided	Meandering	Meandering	Straight	D4	Meandering	single thread channel	from meandering to steep braided
	2	gravel	straight	Braided	Braided	Meandering	Meandering	Straight	D4	Meandering	single thread channel	from meandering to steep braided
	3	gravel	straight	Braided	Braided	Meandering	Meandering	Straight	D4	Meandering	single thread channel	from meandering to steep braided
	Total	gravel	straight	Braided	Braided	Meandering	Meandering	Straight	D4	Meandering	single thread channel	from meandering to steep braided

Table 3-7 Channel Pattern Classification for Cochiti Dam Reach 1962, 1972, 1992, and 2002.

3.3.2 Sinuosity

The sinuosity of the Cochiti Dam reach varied with subreach. Immediately downstream of the dam in subreach 1, the sinuosity varied between 1.3 and 1.4 until the early 1970s. Subreaches 2 and 3 had steadily increasing sinuosities, typically between 1.0 and 1.2, until the early 1970s. After the dam, sinuosity decreased overall to an average of 1.13. Subreach 1, however, continued having a much higher sinuosity (around 1.25), than the downstream subreaches (see Figure 3-10). This result is not typical of other reaches of the Middle Rio Grande, which are generally straight channels with low sinuosities (Leon 1998, Bauer 2000, Richard et al. 2001, Albert 2004). This may be due to the proximity of the reach to the dam itself.

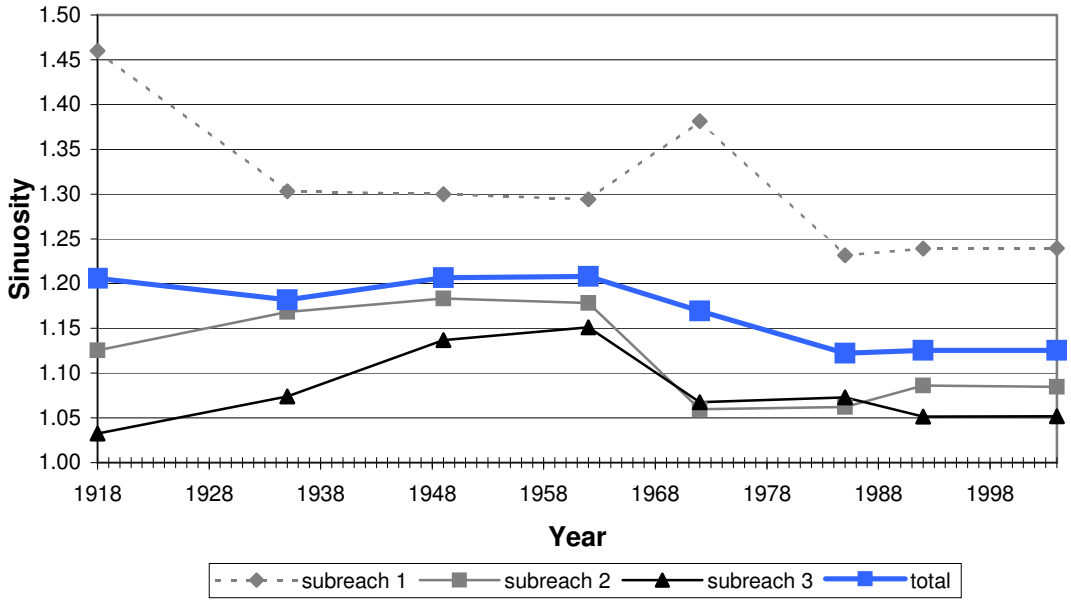

Figure 3-10 Time series of sinuosity of the Cochiti Dam reach as the ratio of channel thalweg length to valley length.

3.3.3 Longitudinal Profile

Thalweg Elevation

Changes in thalweg elevation over time were calculated for each CO-line in the reach. Surveys were available for up to 2004 for CO-lines 2, 3, and 4, and were available up to 1998 for CO-lines 5 through 8. Data in 1973, 1979, 1992, 1995, and 1998 was collected during summer

months. Data from 1974, 1975, 1980, and 2004 was collected during winter months. The overall trend is slight degradation at cross-sections CO-2 through CO-8, with the exception of CO-4, which appears to have aggraded.

Table 3-8 summarizes total temporal thalweg changes. Figure 3-11 shows a longitudinal profile of the changes. From 1973 to 2004, Subreach 1 degraded an average of 1.72 feet. From 1973 to 1998, subreach 2 degraded an average of 0.88 feet, and subreach 3 degraded an average of 2.47 feet. The Cochiti Dam reach degraded an average of 1.57 feet.

CO-line	agg/deg (ft)	Years
2	-2.21	1973-2004
3	-1.23	1973-2004
4	+1.89	1973-2004
5	-2.92	1973-1998
6	-1.61	1973-1998
7	-2.56	1973-1998
8	-2.37	1973-1998

Table 3-8 Average thalweg change at each CO-line from 1962 to 2004.

Subreach 2 had a lower average degradation because the bed appeared to aggrade at CO-4. The cross-section at CO-4 had split channel flow with two large main channels until 1998. The channel then began to favor the left side, leaving the right side available for overbank or flood flows. The thalweg did not actually aggrade; the right channel became the secondary channel instead of the main channel. The average degradation for all range-lines except CO-4 was 2.15 feet. Figure 3-12 graphically shows the change.

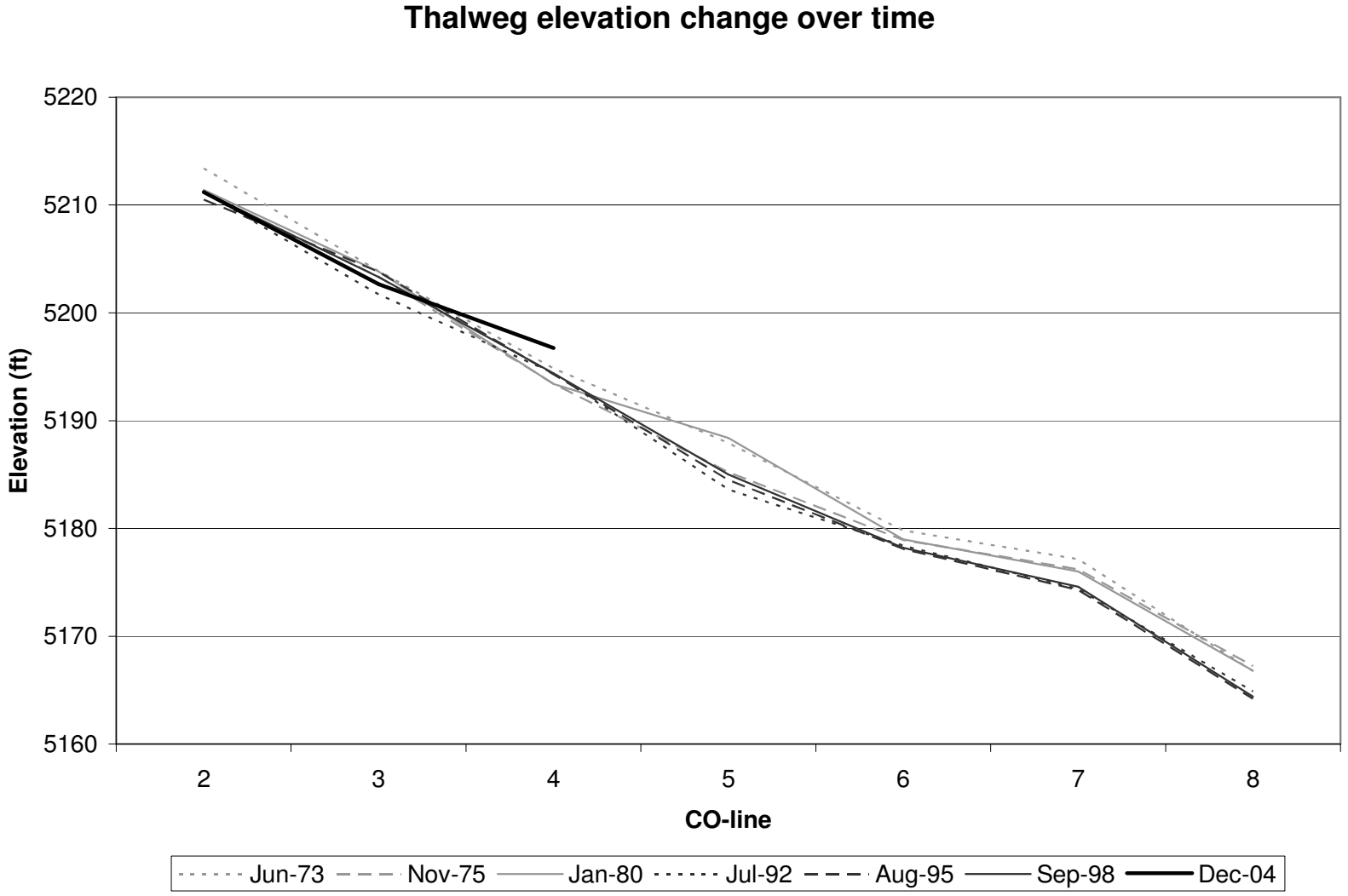

Figure 3-11 Thalweg elevation change with time at CO-lines

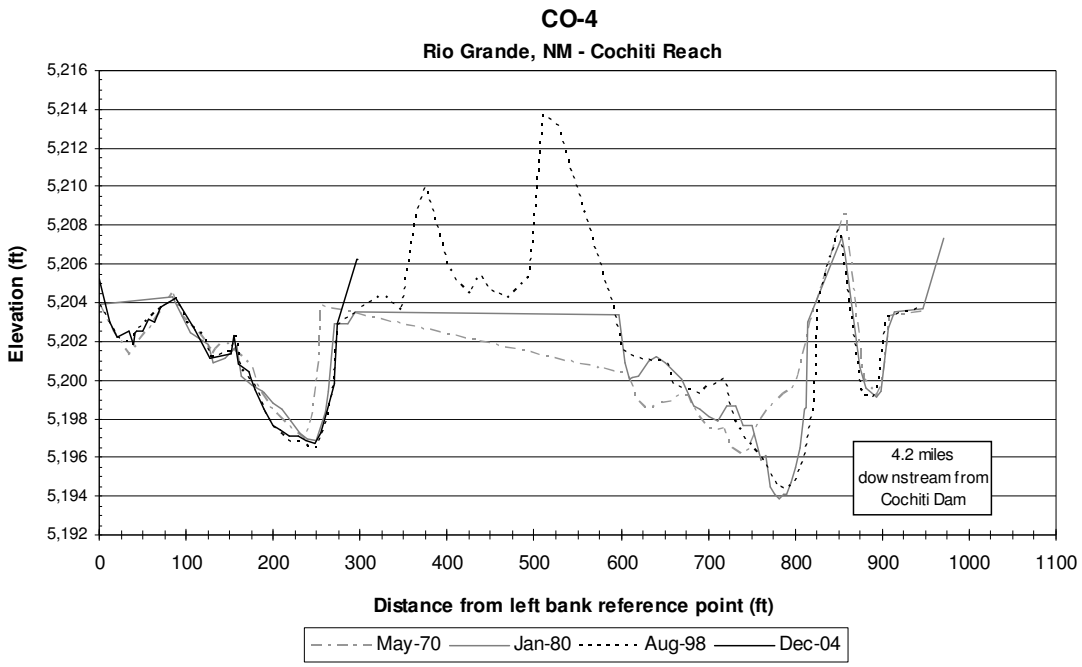

Figure 3-12 Thalweg change at CO-4

Mean Bed Elevation

Mean bed elevation changes were calculated from agg/deg surveys. The channel bed elevation in agg/deg surveys is taken as the mean bed elevation. Agg/deg survey data was available for 1962, 1972, 1992, and 2002. Figure 3-13 shows the cross-section at agg/deg line 57 as an example mean bed elevation over the past 40 years.

Table 3-9 quantifies the aggradational and degradational trends over the length of the reach for the three time periods. From the agg/deg data set, from 1962 to 2002, subreach 1 averaged a total aggradation of 0.81 feet, subreach 2 averaged a degradation of 0.32 feet, and subreach 3 averaged a total aggradation of 0.13 feet. Figure 3-14 shows that while the mean bed has not changed appreciably, it has varied inconsistently around a mean value.

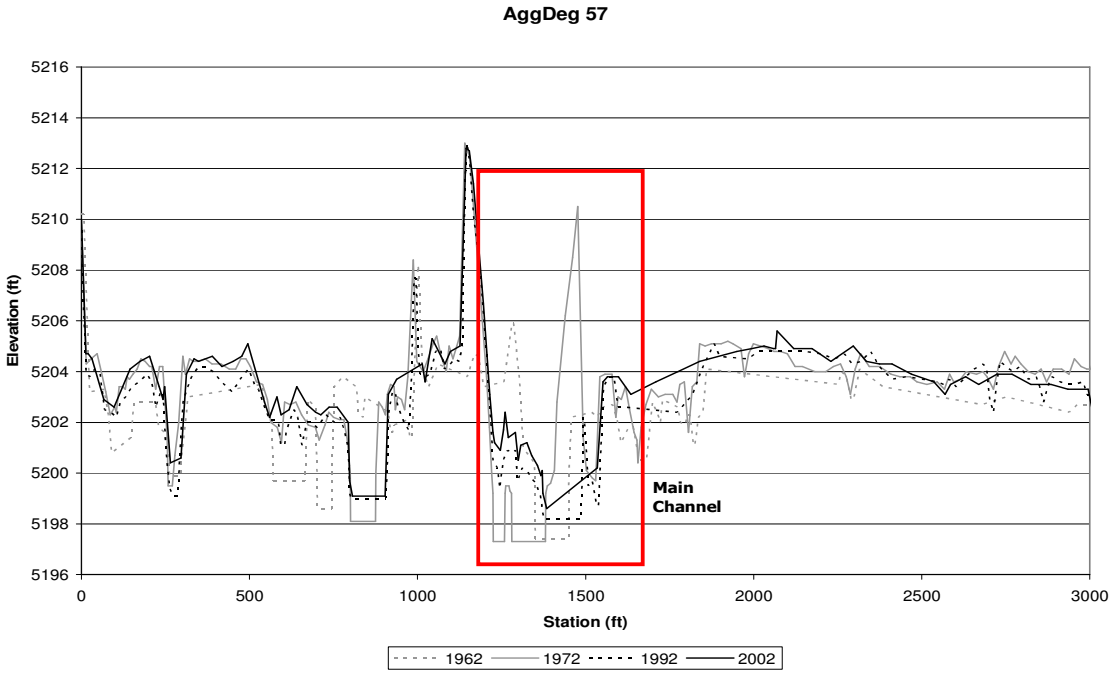

Figure 3-13 Agg/Deg line 57 displaying the aggradation of the mean bed elevation from 1962 to 2002

	Mean Bed Elevation (ft)				Changes in MBE (ft)			
subreach	1962	1972	1992	2002	62-72	72-92	92-02	**62-02**
1	5214.99	5214.96	5215.45	5215.80	-0.03	0.49	0.35	0.81
2	5194.11	5192.77	5193.14	5193.80	-1.34	0.37	0.66	-0.32
3	5173.50	5173.76	5173.54	5173.63	0.26	-0.22	0.09	0.13
total	5194.20	5193.83	5194.04	5194.41	-0.37	0.21	0.37	0.21

Table 3-9 Reach averaged mean bed elevation values and changes.

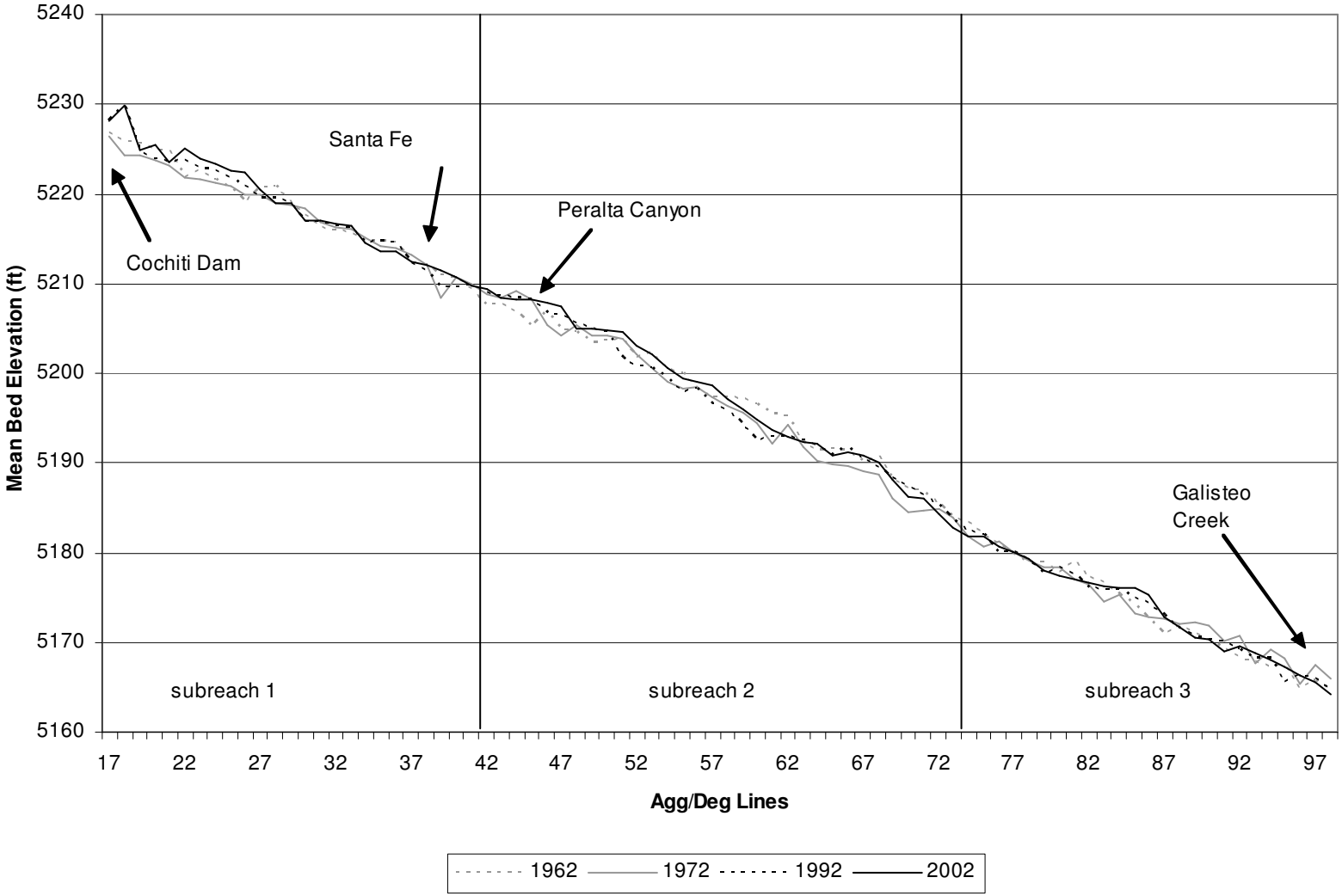

Figure 3-14 Mean bed elevation profile of Cochiti Dam reach for 1962, 1972, 1992, and 2002.

While this slight aggradation seems to contradict the previous findings of thalweg degradation, the explanation for an increase in average mean bed elevation is quite simple. The bed has not actually aggraded with sediment. Agg/deg line surveys are taken photogrametrically, not by surface surveys. The river is surveyed from above, and mean bed elevation is estimated using normal depth calculations (Holmquist-Johnson personal communication 2005). If the bed has narrowed and scoured, the channel geometry may have changed enough to make the average of all active channel elevations higher than that of the original channel. Figure 3-15 shows how the mean bed elevation may have increased.

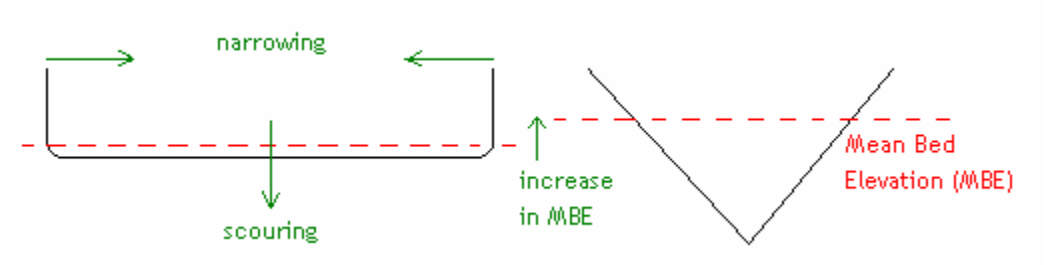

Figure 3-15 Change in mean bed elevation due to channel geometry changes

Instantaneous bed slope was calculated using the difference between mean bed elevations at the agg/deg line just upstream from a cross-section and that of the agg/deg line just downstream. The difference was then divided by the total channel length between those agg/deg lines. The bedslopes calculated from 1962 to 2002 are shown in Table 3-10. The bedslope decreased overall before the dam, and has been increasing since 1972.

	Bed Slope (ft/ft)			
subreach	1962	1972	1992	2002
1	0.0014	0.0013	0.0015	0.0015
2	0.0017	0.0018	0.0016	0.0019
3	0.0015	0.0013	0.0015	0.0015
total	0.0016	0.0014	0.0015	0.0016

Table 3-10 Bed slope 1962-2002 for Cochiti Dam reach

Changes to the cross-sections upstream have been minor since the mid 1990's. The bed appears to have armored and little degradation is expected in the future. The CI lines

near the upstream portion of the reach have been taken every 3 to 4 years since 1990 and show little change near the dam (Figure 3-16).

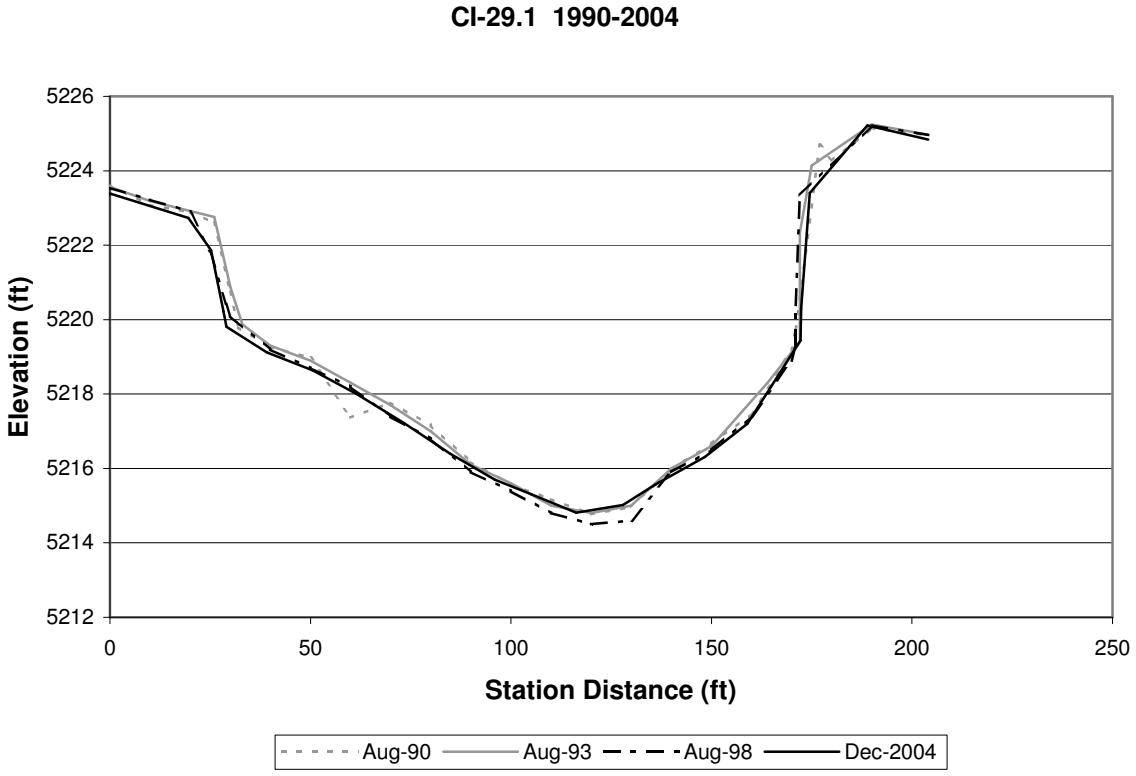

Figure 3-16 Cross-section at CI-29.1 showing armoring just downstream of the dam.

Friction Slope

The average friction slopes for subreaches 1, 2, and 3, and the entire reach average are shown in Figure 3-17. Since 1970, the energy grade slope has increased dramatically. This suggests that the velocity is increasing, as supported by the geometry change and the HEC-RAS results in Section 3.3.4. As a function of the square of flow velocity, the friction slope is also expected to decrease with increasing *n* value (bed material coarsening) and thus decreasing sediment transport capacity.

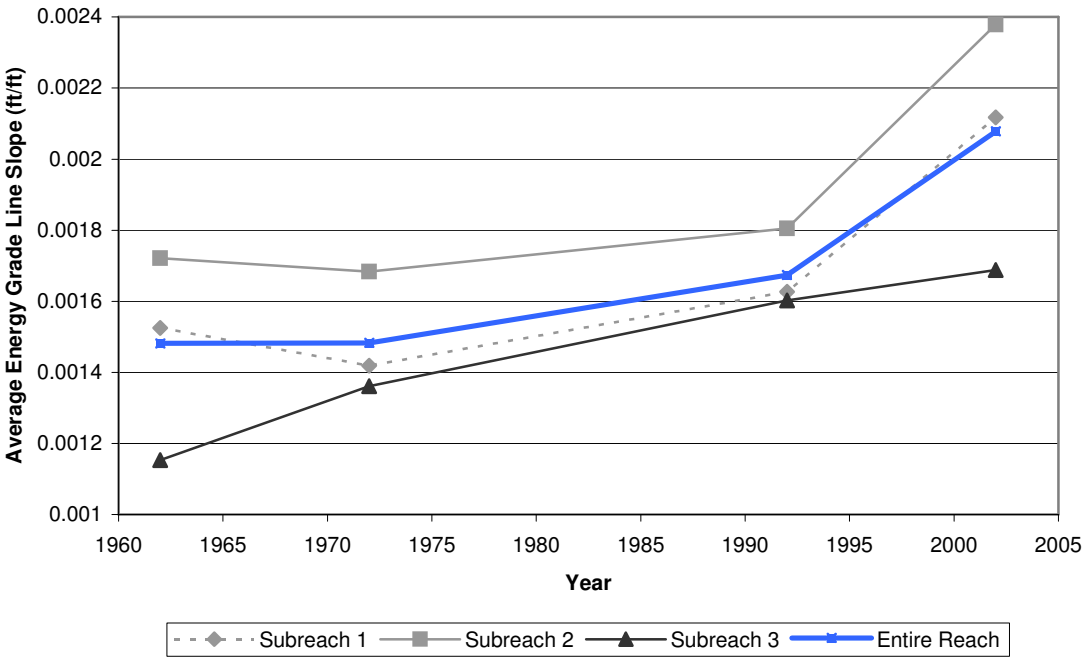

Figure 3-17 Time series of energy grade slope for each subreach and the average over the entire reach from HEC-RAS modeling results at Q=5,000 cfs.

Water Surface Slope

A time series of the water surface slope was generated using the HEC-RAS modeling results. Figure 3-18 displays the results for each subreach and an average for the entire reach. Subreaches 2 and 3 experienced increases in water surface slope over time, while subreach 1 saw a decreasing water surface slope until 1992. The average for the entire reach shows an increasing water surface slope over time.

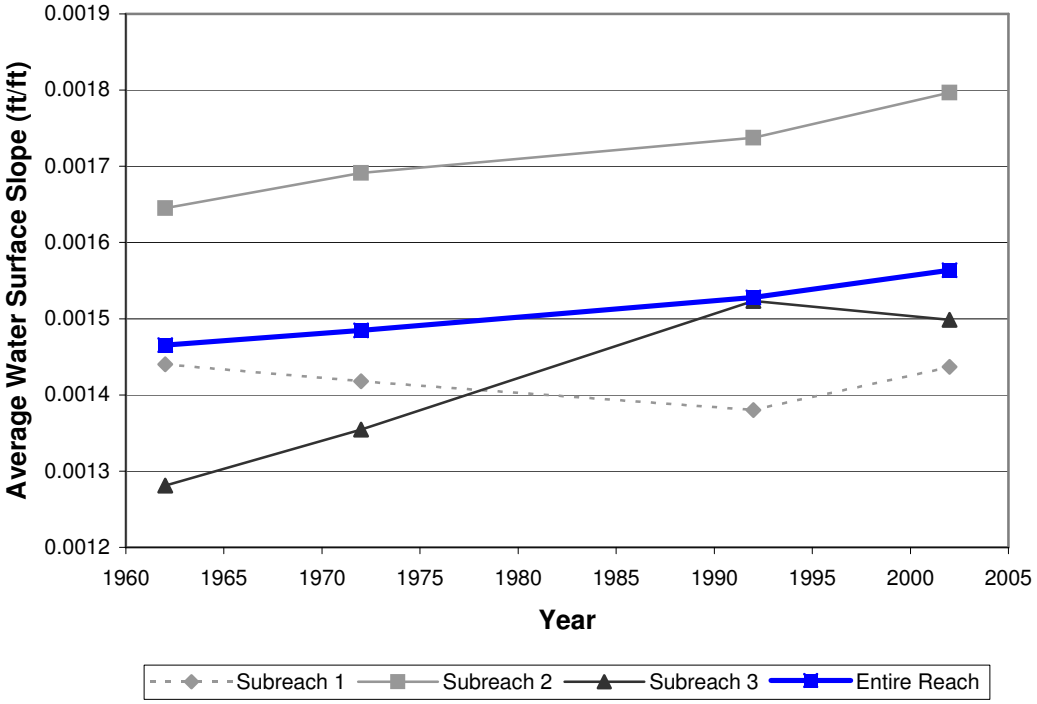

Figure 3-18 Time series of water surface slope (ft/ft) for subreaches 1, 2, and 3, and the entire Cochiti Dam reach from HEC-RAS modeling results at Q=5,000 cfs.

3.3.4 Channel Geometry

Hydraulic Geometry

Changes in channel geometry parameters such as velocity, cross-sectional area, depth, width, and wetted perimeter were calculated using HEC-RAS 3.1.3. The model was run using a channel forming discharge of 5,000 cfs. Average velocity, depth and Froude number have increasing trends over time, while area, wetted perimeter, and width/depth ratio show decreases over time. Subreach 1 consistently has the largest average velocity and depth values, and the smallest average area, wetted perimeter, and width/depth ration values. Subreach 2 tends to have the largest average area, width/depth ratio, and Froude number values, but the smallest average depth values. Subreach 3 tends to have median values for all parameters.

The increase in the average velocity, seen in Figure 3-19, may be due in part to the channel average depth increase (Figure 3-20). Note that the averaged depth increase from 1962

to 2002 is very small. While thalweg degradation was noted in Section 3.3.3, the channel is also experiencing increasing slope over the years, which would decrease the average depth in the channel. Since Froude number is proportional to velocity by a factor of $1/\sqrt{gD}$, where D is hydraulic depth, and velocity is increasing at a rate faster than the hydraulic depth, the Froude number increases over time as shown in Figure 3-21.

At the same time, cross-sectional flow area in each subreach is decreasing (Figure 3-22). Since the channel has transitioned from a braided to meandering planform, the channel width has decreased at a higher rate than the depth has increased. This transition has also decreased the wetted perimeter, seen in Figure 3-23. With increasing depth and decreasing width, the width-depth ratio would be expected to decrease, as shown in Figure 3-24.

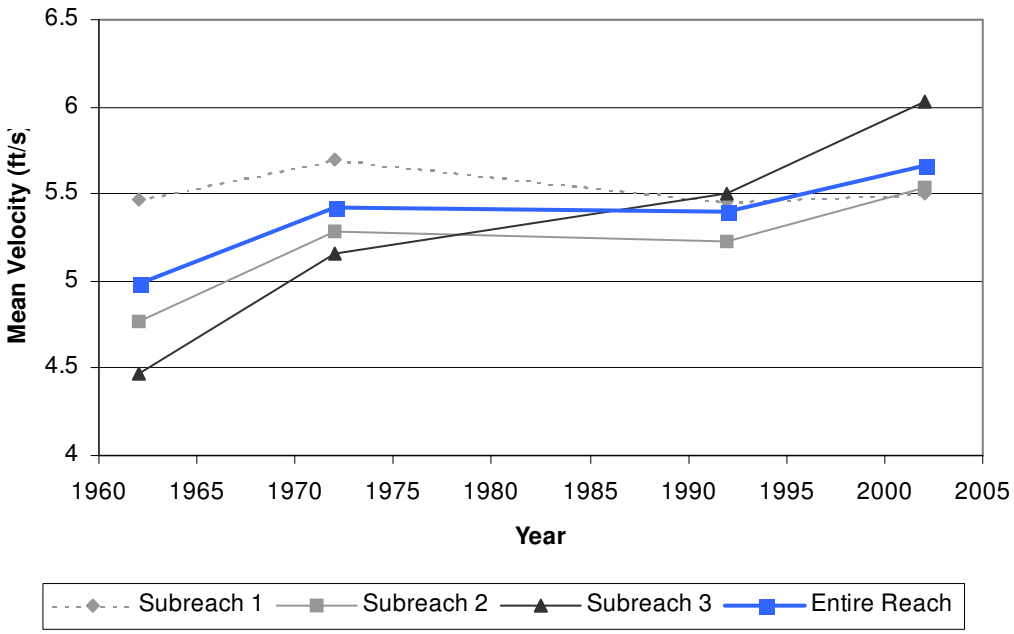

Figure 3-19 Average HEC-RAS results for average main channel velocity for Q=5,000 cfs.

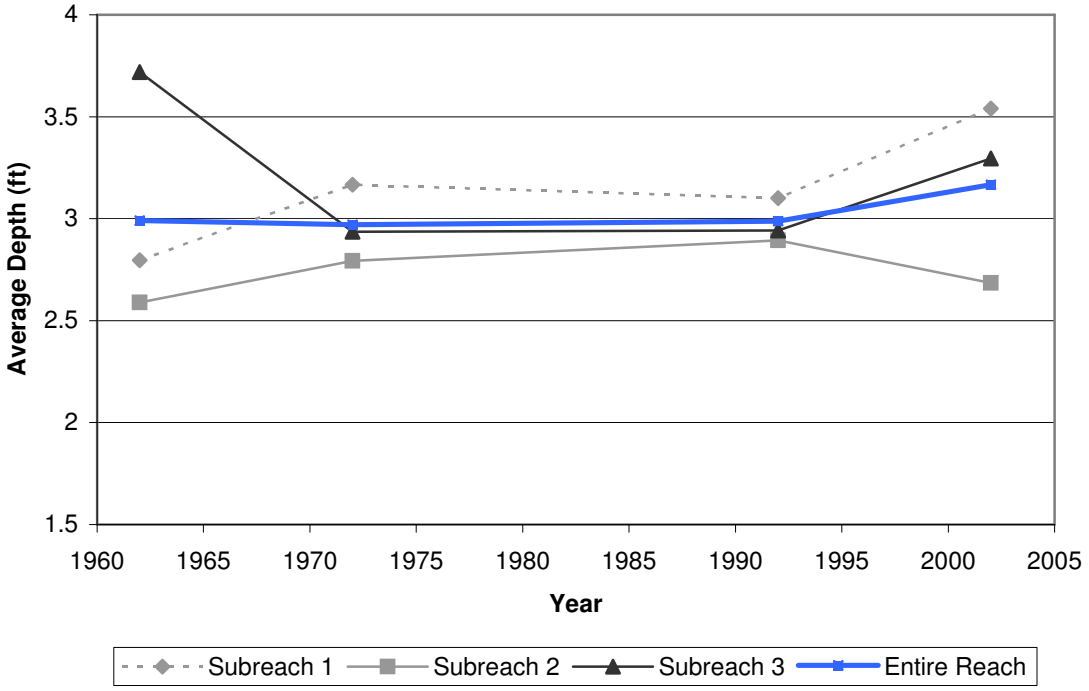

Figure 3-20 Average HEC-RAS results for average channel depth for Q=5,000 cfs

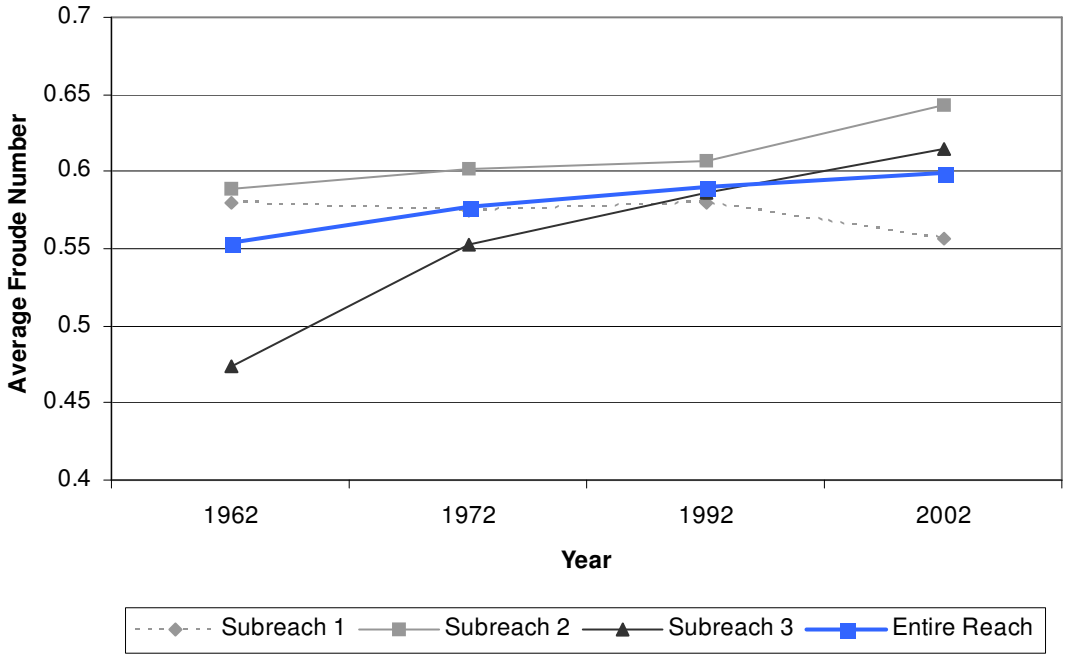

Figure 3-21 Average HEC-RAS results for average channel Froude number for Q=5,000 cfs

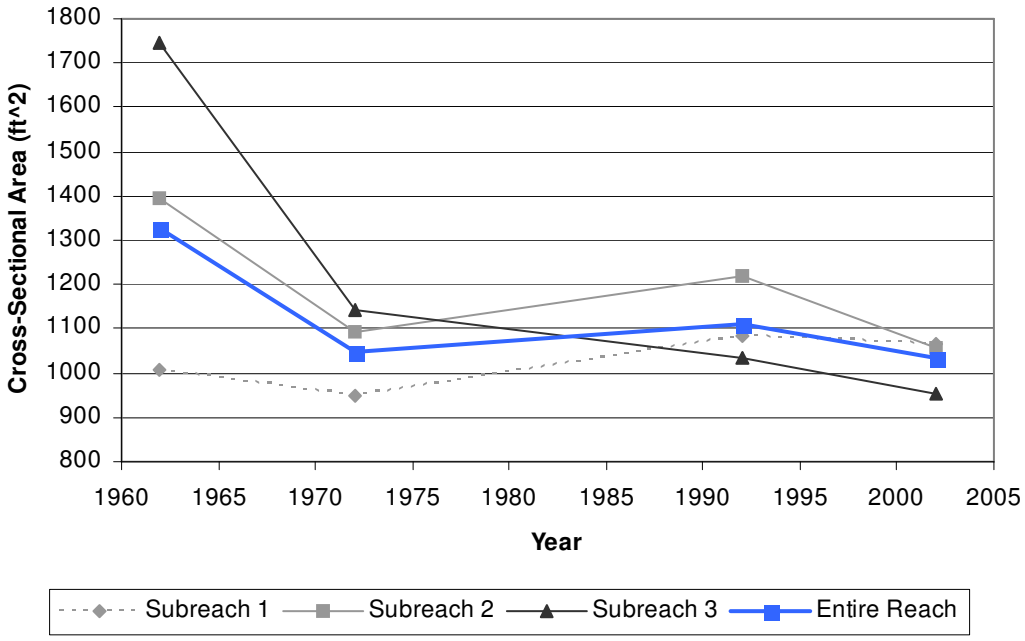

Figure 3-22 Average HEC-RAS results for average channel cross-sectional area for Q=5,000 cfs

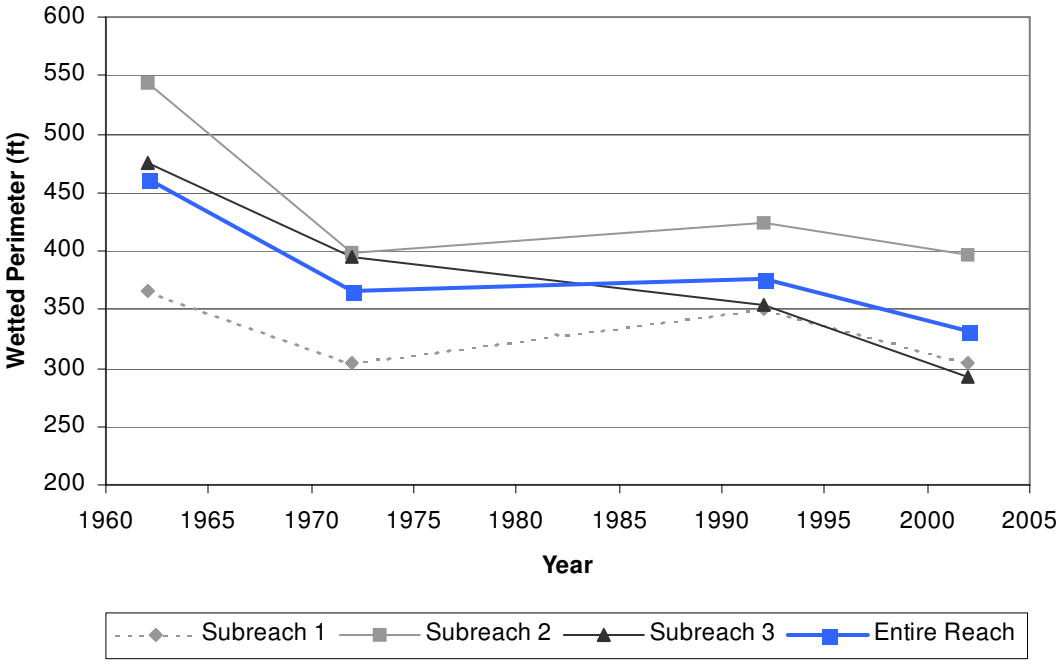

Figure 3-23 Average HEC-RAS results for average channel wetted perimeter for Q=5,000 cfs

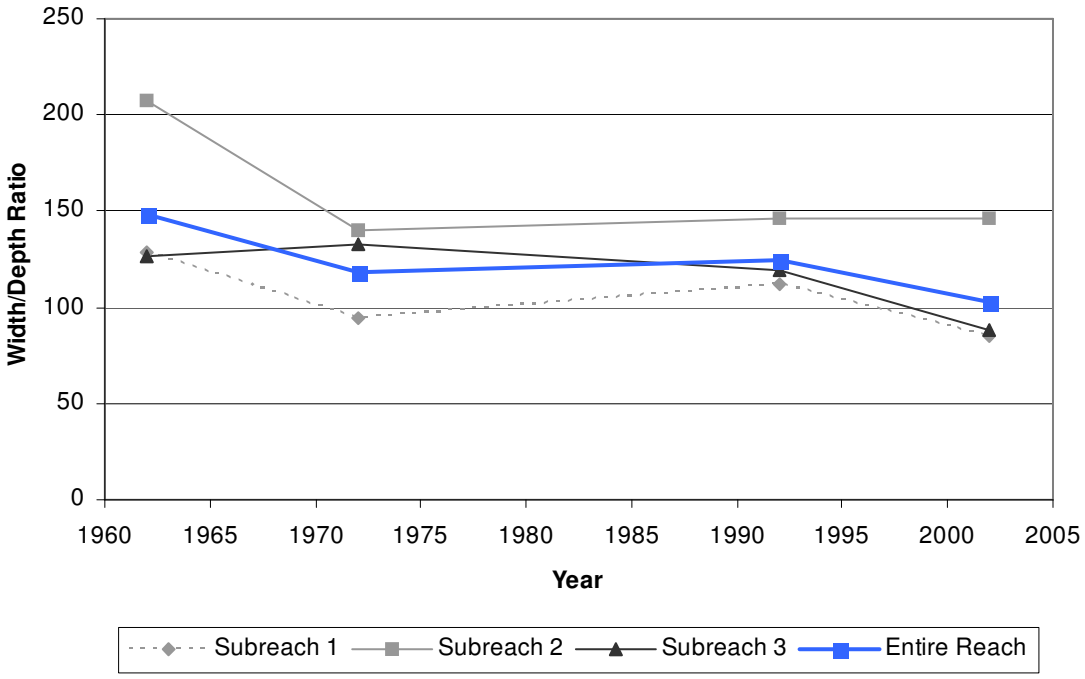

Figure 3-24 Average HEC-RAS results for average channel width/depth ratio for Q=5,000 cfs

Width trends were determined through the use of ArcGIS 9 and the GIS coverages provided by the USBR in Denver. They also were determined from HEC-RAS modeling results under the channel forming 5,000 cfs flow. Figure 3-25 shows the decreasing trends in width, as determined by aerial photographs and topographical surveys in the form of GIS coverages. From 1918 to 1948, increases in width are apparent. After 1948, a dramatic decrease in width is evident for all reaches. The average width for the entire reach was cut in half over the period from 1948 to 1972. The width then remained fairly constant for the next decade, and began to slowly decrease again in the 1990s.

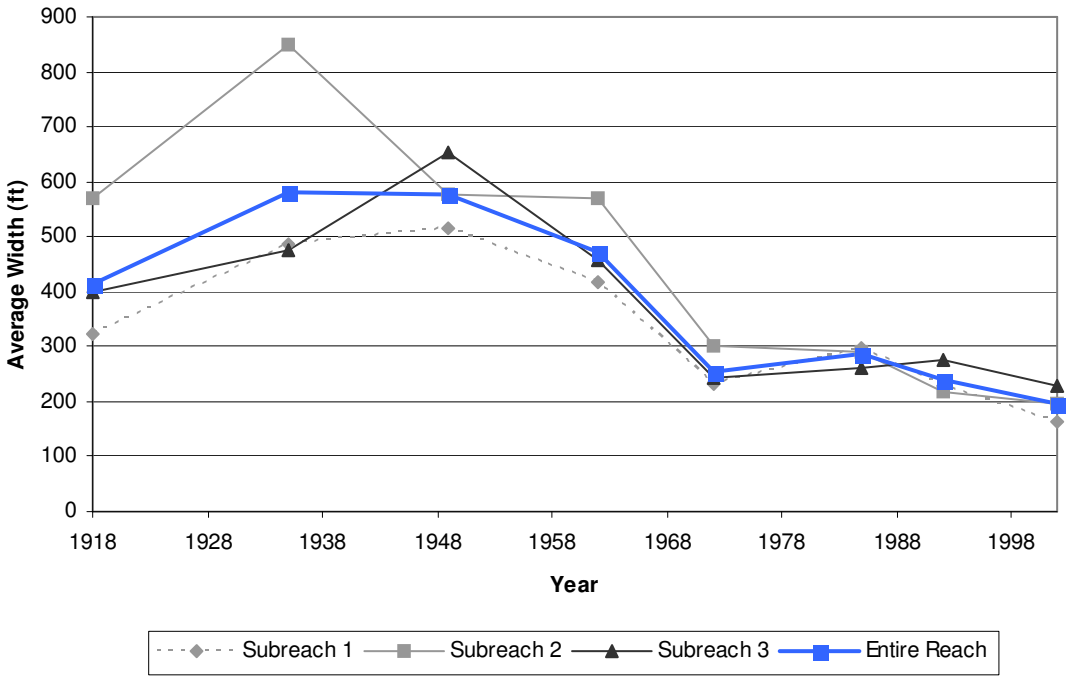

Figure 3-25 Active channel width from digitized aerial photos

The overall decrease in channel width is also shown through HEC-RAS modeling results. A plot of the results from 1962 to 2002 for the 5,000 cfs run is shown in Figure 3-26. This run shows similar results for temporal trends at each subreach. The HEC-RAS widths are larger than the results from the aerial photograph delineation, due to the large discharge routed through HEC-RAS. The change in width from 1962 to 2002 using both HEC-RAS and GIS is on the order of 150 to 200 feet.

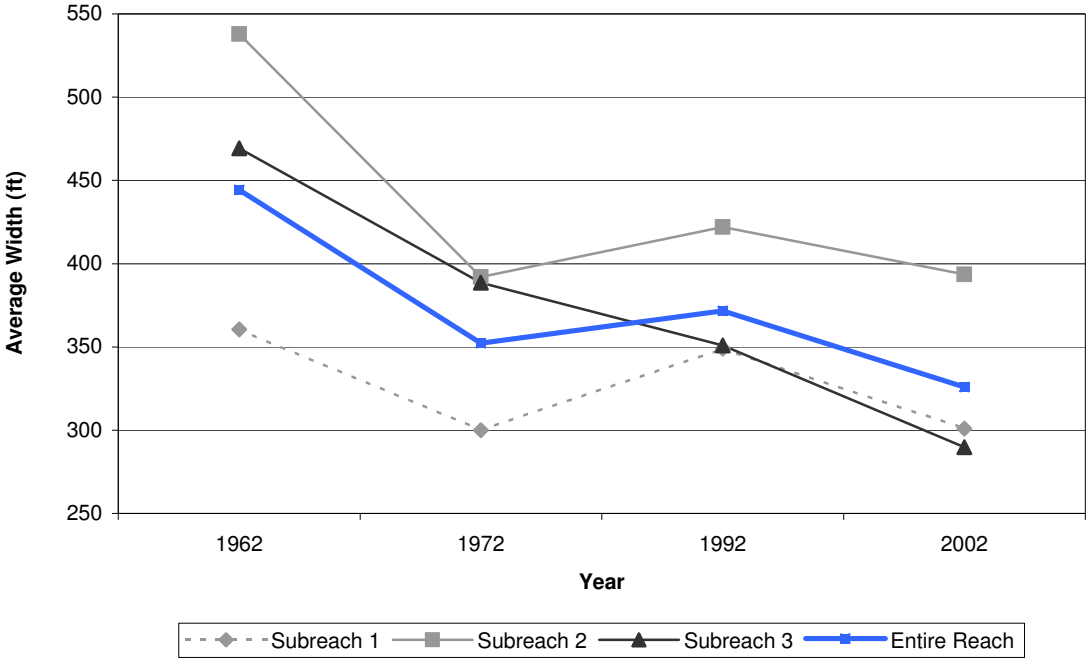

Figure 3-26 Average channel width from HEC-RAS results at Q=5,000 cfs

Overbank Flow/Channel Capacity

Most of the flow occurs in the main channel and not in the overbank region in each time period, according to HEC-RAS model runs at 5,000 cfs. The 2002 run is shown in Figure 3-27. For each year, subreach 2 tended to have a larger amount of overbank flow in the area of CO-4. This may be a partial justification to the aggradational trends seen in this reach. As overbank flow occurs, the velocity of the flow decreases and sediment deposits. This may be an area of increased overbank activity, and thus a sediment deposition area. However, overbank flow will not be taken into account when calculating sediment transport in the reach because most transport occurs in the main channel.

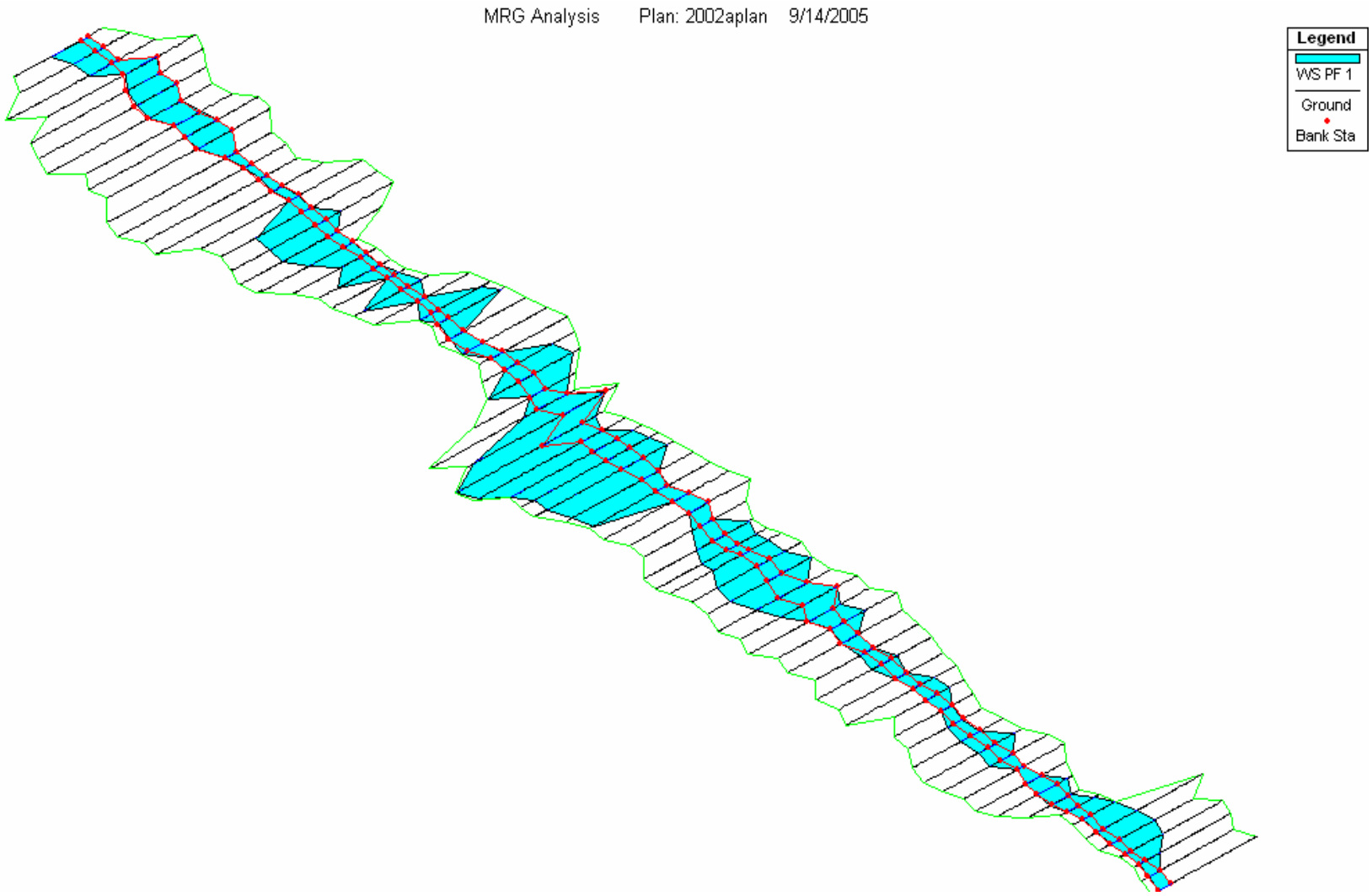

Figure 3-27 HEC-RAS aerial view of Cochiti Dam reach at 5,000 cfs.
A large overbank area occurs in subreach 2. The black lines represent the agg/deg cross-sections defining the reach.

3.3.5 Sediment

Bed Material

The median grain size for each subreach was determined for the available years using data taken at CO-lines. CO-lines 2 through 8 provided sporadic grain size distribution data. CO-lines 3, 5, and 8 were the most complete sets of data and were chosen to represent subreaches 1, 2, and 3 respectively. Average values for each cross-section were computed using all measurements taken.

Table 3-11 summarizes the results of the bed material analysis. The grain size changes over time are shown in Figure 3-28. In 1970, just before the installation of the Cochiti Dam, grain sizes for all reaches were fine to medium sand. The bed armored over time to produce d_{50} values indicating coarse or very coarse gravel by 1998.

Galisteo Creek enters the Middle Rio Grande at the downstream boundary of the Cochiti Dam reach. This tributary will influence the grain size distribution and d_{50} values downstream in the Galisteo reach.

	d_{50} bed material type					
	1970	1972	1975	1980	1992	1998
subreach 1	medium sand	fine sand	medium sand	medium gravel	very coarse gravel	coarse gravel
subreach 2	fine sand	fine sand	very coarse sand	coarse gravel	medium gravel	very coarse gravel
subreach 3	medium sand	medium sand	medium sand	very coarse sand	very coarse gravel	coarse gravel
total reach	medium sand	medium sand	very fine gravel	medium gravel	very coarse gravel	coarse gravel

Table 3-11 Median grain sizes in subreaches 1, 2, 3, and the total reach for selected dates

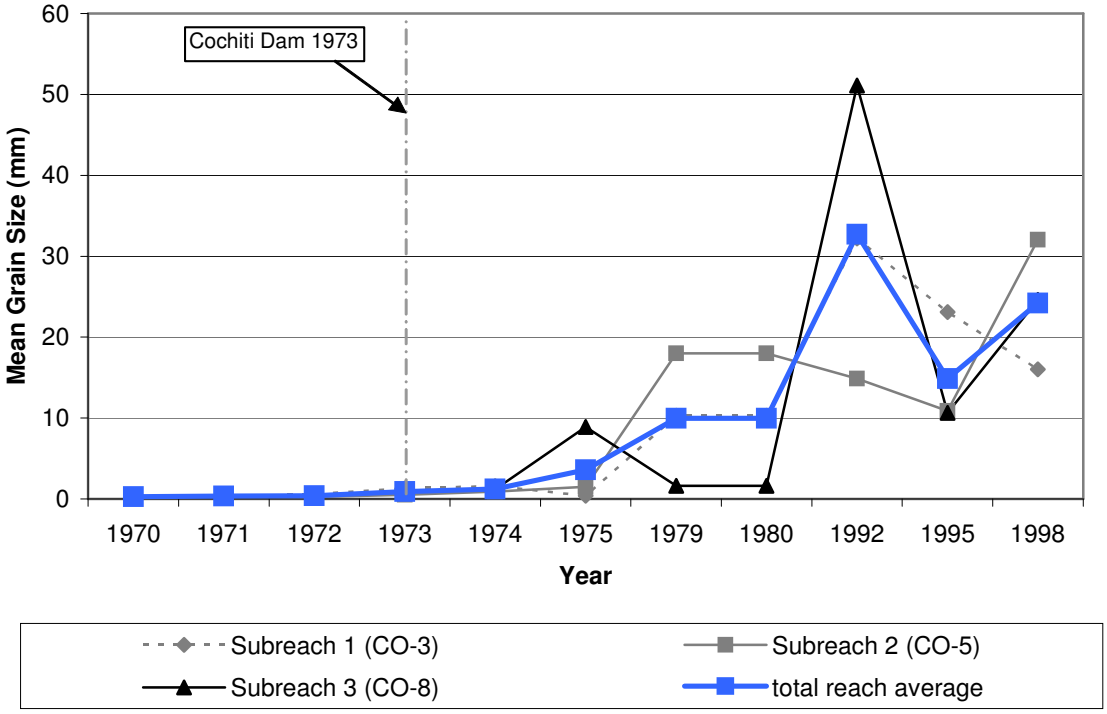

Figure 3-28 Median grain size (d_{50}) for each subreach

Figure 3-29 displays the particle size distribution for each subreach and the entire Cochiti Dam reach in 1972. The particle sizes steadily increase with distance downstream. Note that particle sizes for subreach 3 are smaller than those from subreaches 2 and 1. This may be due in part to the proximity of these range-lines to the confluence with Galisteo Creek and the large sand and silt input from that tributary.

The 1998 particle size distributions are shown in the next figure, Figure 3-30. Again, subreach 3 has smaller sediment sizes than subreach 2, and the overall sizes of the sediments have increased since 1972. The bed seems to have armored more upstream, closer to the dam, than downstream. The average d_{50} for 1998 is near 20 mm while the 1972 d_{50} is less than 1.

Average particle size distributions for each subreach are available in Appendix D. Data was taken during the fall months for each of the years. Bed material data has not been taken on this part of the Pueblo de Cochiti Nation since 1998.

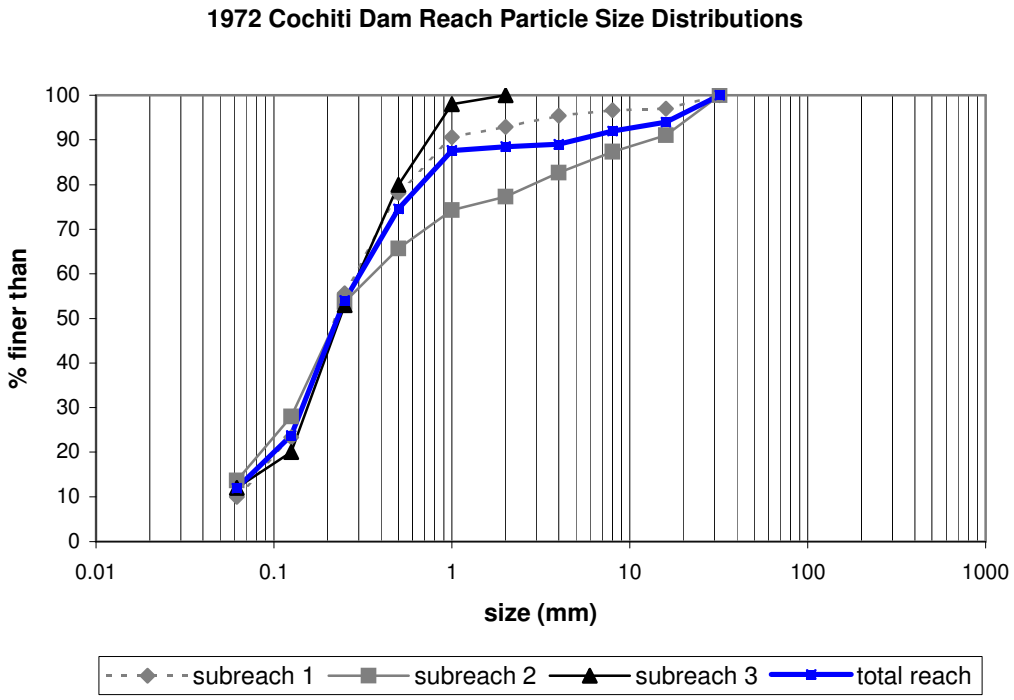

Figure 3-29 1972 plot of particle size distribution for entire reach

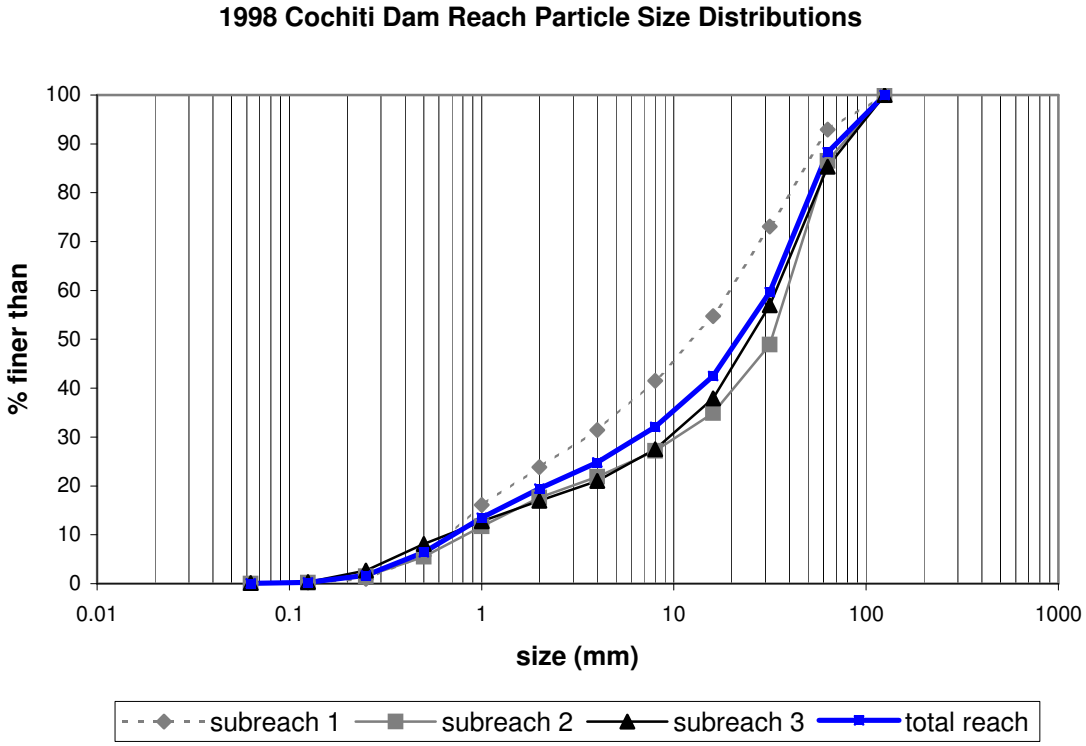

Figure 3-30 1998 particle size distribution for Cochiti Dam Reach

3.3 Suspended Sediment and Water History

3.3.1 Methods

Single and double-mass curves were generated to analyze water and sediment flow trends over the past several decades in the Cochiti Dam reach. Suspended sediment data for the Cochiti gage was limited, so a detailed sediment budget analysis could not be done.

The following curves were developed for the Cochiti gage:

- Mass curve of water discharge (acre-feet/year) from 1931 to 2004
- Mass curve of sediment discharge (tons/year) from 1955-1988
- Double mass curve with water and sediment discharge for trends in sediment concentration (mg/L) from 1955-1988

The slopes of each curve and the time periods of breaks were also estimated.

3.3.2 Single Mass Curve Results

Discharge Mass Curve

The discharge mass curve for the USGS gage below Cochiti Dam is shown in Figure 3-31. Before the dam, the USGS gage was located just upstream in what is now Cochiti Lake. After the dam, the gage was moved to the outlet of the dam. The data is plotted as one continuous data set. A results summary follows in Table 3-12. The first period of time, from 1931 to 1949 has an average volumetric discharge of 1.2-million acre-ft per year. From 1950 to 1978, the discharge rates level off slightly to 770,000 acre-ft per year. A drier period is apparent during this time (refer to Figure 2-7). After 1979, however, the discharge rates increase again to 1.1-million acre-ft per year.

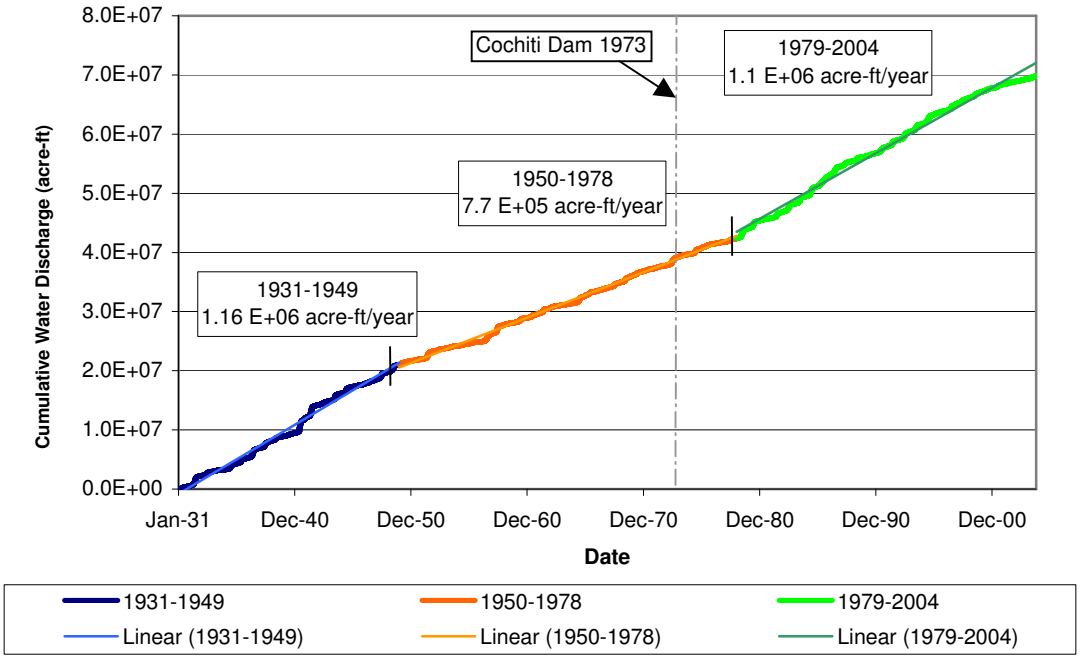

Figure 3-31 Discharge mass curve at Cochiti Dam gage (1931-2004)

Time Period	*Average Water Discharge per year (acre-ft/year)*
1931-1949	1.2 E+06
1950-1978	0.77 E+06
1979-2004	1.1 E+06

Table 3-12 Summary of discharge mass slope breaks at Cochiti Dam (1931-2004)

Suspended Sediment Mass Curve

Suspended sediment data for Cochiti gage, which only existed after the installation of Cochiti dam, recorded sediment data until 1988. Pre-dam suspended sediment data for this reach has been estimated with data from the upstream Otowi gaging station (Richard et al. 2001).

Up until the construction of the dam, the Cochiti Dam reach had a fairly large input flux of sediment each year. Data from the Otowi gage averaged 2.4 million tons per year flowing into the reach. After the dam, the input decreased dramatically to just over 50,000 tons per year. If the Cochiti Dam has a trap efficiency of 87% (USACE 2005), the expected average sediment

discharge after the dam would be 312,000 tons per year. This figure is over 6 times the average from recorded data at the Cochiti dam gage. Judging from the data available for this report, the estimated trap efficiency of Cochiti Dam is closer to 98%. Figure 3-32 displays the single mass curve and Table 3-13 summarizes the results.

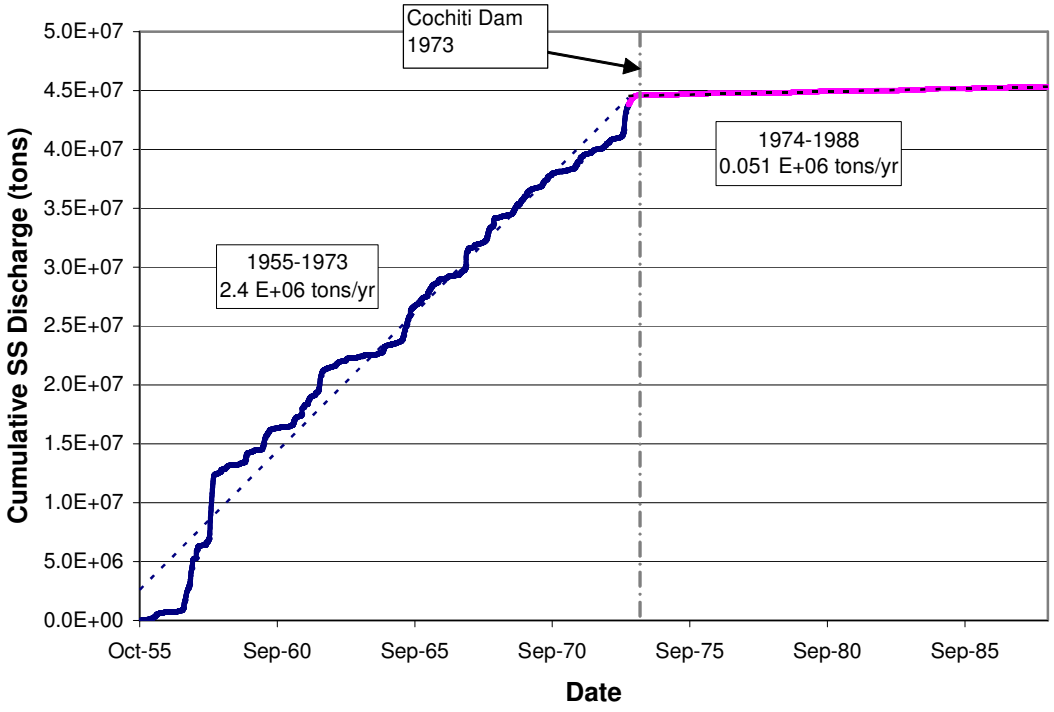

Figure 3-32 Suspended sediment mass curve at Otowi gage (1955-1974) and Cochiti gage (1975-1988)

Time Period	*Average Suspended Sediment Discharge (tons/year)*
1955-1973	2.4 E+06
1974-1988	0.051 E+06

Table 3-13 Summary of suspended sediment concentrations at Otowi and Cochiti gages (1955-1988)

3.3.3 Double Mass Curve Results

The double mass curve of cumulative discharge (acre-ft) versus cumulative sediment discharge (tons) is shown in Figure 3-33 and a summary table is shown in Table 3-14. The figure shows higher concentrations of suspended sediment from 1955 to 1973 with an average concentration of 2200 mg/L and a yearly accumulation of 3 tons/acre-ft of sediment. The pre-

dam data is from the Otowi gage. After 1973, a clear drop in sediment concentration is visible, with a concentration less than 2% of its original. The yearly accumulation of sediment dropped to 0.05 tons/acre-ft and the concentration dropped to 38 mg/L.

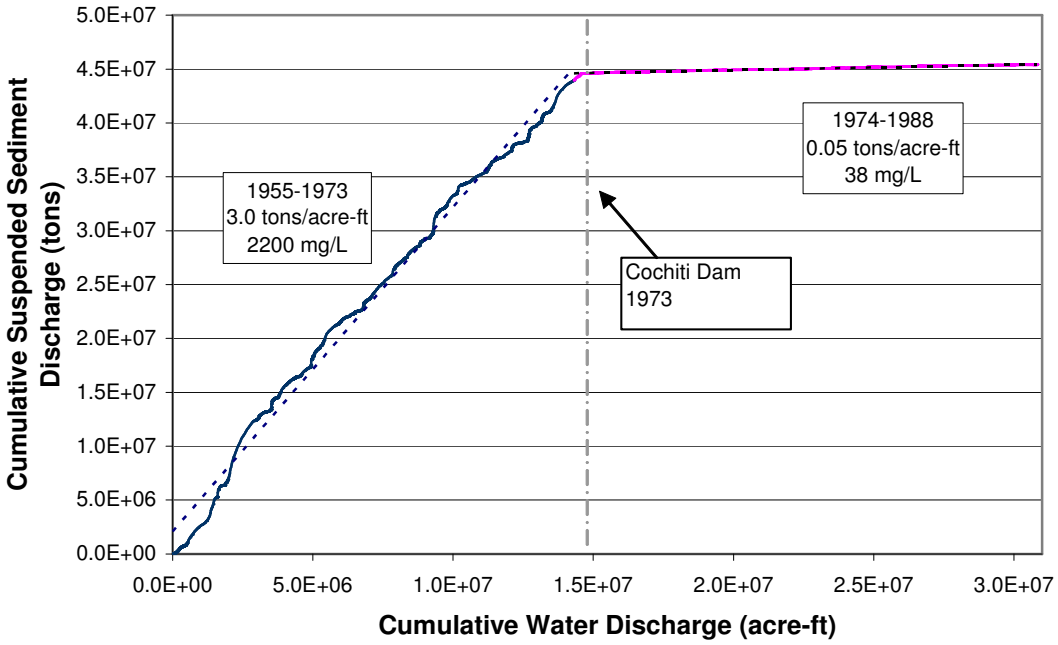

Figure 3-33 Double mass curve of discharge and suspended sediment for Cochiti Dam reach using Otowi (1955-1974) and Cochiti (1974-1988) gage data

	Concentration	
Time Period	*tons/acre-ft*	*mg/L*
1955-1973	3.0	2200
1974-1988	0.05	38

Table 3-14 Summary of suspended sediment concentrations at Cochiti Dam reach using Otowi (1955-1974) and Cochiti (1974-1988) gage data

Chapter 4: Equilibrium State Predictors

4.1 Introduction

Equilibrium state predictors were used on the Cochiti Dam reach to estimate potential future conditions. Analyses were done using hydraulic geometry methods, equilibrium width and slope methods, regime equations, empirical equations, and stable channel analysis programs to determine the equilibrium state of the reach and the direction in which the system is moving. Appendix F contains detailed methods and results from the Stable Channel Analysis run on the Cochiti Dam reach.

Mackin (1948) describes an equilibrium, or "graded" channel as "…one in which, over a period of years, slope is delicately adjusted to provide, with available discharge and with prevailing channel characteristics, just the velocity required for the transportation of the load supplied from the drainage basin. The graded stream is a system in equilibrium." A graded stream does not have to be fixed in space or time, but is allowed to vary around some mean value in response to extreme events. However, as long as the recovery time (time required for the system to return to equilibrium conditions) is shorter than the recurrence interval (the return period for the extreme event), then the stream is considered to be dynamically stable. This is called "dynamic equilibrium" or "dynamic stability" (Watson et al. 2005). Figure 4-1 is a plot of the concept of dynamic equilibrium. The system shown is a "negative feedback" system, meaning it minimizes variance around $\Delta_{eq}=0$ with increasing time.

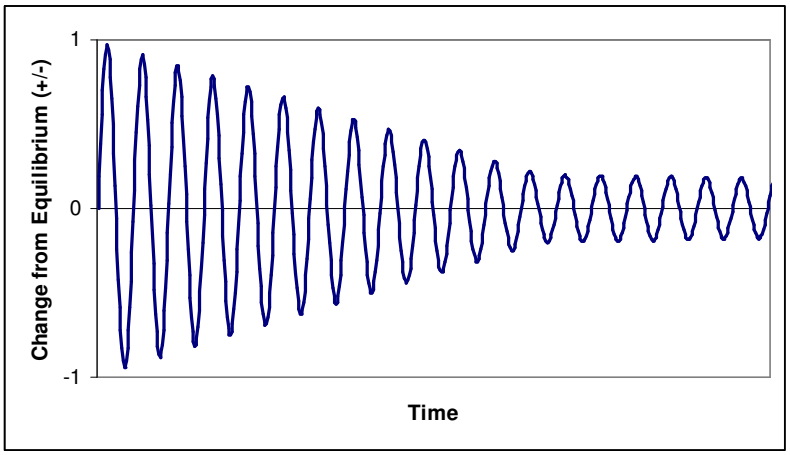

Figure 4-1 Graphical interpretation of concept of dynamic equilibrium.

Lane's 1955 balance model applies to the concept of dynamic equilibrium. Lane's balance, $QS \sim Q_s D_{50}$, shows how a change in any of the four driving variables in a stream (discharge, slope, median grain size, and sediment discharge) produces a response in the others to tend towards equilibrium. Figure 4-2 displays this concept.

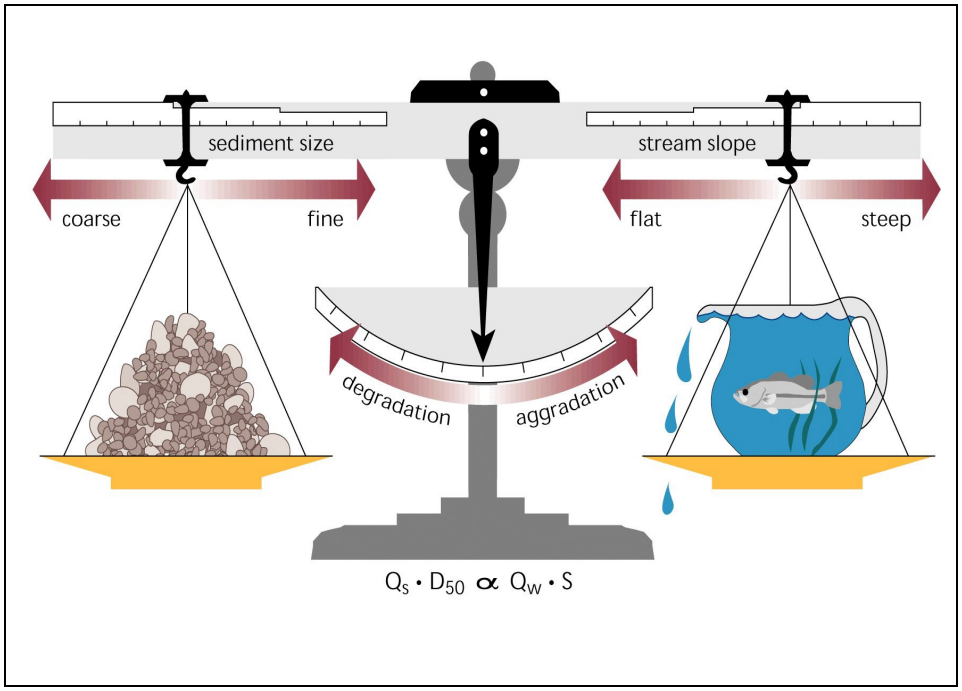

Figure 4-2 Lane's balance (1955)

Lane's balance reaffirms Mackin's statement of graded stream response. It shows that a dynamically stable stream has adjusted these four variables in order to produce neither

aggradation nor degradation in the stream, effectively transporting all available sediment through the reach. In actuality, the situation of dynamic stability, when sediment input exactly matches output, is a special case that won't persist over long periods of time and that may only occur in subreaches of a system (Watson et al. 2005).

Thus, in the Middle Rio Grande, major events such as floods, droughts, construction, or other temporary variations may affect the channel regime. These local instabilities are the stream's response to the varying hydrologic inputs. This chapter will assess whether or not equilibrium conditions can potentially exist, and if so, it will attempt to quantify these conditions.

4.2 Methods

4.2.1 Sediment Transport Analysis

The sediment load exiting Cochiti Dam is quite small (refer to Figure 3-31). After 1973, the suspended sediment discharge out of the dam was only 0.05 tons/acre-ft (38 mg/L), or approximately 2% of the suspended sediment discharging at the Otowi gage. This amount was also approximately 9% of the sediment discharge occurring at the same time period at the Bernalillo gage. The sediment discharge from Cochiti Dam may be assumed to be entirely washload, due to the large settling basin upstream (Cochiti Reservoir) and the concrete footing at the base of the dam, which prevents initial bedload transport. Since the sediment estimated from Figure 3-33 is very small, the sediment discharge entering the reach is assumed to average 38 mg/L of washload. The equilibrium slope was calculated using the program developed by Claudia Leon (2003) which estimates equilibrium slope for a reach with varying widths. This will be discussed in the Equilbrium Channel Slope Analysis section.

Channel transport capacities for each subreach in the Cochiti Reach were estimated for 1962, 1972, 1992, and 2002 using the stable channel design tool in HEC-RAS 3.1.3. This program utilized several different sediment transport equations: Laursen (1958), Engelund and

Hansen (1967), Ackers and White (1973), Yang (sand-1973, gravel-1984), and Toffaleti (1968) (Stevens et al. 1989, Julien 1995, USACE 2002). Based on the gradation of bed material for 1962 and 1972, most of the bed material transport relationships are appropriate. In 1992 and 2002, most of the subreaches contained medium to coarse gravel, making many of the bed material transport relationships inadequate. Different equations based on type of calculation and bed material type are shown in Table 4-1. The assumptions and limitations of each model used in the HEC-RAS run are described in Appendix E.

	1962-1972		1992-2002	
	BML	BL	BML	BL
Ackers and White (1973)	X		X	
Einstein BL (1950)		X		X
Einstein BML (1950)	X			
Engelund and Hansen (1967)	X			
Kalinske		X		X
Laursen (1958)	X			
Meyer-Peter and Müller (1948)		X		X
Rottner		X		X
Schoklitsch (1934)		X		X
Toffaleti (1968)	X			
Yang - gravel (1984)			X	
Yang - sand (1973)	X			

Table 4-1 Appropriateness of bedload and bed-material load transport equations (Stevens et al. 1989)

The transport capacity equations are functions of the channel slope. The transport capacity was estimated over the length of the entire reach, broken by 15 agg/deg lines spaced 2500 feet apart. This was the optimum spatial step HEC-RAS could use with minimal numerical instability. Input values were taken from HEC-RAS runs at 5,000 cfs from chapter 3. Width, depth, velocity, and water surface slope varied over each cross-section. Particle size distribution data for the channel bed were taken from the particle size distributions in Chapter 3 and Appendix D.

4.2.2 Equilibrium Channel Slope Analysis

The equilibrium slope of the channel was estimated using the program created by Claudia Leon (2003) for the Bosque del Apache reach of the Middle Rio Grande. This program utilizes discharge, temperature, mean bed elevation, width, and sediment data to estimate the equilibrium slope, time to equilibrium, aggradation, and degradation of the channel bed under certain specified conditions. The program assumes that the width of the channel remains fixed over time, although it may vary spatially.

The program was run using mean bed elevation, bed slope and width data from the three subreaches from 1972, daily discharge and temperature data from the USGS from 1970 to 2004, and median grain sizes from 1972.

In addition, depth to armoring was calculated to provide a base elevation in the reach to which scouring was possible for each of the three subreaches. This was calculated by estimating the minimum grain size at the beginning of motion, d_{sc}, in each subreach. The scour depth, Δz, was then calculated based on the percent-finer value of each size claste at each subreach in each year. Next, a maximum peak flow scouring was calculated. This result was added to the scour calculated from 1972 to 1998 to estimate the total depth to armoring that is possible in the reach. Each subreach retained a maximum scour depth during the model run to prevent infinite degradation.

4.2.3 Hydraulic Geometry

Hydraulic geometry equations were obtained from several different sources. These equations were developed to estimate the characteristics of stable channels under channel forming discharge. These methods may incorporate bed material size, channel slope, sediment concentration, or a combination of these. The equations were developed for simplified situations, such as man-made canals or single-thread channels. Unless specified differently, the variable Q

refers to bankfull (channel-forming) discharge. In the case of the Cochiti Dam reach, Q is equal to 5,000 cfs (the two-year return flow).

The methods used in the estimation of equilibrium width are described below.

Leopold and Maddock (1953) developed empirical equations, which relate width, depth, and velocity to discharge with power functions.

$$W = aQ^{b} \quad (4.1a)$$

$$D = cQ^{e} \quad (4.1b)$$

$$V = kQ^{m} \quad (4.1c)$$

In this set of equations, ack=1 while b+e+m=1, and b, e, and m are usually equal to 0.5, 0.4, and 0.1, respectively, regardless of stage, discharge, sediment characteristics, or flow regime (ASCE Task Committee on Hydraulics 1998).

Julien and Wargadalam (1995) developed semi-theoretical regime hydraulic geometry equations based on continuity, resistance, sediment transport, and secondary flow.

$$D = 0.200 Q^{\frac{2}{6m+5}} d_s^{\frac{6m}{6m+5}} S^{-\frac{1}{6m+5}} \quad (4.2a)$$

$$W = 1.330 Q^{\frac{4m+2}{6m+5}} d_s^{-\frac{4m}{6m+5}} S^{-\frac{2m+1}{6m+5}} \quad (4.2b)$$

$$V = 3.758 Q^{\frac{2m+1}{6m+5}} d_s^{-\frac{2m}{6m+5}} S^{\frac{2m+2}{6m+5}} \quad (4.2c)$$

$$\tau_* = 0.121 Q^{\frac{2}{6m+5}} d_s^{-\frac{5}{6m+5}} S^{\frac{6m+4}{6m+5}} \quad (4.2d)$$

$$m = \frac{1}{\ln(\frac{12.2D}{d_s})} \quad (4.2e)$$

In these equations, D stands for average depth (m), Q is discharge (cms), W is average width (m), v is average one-dimensional velocity (m/s), d_s is median grain size (m), and τ_* is shear stress. The Julien-Wargadalam equations were also used to estimate a stable slope for the reach using 1998 conditions.

Simons & Albertson (1963), developed equations from analysis of Indian and American canals. Five data sets were used in the development of the equations. Simons and Bender's data were collected from irrigation canals in Wyoming, Colorado and Nebraska during the summers of 1953 and 1954 and consisted of cohesive and non-cohesive bank material. The USBR data were collected from canals in the San Luis Valley of Colorado. This data consisted of coarse non-cohesive material. Indian canal data were collected from the Punjab and Sind canals. The average diameter of the bed material is approximately 0.43 mm for the Punjab canals and between 0.0346 mm to 0.1642 mm for the Sind canals. The Imperial Valley canal data were collected in the Imperial Valley canal systems. Bed and bank conditions of these canals are similar to the Punjab, Sind and Simons and Bender canals (Simons et al. 1963).

The relationship between wetted perimeter (P) and water discharge is represented in Figure 4-3. Once the wetted perimeter is obtained from Figure 4-1, the averaged channel width is estimated using Figure 4-4.

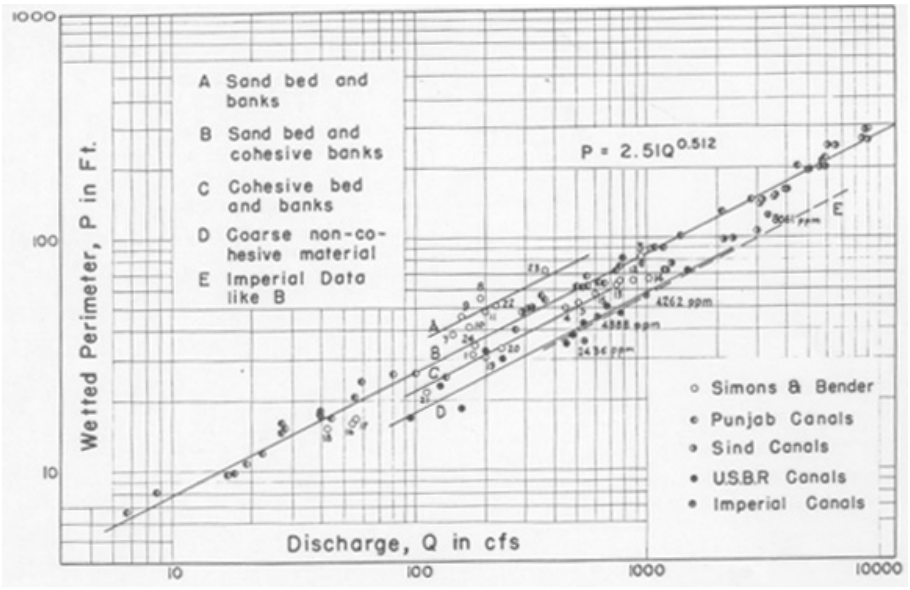

Figure 4-3 Variation of wetted perimeter *P* with discharge *Q* and type of channel (after Simons and Albertson 1963)

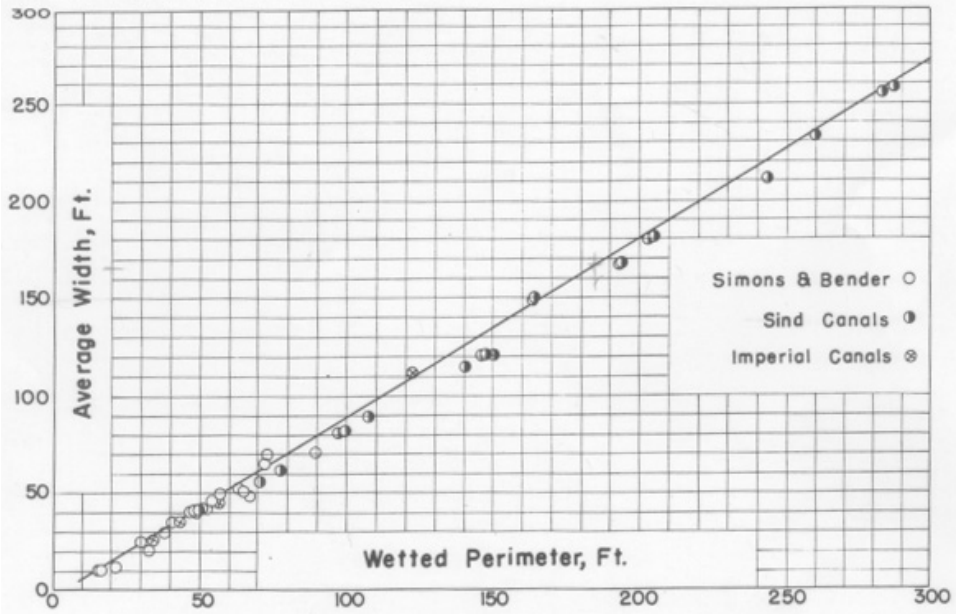

Figure 4-4 Variation of average width *W* with wetted perimeter *P* (after Simons and Albertson 1963)

Blench (1957) developed regime equations from flume data. The equations account for the differences in bed and bank material by means of a bed and a side factor (F_s) (Thorne et al. 1997). The range of application of Blench's equation is (Thorne et al. 1997):

Discharge (Q): 0.03-2800 m^3/s

Sediment concentration (c): 30-100 ppm

Bed material size (d_s): 0.1-0.6 mm

Bank material type: cohesive

Bedforms: ripples – dunes

Planform: straight

Profile: uniform

The size factor is defined by $F_s = V^3/b$, where b is defined as the breadth, that multiplied by the mean depth d, gives the area of a mean trapezoidal section, and V is the mean flow velocity (Blench 1957).

The regime equation for channel width (W) is [from Wargadalam (1993)]:

$$W(ft) = \left(\frac{9.6(1 + 0.012c)}{F_s} \right)^{\frac{1}{2}} d^{\frac{1}{4}} Q^{\frac{1}{2}} \qquad (4.3)$$

Where,

c = sediment load concentration (ppm),

$d = d_{50}$ (mm), and

F_s = 0.1 for slight cohesiveness of banks

Lacey [(1930-1958), from Wargadalam (1993)] developed the equation

$$P(\text{ft}) = 2.667Q^{0.5} \qquad (4.4)$$

Where,

P = wetted perimeter (feet)

Q = water discharge (ft^3/s)

Klaassen-Vermeer (1988) developed a width relationship for braided rivers based on work on the Jamuna River in Bangladesh:

$$W(\text{m}) = 16.1Q^{0.53} \qquad (4.5)$$

Where,

Q = water discharge (m^3/s)

Nouh (1988) developed regime equations from ephemeral channels located in the South and Southwest regions of Saudi Arabia. The equations provide information of channel dimensions under varying flash flood and sediment flow conditions in an extremely arid zone. The following regression equation was obtained for the channel width:

$$W(m) = 28.3\left(\frac{Q_{50}}{Q}\right)^{0.83} + 0.018(1+d)^{0.93} c^{1.25} \qquad (4.6)$$

Where,

Q_{50} = peak discharge for 50 yr. return period (m^3/s)

Q = annual mean discharge (m^3/s)

$d = d_{50}$ (mm)

c = mean suspended sediment concentration (kg/m^3).

Additionally, an empirical width-discharge specific to the Cochiti Dam reach was developed from digitized active channel widths from GIS coverages and the peak flows from 5 years prior to the survey date. Peak flows were obtained from the Rio Grande at Otowi gage for 1918 and Rio Grande at Cochiti Gage for the remaining years. The equation that results takes the form:

$$W = aQ^b \qquad (4.7)$$

Where,

W = active channel width (ft)

Q = peak discharge (cfs)

Table 4-2 contains the input data for the empirical width-discharge equations. This includes the averages of peak flows over the five years before the survey date, as well as the total average channel width for the entire Cochiti Dam reach for each year studied.

		1918	1935	1949	1962	1972	1985	1992	2001	2004
	Averaged 5-year peak flows (cfs)	11630	7232	7996	5546	3560	5958	4172	4252	2410
Total Width (ft)	subreach 1	323	487	515	419	232	299	227	165	160
	subreach 2	571	849	575	570	301	292	217	196	200
	subreach 3	400	477	655	458	244	263	276	229	240
	total reach	415	580	578	472	254	285	240	194	201

Table 4-2 Input data for empirical width-discharge relationship

Table 4-3 contains input data for the hydraulic geometry calculations. The peak discharges for the 50-year return period were taken from the Bullard and Lane (1993) report. The average suspended sediment concentration values were estimated from the double mass curve (Figure 4-3), which was developed from the Rio Grande at Otowi and the Rio Grande below Cochiti Dam gages. Note that since the suspended sediment data is reported only until 1988, the trend line resulting after Cochiti Dam (1973) was extrapolated to estimate data for 1992 and 2002 dates.

		Q (cfs)	Q50 (cfs)	d50 (mm)	So (ft/ft)	Avg C (ppm)
1962	subreach 1	5000	23500	0.21	0.0007	2200
	subreach 2	5000	23500	0.21	0.0008	2200
	subreach 3	5000	23500	0.21	0.0010	2200
	total reach	5000	23500	0.21	0.0008	2200
1972	subreach 1	5000	10000	0.21	0.0009	2200
	subreach 2	5000	10000	0.21	0.0009	2200
	subreach 3	5000	10000	0.24	0.0010	2200
	total reach	5000	10000	0.22	0.0009	2200
1992	subreach 1	5000	10000	1.38	0.0008	38
	subreach 2	5000	10000	1.09	0.0011	38
	subreach 3	5000	10000	5.73	0.0007	38
	total reach	5000	10000	2.73	0.0009	38
2002	subreach 1	5000	10000	15.425	0.0011	38
	subreach 2	5000	10000	11.29	0.0008	38
	subreach 3	5000	10000	1.2375	0.0008	38
	total reach	5000	10000	9.32	0.0008	38

Table 4-3 Input data for hydraulic geometry calculations

4.2.4 Equilibrium Channel Width

Williams and Wolman (1984) studied the downstream effects of dams on alluvial rivers. The method developed describes the changes in channel width with time using hyperbolic equations of the form:

$$(1/(W_t/W_i)) = C_1 + C_2\,(1/t) \qquad (4.8)$$

Where,

W_t/W_i = the relative change in channel width,

C_1 and C_2 = empirical coefficients, and

t = time in years after the onset of the particular channel change.

The relative change in channel width is equal to the ratio of the width at time t (W_t) to the initial width (W_i). Coefficients C_1 and C_2 may be functions of flow discharges and boundary materials.

Hyperbolic equations were fitted to the entire Cochiti Dam reach and to each subreach data set from 1949 to 2004. The time $t = 0$ was taken as 1949, when narrowing of the channel began. The data to which the hyperbolic regressions were applied are in Table 4-4.

	Reach	t (year)	1/t	W_i (ft)	W_t (ft)	$1/(W_t/W_i - 1)$
1949	subreach 1	31	0.0323	515		1.68
	subreach 2	31	0.0323	575		127
	subreach 3	31	0.0323	655		1.56
	total reach	31	0.0323	578		2.54
1962	subreach 1	44	0.0227		419	3.36
	subreach 2	44	0.0227		570	-1141
	subreach 3	44	0.0227		458	6.84
	total reach	44	0.0227		472	7.17
1972	subreach 1	54	0.0185		232	-3.55
	subreach 2	54	0.0185		301	-2.11
	subreach 3	54	0.0185		244	-2.56
	total reach	54	0.0185		254	-2.59
1985	subreach 1	67	0.0149		299	-13.7
	subreach 2	67	0.0149		292	-2.04
	subreach 3	67	0.0149		263	-2.93
	total reach	67	0.0149		285	-3.20
1992	subreach 1	74	0.0135		227	-3.36
	subreach 2	74	0.0135		217	-1.61
	subreach 3	74	0.0135		276	-3.22
	total reach	74	0.0135		240	-2.38
2001	subreach 1	83	0.0120		165	-2.04
	subreach 2	83	0.0120		196	-1.52
	subreach 3	83	0.0120		229	-2.35
	total reach	83	0.0120		194	-1.88
2004	subreach 1	86	0.0116		160	-1.98
	subreach 2	86	0.0116		200	-1.54
	subreach 3	86	0.0116		240	-2.51
	total reach	86	0.0116		201	-1.94

Table 4-4 Hyperbolic regression input data

Richard (2001) selected an exponential function to describe the changes in width with time of the Cochiti reach of the Rio Grande. The hypothesis of the model is that the magnitude of the slope of the width vs. time curve increases with deviation from the equilibrium width, W_e. The exponential function is:

$$W = W_e + (W_0 - W_e).\, e^{-k_1 t} \qquad (4.9)$$

Where,

k_1 = rate constant;

W_e = Equilibrium width toward which channel is moving (ft),

W_0 = Channel width (ft) at time t_0 (yrs), and

W = Channel width (ft) at time t (yrs).

Richard used three methods to estimate k_1 and W_e. The first method consists of empirically estimating the value of k_1 and W_e by plotting the width change rate vs. the width and generating a regression line. The rate constant, k_1, is the slope of the regression line and the intercept is $k_1 W_e$. The second method consists of using the empirically determined k-values from the first method and varying the equilibrium width values to produce a "best-fit" equation that minimized the sum-square error (SSE) between the predicted and observed widths. This method was developed in an effort to better estimate the equilibrium width. The third method consists of estimating the equilibrium width, W_e, using a hydraulic geometry equation. The k_1-value was determined by varying it until the SSE between the predicted and observed width was minimized.

In addition, a "Best Engineering Estimate" equation was estimated visually, as well as a least-squares regression. These were plotted in addition to Richard's method in an effort to develop a better fit to the data. The least squares fit was developed by taking the partial derivative of the exponential equation $W=(a-c)e^{(-bt)}+c$ with respect to each variable and setting them equal to zero. This produced three equations and three variables which were solved simultaneously.

4.3 Results

4.3.1 Sediment Transport Analysis

Sediment transport capacities were calculated for the Cochiti Dam reach using several methods in HEC-RAS. Assuming all suspended sediment discharge consists of washload when entering the reach, Figure 4-5 shows the sediment rating curve for suspended sediment

(washload) discharge for summer and winter at Cochiti Dam for the entire period of record (1974 to 1988).

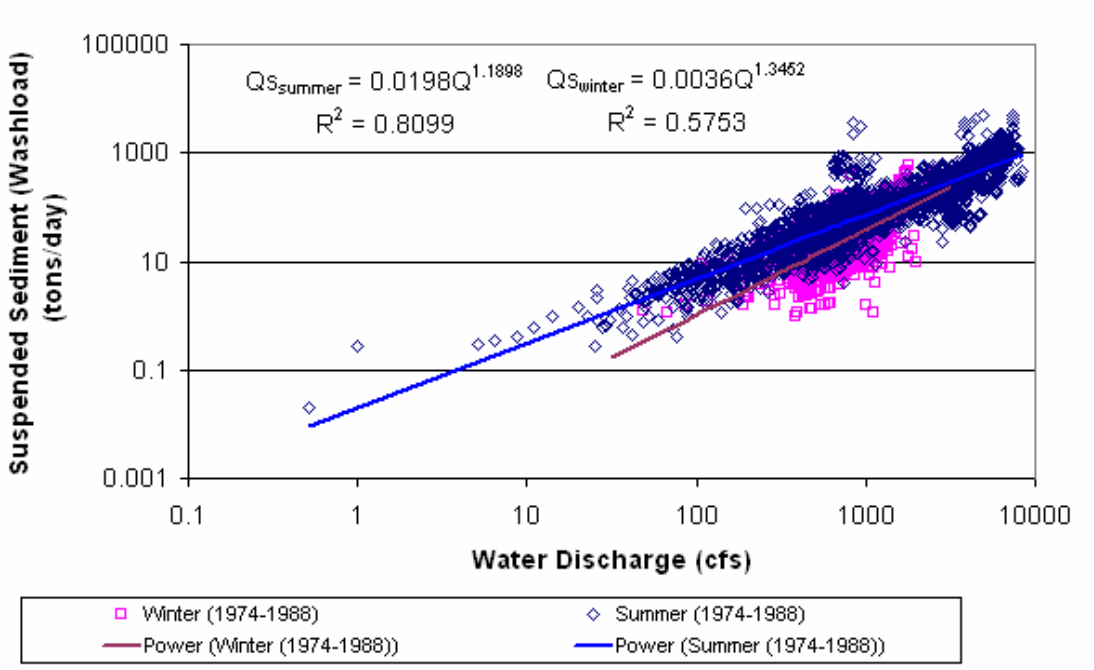

Figure 4-5 Cochiti Dam gage sediment rating curve for summer and winter months from 1974 to 1988.

The sediment transport capacities were calculated using HEC-RAS 3.1.3, as described in the methods. The width, depth, water surface slope, bank roughness, valley slope, and cross-sectional geometries were taken directly from the HEC-RAS runs in Chapter 3 at 5,000 cfs. A constant sediment concentration of 32 mg/L (140 tons/day) was used in the input data for the 1992 and 2002 runs. This concentration corresponds to 5,000 cfs of flow after the installation of the Cochiti Dam. For 1962 and 1972 (pre-dam conditions), the 5,000 cfs discharge corresponded to a larger sediment concentration of 2000 mg/L (6575 tons/day).

Transport capacities varied from year to year but were with in an order of magnitude of each other. For 1962 and 1972, total load equations by Laursen, Engelund and Hansen, and Yang were most appropriate. Acker's and White, while a total load equation, tended to overestimate sediment transport of fine and very fine sands, was thrown out of these runs.

In 1992 and 2002, the bed coarsened and became bedload-transport dominated. Thus, Meyer-Peter and Muller's equation may be more suitable, as it is a bedload transport equation. Engelund and Hansen's method works well for all years.

Table 4-5 displays the transport capacities calculated by HEC-RAS over the Cochiti Dam reach for 1972 and 1992. Plots for each method for all runs (1962, 1972, 1992, and 2002) are available in Appendix E.

	Method	1962	1972	1992	2002
subreach 1	Ackers-White			8,530	5,250
	Engelund-Hansen	40,000	50,000	18,000	18,000
	Laursen	230,000	180,000		
	Meyer-Peter and Muller			7,800	6,900
	Toffaleti			23,000	24,000
	Yang	56,000	55,000	25,000	26,000
subreach 2	Ackers-White			7,300	1,700
	Engelund-Hansen	48,000	85,000	19,000	13,000
	Laursen	180,000	340,000		
	Meyer-Peter and Muller			7,100	6,000
	Toffaleti			38,000	28,000
	Yang	64,000	94,000	27,000	23,000
subreach 3	Ackers-White			5,600	790
	Engelund-Hansen	45,000	49,000	15,000	8,800
	Laursen	290,000	180,000		
	Meyer-Peter and Muller			6,000	3,700
	Toffaleti			18,000	14,000
	Yang	66,000	58,000	19,000	13,000
total reach	Ackers-White			7,200	2,600
	Engelund-Hansen	44,000	61,000	17,000	13,000
	Laursen	230,000	230,000		
	Meyer-Peter and Muller			7,000	5,600
	Toffaleti			26,000	22,000
	Yang	62,000	69,000	24,000	20,000

Table 4-5 Reach-averaged sediment transport capacities calculated by HEC-RAS.

Sediment transport capacities were reduced over time with the drastic increase in bed sediment sizes. Sediment transport capacity would be expected to increase after the dam closure, due to the input of a low concentration of sediment and a highly erodable bed. Over time, however, the armoring of the bed seems to have decreased the overall sediment transport capacity of the reach.

By the equation $L_T=L_w+L_{bm}$, where L_T is the total sediment load, L_W is the washload transported, and L_{bm} is the bed material transported, rough estimates of bed material transported through the reach were made (Julien 1998). Table 4-6 displays the results of this calculation.

	Method	Transport Capacity (tons/day)	Average Gage L_w (tons/day)	Estimated L_{BM} (tons/day)
1962	Engelund-Hansen	44,000	6575	37,425
	Laursen (Copeland)	230,000	6575	223,425
	Yang	62,000	6575	55,425
1972	Engelund-Hansen	61,000	6575	54,425
	Laursen (Copeland)	230,000	6575	223,425
	Yang	69,000	6575	62,425
1992	Ackers-White	7,200	140	7,060
	Engelund-Hansen	17,000	140	16,860
	Meyer-Peter and Muller	7,000	140	6,860
	Toffaleti	26,000	140	25,860
	Yang	24,000	140	23,860
2002	Ackers-White	2,600	140	2,460
	Engelund-Hansen	13,000	140	12,860
	Meyer-Peter and Muller	5,600	140	5,460
	Toffaleti	22,000	140	21,860
	Yang	20,000	140	19,860

Table 4-6 Bed material transport calculations from sediment transport capacity calculations and known washload discharge

4.3.2 Equilibrium Channel Slope Analysis

Using the model created by Leon (2003), an equilibrium slope was obtained for each of the three subreaches of the Cochiti Dam reach. Data was input by subreach and run for approximately 40 years (12419 days). Depth to armoring was attained along most of the upstream part of the reach, while the downstream portion aggraded. Equilibrium was reached in only a few years, contradictory to the real conditions of the Cochiti Dam reach. A sumary of equilibrium slopes calculated by the program is available in Table 4-7. Figure 4-6 displays the initial and final conditions of the model.

There were several limitations in using this model. In Leon's model, the width cannot change over time. Obviously, one of the major changes to the Middle Rio Grande during this

time period was the narrowing of the channel. In addition, this model cannot handle grain size distributions, or changes in grain size over time. The Cochiti Dam reach of the Middle Rio Grande contains sediments as small as sand and as large as very coarse gravel. The median grain size has also increased by fifty times since the 1970s. These changes are not taken into account by the model.

The model is quasi-unsteady. While discharge can change from day to day in this model, each day is run as steady state. Real-life conditions are unsteady. This may be one of the reasons equilibrium was reached so quickly.

Data inadequacies also caused limitations to the model's accuracy. The particle size distributions used to estimate the median grain size was done from a visual bed inspection, not from a deep bed excavation. This limited the accuracy of the depth to armoring calculation. The armoring calculation showed correct trends in observed degradation of the channel, but overestimated the actual degradation in the reach. From 1972 to 1998, the equations calculated a depth to armoring of over three feet in subreach 1, over one foot in subreach 2, and over six feet in subreach 3. With the exception of subreach 2, the actual thalweg degradations that have occurred are much smaller, as shown in Figure 3-11. The overestimation may be due, in part, to the inadequacies of the particle size distributions used.

Figure 4-6 displays the initial and final conditions of the model run. Dotted lines represent initial conditions and solid lines represent final conditions. A large amount of degradation appears to occur in subreach 3, also contradictory to observations

The entire Cochiti Dam reach was evaluated as three subreaches in this model. This may have simplified the problem and smoothed over small scale changes in aggradation and degradation in the reach, but it was necessary to avoid numerical instability in the model.

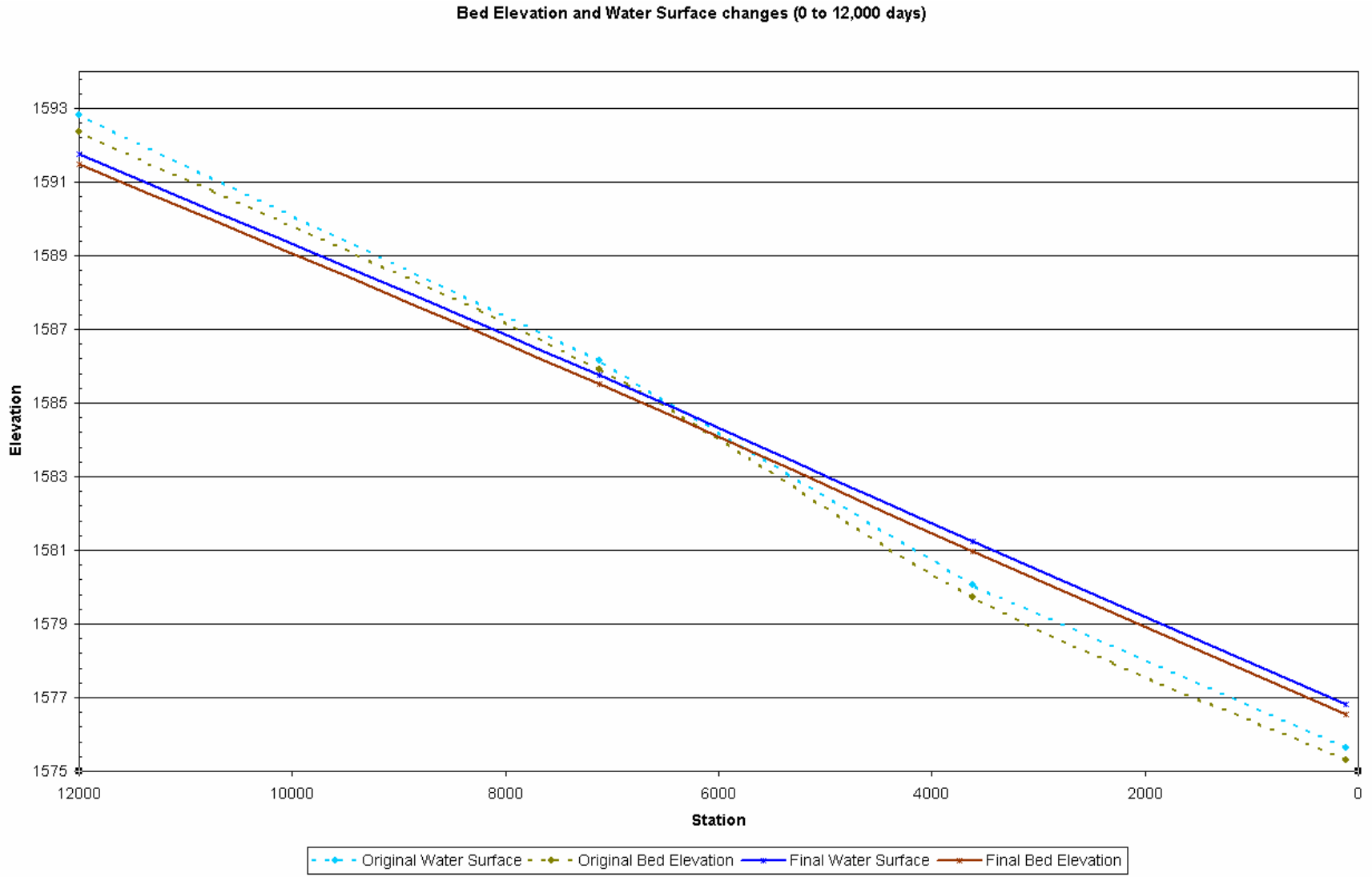

Figure 4-6 Equilibrium Slope determination using program developed by Leon (2001)

In addition, the model had a fourth upstream "dummy" reach to represent upstream conditions that would take the place of Cochiti Dam. Without this reach, the upstream part of the bed would not have been allowed to degrade.

	Equilibrium Slopes	
Reach	Water	Bed
subreach 1	0.001261	0.001261
subreach 2	0.001287	0.001297
subreach 3	0.001234	0.001224
total reach	0.001258	0.001256

Table 4-7 Equilibrium slopes predicted by Leon's (2001) model

4.3.3 Hydraulic Geometry

The equilibrium widths predicted by the hydraulic geometry equations for HEC-RAS model data run at 5,000 cfs are summarized in Table 4-8 and displayed graphically in Figure 4-7. Simons and Albertson's, Julien-Wargadalam's and Lacey's equations all underestimate the width for all subreaches for all years. Blench's equation overestimates the width for all subreaches in 1962 and 1972, but predicts widths fairly closely to the observed values in 1992 and 2002. Nouh's equation vastly overestimates the width for all subreaches in 1962 and 1972, and also greatly underestimates the widths for all subreaches in 1992 and 2002. Klassen and Vermeer's equation overestimates the width for all subreaches for all years analyzed.

From Figure 4-9, Blench's 1992 and 2002 calculations produce width values close to the channel width obtained by HEC-RAS analysis. The most accurate regime equations are from Julien-Wargadalam, which underpredicts the HEC-RAS values. Overall, the regime equations tend to inaccurately predict historical widths. However, they correctly predict little change in channel width with time, as observed in this reach since the 1960's. The Julien-Wargadalam, Simons and Albertson, and Lacey equations also predict that the channel is becoming close to equilibrium with time. This is indicated by the movement of the predicted widths towards the 1:1 line with observed widths.

Year	subreach	Reach-Avg HEC-RAS Channel Width (ft)	Klassen & Vermeer	Nouh	Blench	Simons and Albertson	Julien-Wargadalam	Lacey
1962	1	361	729	1069	1096	245	283	189
	2	538	729	1069	1096	245	273	189
	3	469	729	1069	1096	245	265	189
	Total	**444**	**729**	**1069**	**1096**	**245**	**274**	**189**
1972	1	300	729	1066	1096	245	269	189
	2	392	729	1066	1096	245	264	189
	3	389	729	1090	1133	245	263	189
	Total	**352**	**729**	**1074**	**1109**	**245**	**265**	**189**
1992	1	349	729	16	404	245	263	189
	2	422	729	15	381	245	262	189
	3	351	729	36	577	245	263	189
	Total	**372**	**729**	**23**	**480**	**245**	**261**	**189**
2002	1	524	729	79	740	245	259	189
	2	584	729	61	684	245	269	189
	3	598	729	15	394	245	269	189
	Total	**563**	**729**	**52**	**652**	**245**	**262**	**189**

Table 4-8 Predicted equilibrium widths (in feet) from hydraulic geometry equations for Q=5,000 cfs

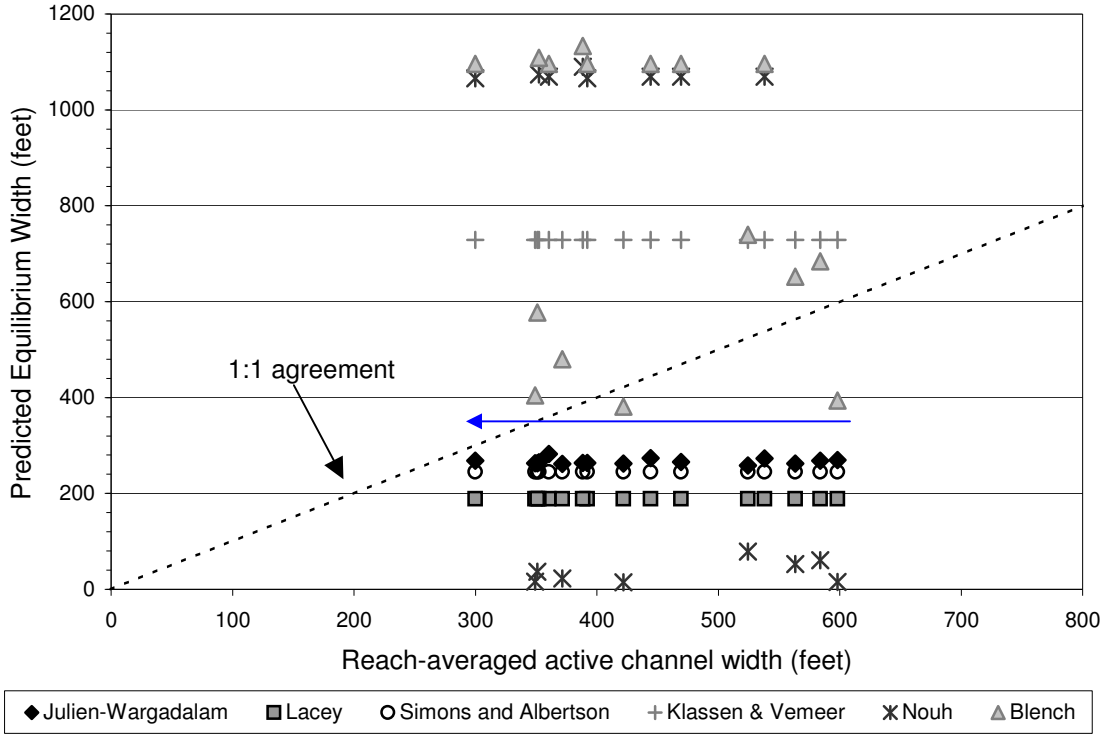

Figure 4-7 Hydraulic geometry equation results of predicted equilibrium width versus reach-averaged active channel width. The arrow indicates the direction of increasing time.

The Julien-Wargadalam equations were also used to predict a stable slope and width for the reach. The shear stress, τ*, was taken to be 0.047, or at incipient motion of the bed particles, with a d_s of 24 mm (1998 conditions). This analysis predicts a stable channel slope for the reach of 0.001025 ft/ft and a stable width of 267 ft, values that are very close to 1998 observations.

Empirical width-discharge relationships were developed for each subreach using active channel widths measured from aerial photos and topographic maps. The non-vegetated active channels were measured using GIS. Table 4-9 displays the numerical results of the analysis, while Figure 4-8 is a plot of the downstream hydraulic geometry relationships.

		1918	*1935*	*1949*	*1962*	*1972*	*1985*	*1992*	*2001*	*2004*
	Averaged 5-year peak flows (cfs)	11630	7232	7996	5546	3560	5958	4172	4252	2410
GIS Width (ft)	subreach 1	323	487	515	419	232	299	227	165	160
	subreach 2	571	849	575	570	301	292	217	196	200
	subreach 3	400	477	655	458	244	263	276	229	240
	total reach	**415**	**580**	**578**	**472**	**254**	**285**	**240**	**194**	**201**
Predicted Width (ft)	subreach 1	512	367	394	305	224	321	250	253	170
	subreach 2	730	476	521	375	251	400	290	295	177
	subreach 3	543	412	437	353	273	368	299	303	218
	total reach	**562**	**401**	**431**	**332**	**243**	**350**	**271**	**275**	**184**

Table 4-9 Measured and predicted widths using empirical width-discharge relationships.

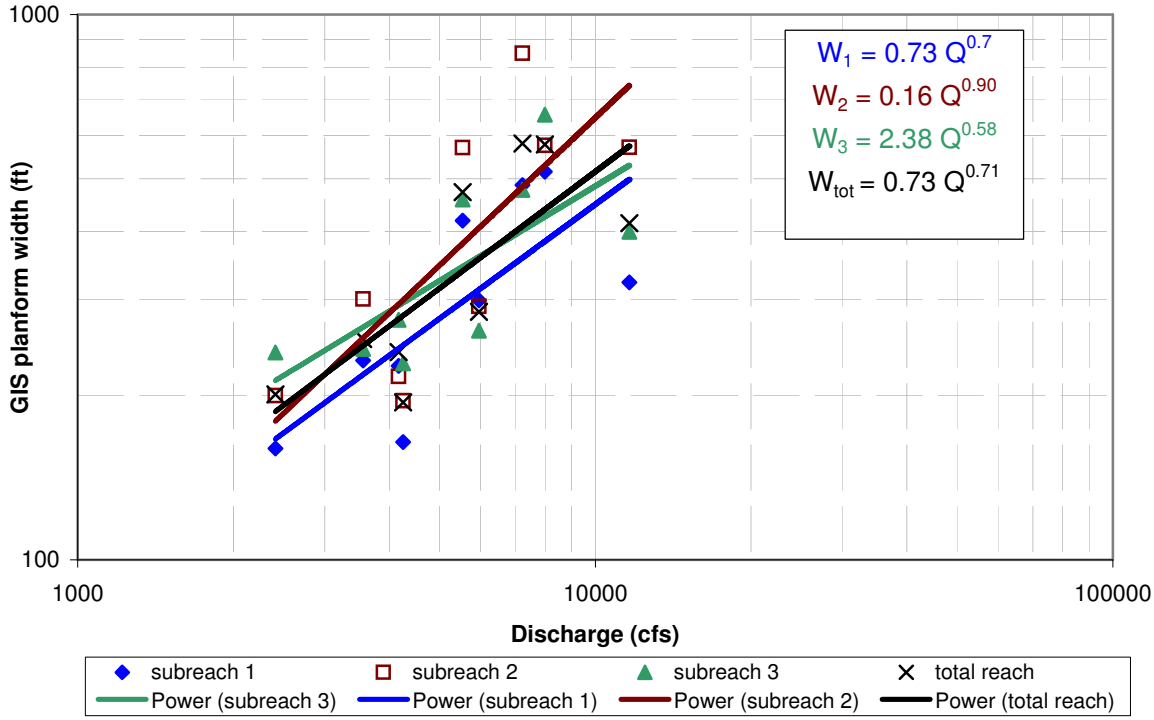

Figure 4-8 Empirical downstream hydraulic geometry relationships for Cochiti Dam Reach from 1918 to 2004

The river was wide and braided from 1918 to 1949 and peak annual flows were high. After 1962, the river was single-thread for the most part, and much more narrow. Coupled with the controlled peak flows out of Cochiti Dam after 1972, the empirical downstream hydraulic geometry relationship is quite steep, with *Q* exponents of well over 0.5 in Figure 4-10. This is not due to the hydraulic regime of the river, but rather due to the drastic changes that have taken place over the past 60 years. Figure 4-9 shows the empirical downstream hydraulic geometry after installation of the dam. Width changes are not as drastic after 1973 and *Q* exponents are much lower.

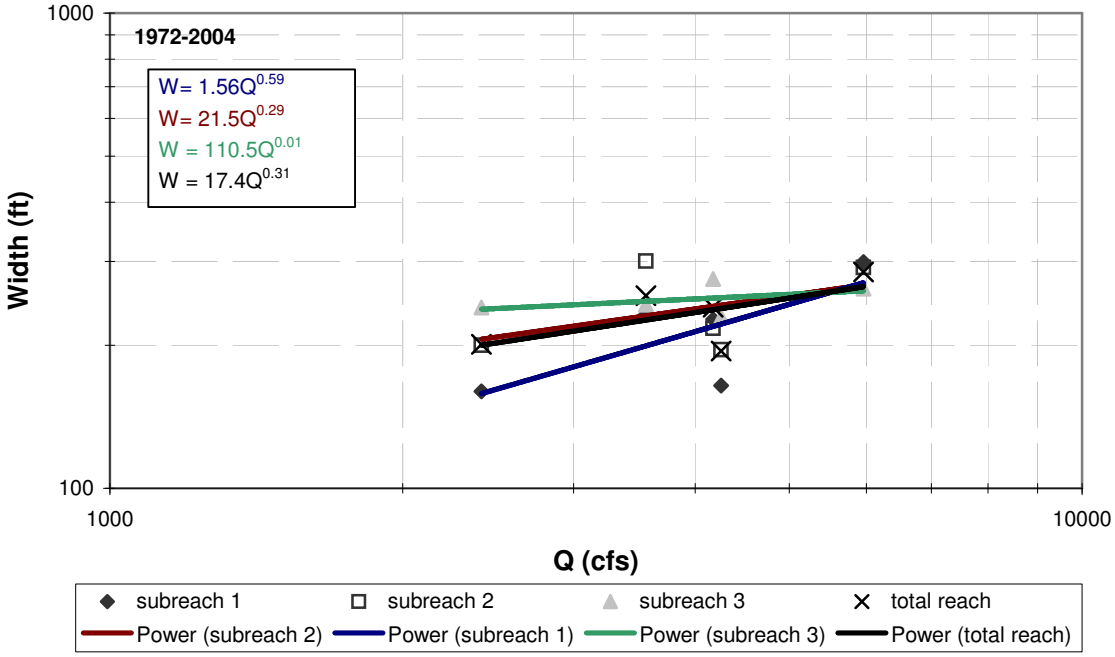

Figure 4-9 Post-dam empirical Downstream Hydraulic Geometry for the Cochiti Dam reach.

4.3.4 Equilibrium Channel Width Analysis

Williams and Wolman (1984) constructed a hyperbolic model described in the methods section. Four hyperbolic equations were fit to the data from 1949 to 2004. The hyperbolic functions were calculated by hand using the least-squares method. The equations fit fairly well and may be used to predict channel trends in width. Figure 4-10 displays the hyperbolic equations fit to the plots. The trends indicate that the width decreased at a much slower rate after 1979. Table 4-10 displays the equations fit to the data.

The hyperbolic model does not predict equilibrium widths adequately. Equilibrium widths for all reaches are less than 100 ft, including negative values. These values do not match those from the hydraulic geometry relationships. While the model fits the data itself, the width changes are too widely scattered to make accurate predictions.

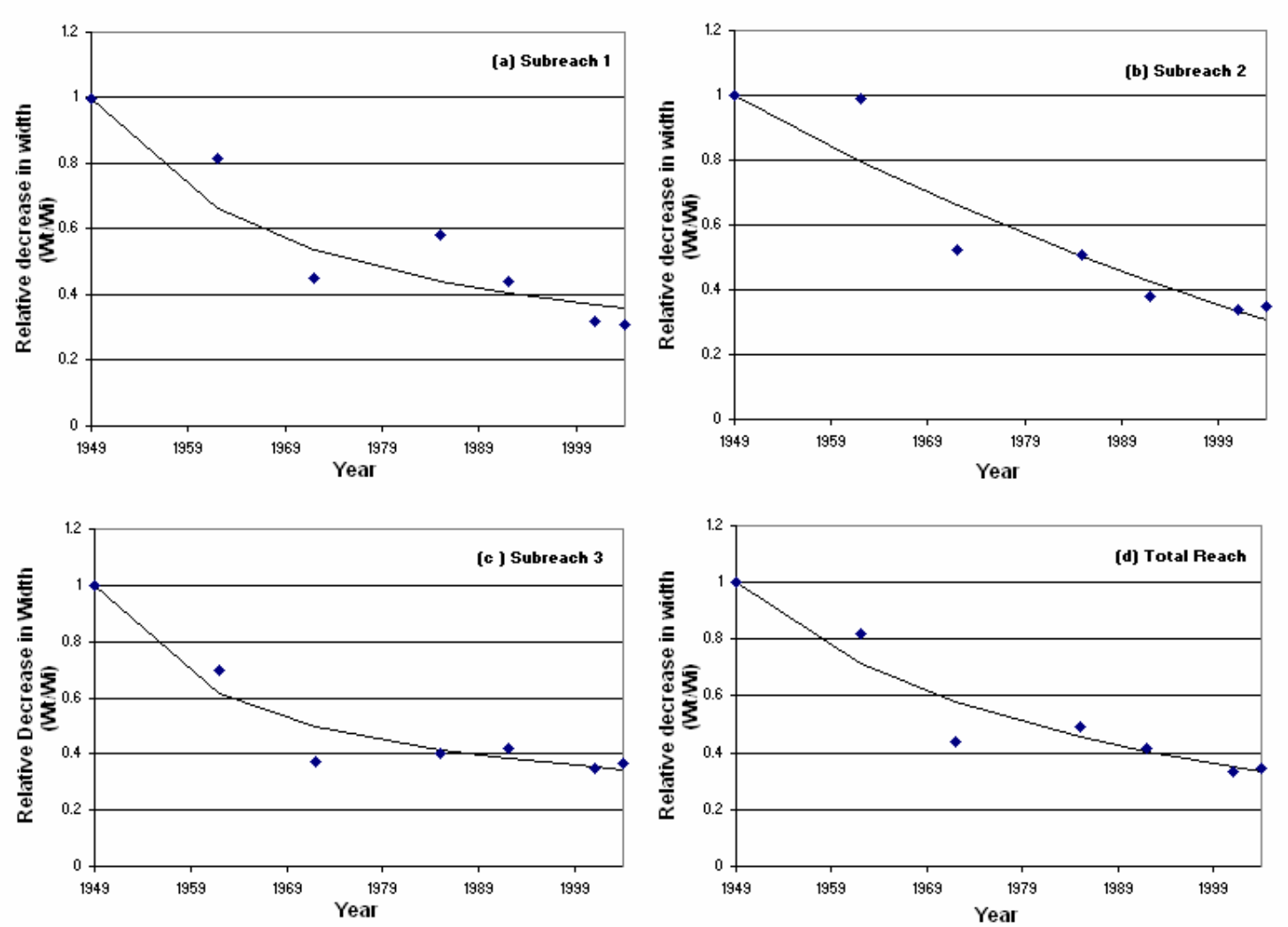

Figure 4-10 Hyperbolic fits to relative decreases in width from 1949 to 2004 for (a) subreach 1, (b) subreach 2, (c) subreach 3, and (d) the entire Cochiti Dam reach.

subreach	Fitted Hyperbolic Equation	r^2	W_e (ft)
1	$\frac{W_t}{W_i} = \frac{t}{-1.2t - 23.9} + 1$	0.77	56
2	$\frac{W_t}{W_i} = \frac{t}{-0.36t - 59.4} + 1$	0.88	-1020
3	$\frac{W_t}{W_i} = \frac{t}{-1.2t - 17.9} + 1$	0.93	109
total	$\frac{W_t}{W_i} = \frac{t}{-0.88t - 34.1} + 1$	0.92	-76

Table 4-10 Hyperbolic fits to relative width plots using least-squares method.

Richard's (2001) exponential model was fitted to the observed active channel width data from aerial photos and topographic surveys of the Cochiti Dam reach. The k_1 and W_e values were estimated using methods 1 and 2. Due to the inexact results from the hydraulic geometry equations, method 3 was not implemented.

Figure 4-11 shows the results of method 1. Change in active channel width was plotted against active channel width to estimate the initial k_1 and W_e values. Table 4-11 summarizes the results. Method 2 produced very similar results with a slightly higher degree of accuracy. In this method, the value of W_e was varied until the sum of the square of errors was minimized between W_e and the observed width. The results are shown in Table 4-12 and a plot of the results of methods 1 and 2 is shown in Figure 4-14. The exponential equations produced by methods 1 and 2 are summarized in Tables 4-13 and 4-14.

Richard's model computes an exponential line from the first data point in 1949. Because the widths in the Cochiti Dam reach vary so widely from year to year, this method does not make a best-fit estimate for all the data points. For this reason, a Best Engineering Estimate fit was also applied visually. The fits and resulting equations are shown in Figure 4.12, Table 4.13, and Table 14.

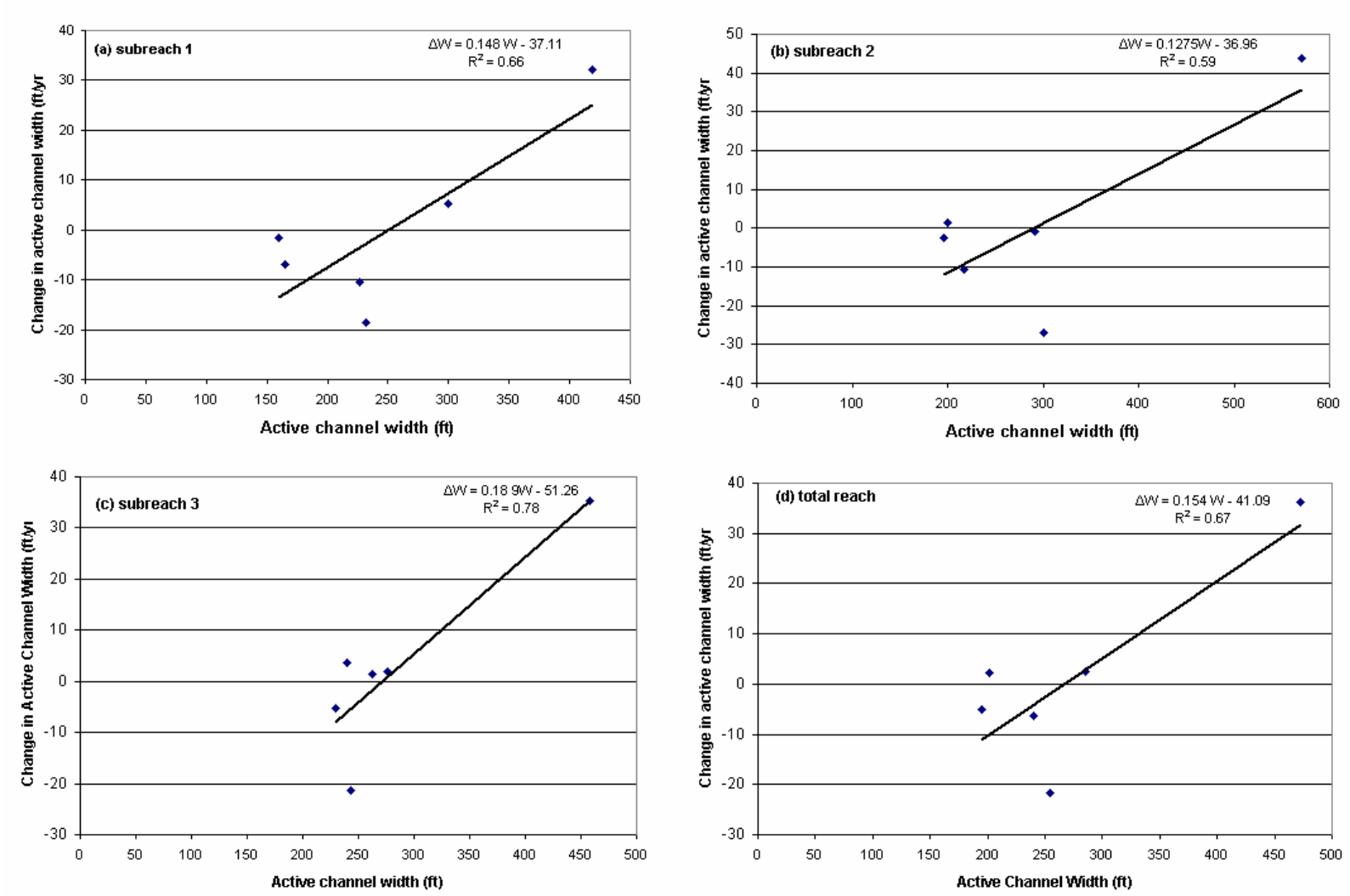

Figure 4-11 Linear regression results of Cochiti Dam reach for Richard's method 1.
Plot of observed width change (ft/year) versus observed channel width (ft) for values from 1918 to 2004.

	k_1 (yr^{-1})	k_1W_e (ft/yr)	W_e (ft)	r^2
subreach 1	0.148	37.11	251	0.66
subreach 2	0.127	36.96	291	0.59
subreach 3	0.189	51.26	271	0.78
total reach	0.154	41.09	267	0.67

Table 4-11 Empirical estimation of k_1 and W_e from linear regressions of width versus change in width data using Richard's method 1 from Figure 4-11.

	Year	W_t (ft)	Method 1 W (ft)	Method 2 W (ft)	W_e guess	SSE	Sum SSE
subreach 1	1949	515	515	515	238	0	
	1962	419	289	279		19686	
	1972	232	260	248		240	
	1985	299	252	240		3561	
	1992	227	251	239		143	
	2001	165	251	238		5467	
	2004	160	251	238		6146	35244
subreach 2	1949	575	419	419	281	24414	
	1962	570	316	308		68873	
	1972	301	298	289		142	
	1985	292	292	283		75	
	1992	217	292	282		4225	
	2001	196	291	282		7371	
	2004	200	291	282		6650	111750
subreach 3	1949	655	232	232	283	178929	
	1962	458	268	279		32080	
	1972	244	271	283		1523	
	1985	263	271	283		409	
	1992	276	271	283		59	
	2001	229	271	283		2925	
	2004	240	271	283		1874	217798
total reach	1949	578	299	299	269	77469	
	1962	472	271	273		39577	
	1972	254	268	270		256	
	1985	285	267	269		246	
	1992	240	267	269		836	
	2001	194	267	269		5618	
	2004	201	267	269		4671	128674

Table 4-12 Exponential results using Richard's method 1 and 2

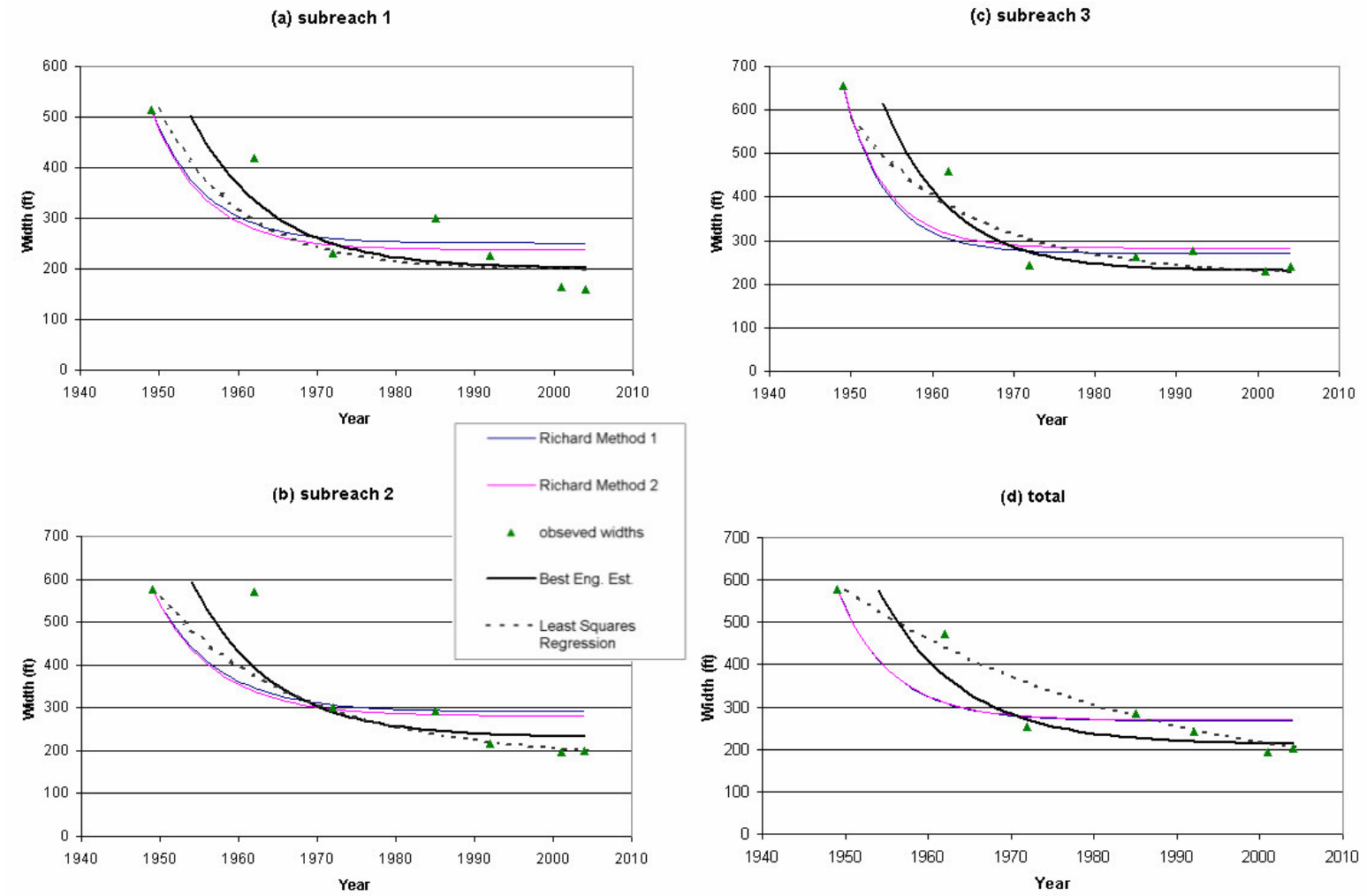

Figure 4-12 Application of Richard's exponential model Methods 1 and 2 plotted against observed width values, Best Engineering Estimates, and Least Squares regressions for (a) subreach 1, (b) subreach 2, (c) subreach 3, and (d) the entire Cochiti Dam reach.

Best Engineering Estimate			Least Squares Regression		
k_1	W_e	r^2	k_1	W_e	r^2
0.1	200	0.73	0.096	197	0.99
0.1	230	0.42	0.054	181	0.90
0.12	230	0.79	0.065	217	0.76
0.1	210	0.72	0.028	96	0.99

Table 4-13 Rate coefficients, equilibrium width, and r2 values for Best Engineering Estimate and Least Squares Regression.

	Richard's Method 1		Richard's Method 2	
subreach	*Equation*	R^2	*Equation*	R^2
1	$W=251+ 264*e^{(-0.148t)}$	0.94	$W=238+ 277*e^{(-0.148t)}$	0.94
2	$W=291+284*e^{(-0.127t)}$	0.86	$W=281+294*e^{(-0.127t)}$	0.86
3	$W=271+284*e^{(-0.189t)}$	0.73	$W=283+372*e^{(-0.189t)}$	0.73
total	$W=267+311*e^{(-0.154t)}$	0.82	$W=269+308*e^{(-0.154t)}$	0.82
	Best Engineering Estimate		**Least Squares Regression**	
subreach	*Equation*	R^2	*Equation*	R^2
1	$W=200+ 600*e^{-0.1(t+5)}$	0.95	$W=197+ 318*e^{(-0.096t)}$	0.99
2	$W=230+ 600*e^{-0.1(t+5)}$	0.92	$W=181+373*e^{(-0.054t)}$	0.90
3	$W=230+ 700*e^{-0.12(t+5)}$	0.97	$W=217+363*e^{(-0.065t)}$	0.76
total	$W=210+ 600*e^{-0.1(t+5)}$	0.96	$W=96+482*e^{(-0.028t)}$	0.99

Table 4-14 Exponential equations from Richard's methods 1 and 2, the best Engineering Estimate, and the Least Squares estimation for each subreach and the Cochiti Dam reach. Time is in years.

The R^2 values for each fit were calculated using the following equation:

$$R^2 = 1 - \frac{SSE}{SST}$$

where

$$SSE = \sum \left(Y_i - \hat{Y}_i \right)^2$$

and

$$SST = \left(\sum Y_i^2 \right) - \frac{\left(\sum Y_i \right)^2}{n}$$

The k_1 rate constant values obtained using Richard's exponential method were compared with values obtained by Richard (2005) for several other alluvial rivers following dam installations similar to the Middle Rio Grande. The rate constants for these other rivers are smaller than those obtained in this analysis. This is most likely due to the fact that the Cochiti

Dam reach is a very short reach just downstream of the dam, and is directly affected by the dam while Richard's examples are longer (20 to 50 miles long) and include other inputs besides the dam (tributaries, floodways, etc.). Table 4-15 compares the values obtained by Richard with the total reach-averaged value from this analysis.

Study Area	k_1 value
Middle Rio Grande	0.0219
Jemez River	0.111
N. Canadian River	0.077
Wolf Creek	0.1132
Arkansas River	0.038
Cochiti Dam Reach	**0.154**

Table 4-15 Richard's k_1 rate change values for various alluvial rivers.

All computed equilibrium values are compiled in Table 4-16. As the table shows, the average equilibrium width for most methods is between 200 and 300 ft. Julien-Wargadalam's equations predict the highest widths while Lacey's equations predict the smallest widths. William's and Wolman's method does not predict reasonable widths for any reach of the river and the Least Squares regression predicts fairly accurate widths for each subreach, but not for the total reach.

sub reach	Downstream Hydraulic Geometry	Simons and Albertson	Julien-Wargadalam	Lacey	Richard	Best Eng. Est.	Least Squares Regression	Max	Mean	Min	Stand. Dev
1	237	250	280	190	251	200	197	280	229	190	34
2	254	250	275	190	291	230	181	291	239	181	41
3	120	250	275	190	271	230	217	275	222	120	54
total	243	250	277	190	267	210	96	277	219	96	62

Table 4-16 Compilation of We values for bankfull (2-year) discharge of 5,000 cfs.

4.4 Schumm's (1969) River Metamorphosis Model

Schumm's (1969) qualitative model of channel metamorphosis is based on the concept that the dimensions, shape, gradient, and pattern of stable alluvial rivers are controlled by the quantity of water and sediment as well as the type of sediment moved through their channels.

This model is appropriate for rivers in semi-arid regions, like the Middle Rio Grande, due to their less cohesive and less developed bank vegetation. The following equations summarize Schumm's results. A plus (+) indicates an increase in the magnitude of the parameter and a minus (-) denotes a decrease.

- Decrease in bed material load:

$$Q_s^- \sim \frac{W^- L^- S^-}{D^+ P^+}$$

- Increase in bed material load:

$$Q_s^+ \sim \frac{W^+ L^+ S^+}{D^- P^-}$$

- Increase in water discharge:

$$Q^+ \sim \frac{W^+ D^+ L^+}{S^-}$$

- Decrease in water discharge:

$$Q^- \sim \frac{W^- D^- L^-}{S^+}$$

- Increase in water discharge and bed material load:

$$Q^+ Q_t^+ \sim \frac{W^+ F^+ L^+ S^{\pm} D^{\pm}}{P^-}$$

- Decrease in water discharge and decrease in bed material load:

$$Q^- Q_t^- \sim \frac{W^- F^- L^- S^{\pm} D^{\pm}}{P^+}$$

Where,

Q = water discharge,

Q_s = bed material load,

Q_t = percentage of total sediment load that is bed-load or ratio of bedload (sand size or larger) to total sediment load x 100 at mean annual discharge,

W = channel width,

D = flow depth,

F = width/depth,

L = meander wavelength,

P = sinuosity, and

S = channel slope.

These equations are summarized in Table 4-17. Table 4-18 summarizes the trends in channel changes in the Cochiti Dam reach for the 1962 to 1972, 1972 to 1992, and 1992 to 2002 time periods in a similar manner as Table 4-17 for comparison. Note that over time, the depth of the channels has increased at a faster rate than the decrease of the channel width, causing the width-depth ratio to decrease.

	W	D	S	W/D =F	P	L
Qs^-	-	+	-		+	-
Q^+	+	+	-			+
Qs^+	+	-	+		-	+
Q^-	-	-	+			-
Q^-Qs^-	-	+ -	+ -	-	+	-
Q^+Qs^+	+	+ -	+ -	+	-	+

Table 4-17 Summary of Schumm's (1969) channel metamorphosis model.

1962-1972

Reach	W	D	F=W/D	EG-Slope	P
1	-	+	-	-	+
2	-	+	-	-	-
3	-	-	+	+	-
total	-	-	-	=	-

1972-1992

Reach	W	D	F=W/D	EG-Slope	P
1	-	-	+	+	-
2	-	+	+	+	+
3	+	=	-	+	-
total	-	=	+	+	-

1992-2002

Reach	W	D	F=W/D	EG-Slope	P
1	-	+	-	+	+
2	-	-	+	+	-
3	-	+	-	+	=
total	-	+	-	+	=

Table 4-18 Summary of channel changes during the 1962-1972, 1972-1992, and 1992-2002 time periods for the Cochiti Dam Reach

Schumm's (1969) metamorphosis model suggests that changes in channel geometry, slope and planform in the Cochiti Dam reach from 1962 to 1992 were most likely responding to a decrease in mean annual flood (Q-) and an increase in sediment load (Qs+). Figure 3-5 confirms the decrease in mean annual flood. However, according to Figure 4-2 sediment discharge did not increase at the Otowi gage from 1962 to 1992. In fact, from 1972 to 1992, the sediment discharge out of Cochiti Dam decreased to less than two percent of its original concentration and discharge. However, bed material transport in the region may have increased drastically due to the increased sediment capacity of the water entering the reach. Bed material transport is not included in the suspended sediment single mass curves shown in Figure 3-32.

From 1992 to 2002, the trends in channel geometry, slope and planform suggest several different possibilities. The tendencies most closely resemble a decrease in sediment discharge and an increase in mean annual flood. However, the overall trends of the Cochiti Dam reach for this time period do not fit into any one Schumm category. Table 4-18 displays the expected Schumm metamorphosis model fitting each subreach for each time period and the validation with

the observed data. Again, suspended sediment values were extrapolated from 1988. Observed data was taken from the mass curves in Figures 3-31 and 3-32.

As the bed has become armored upstream, the total sediment discharge has been decreasing. However, the sediment discharge from the dam is already very small (Figure 3-33), only 38 mg/L or 0.05 tons/acre-ft. Since no sediment discharge data exists from 1988 to present, the change in discharge from 1992 to 2002 in Table 4-19 was estimated to remain the same as it was before 1988. If a change in sediment discharge has occurred, it must be relatively small since it takes place at a controlled dam. For this reason, it is relatively easy to predict sediment and discharge changes, at least at the upstream end of the reach, since it is at the outlet of a controlled dam.

			Observed Data	
	Reach	*Schumm Model*	*Q*	*Qs*
1962-1972	subreach 1	Q- Qs-	-	-
	subreach 2	Q- Qs+		
	subreach 3	Q- Qs+		
	total reach	**Q- Qs+**		
1972-1992	subreach 1	Q- Qs+	+	-
	subreach 2	Q+ Qs-		
	subreach 3	Q+ Qs+		
	total reach	**Q- Qs+**		
1992-2002	subreach 1	Q+ Qs-	=	=
	subreach 2	Q- Qs+		
	subreach 3	Q+ Qs+ / Q- Qs-		
	total reach	**Q+ Qs+ / Q- Qs-**		

Table 4-19 Schumm model results compared to observed data in the Cochiti Dam reach.

Chapter 5: Summary and Conclusions

The morphologic analysis of the Cochiti Dam reach of the Middle Rio Grande entailed a detailed examination of channel characteristics including geometry, planform, and bed material. Discharge and suspended sediment were also studied and were input into several modeling programs for further analysis.

5.1 Summary

Discharge – Total annual discharge at the Cochiti gage decreased after 1950 to two-thirds of its previous annual discharge from 1931 to 1950 (see Figure 4-1). After 1978, the total annual discharge increased again by a factor of 1.5. Factors such as dam management, climate changes, irrigation and other water diversions may be responsible for these changes.

Suspended Sediment – The total annual suspended sediment discharge at the Cochiti gage reveals staunch evidence of the trap efficiency of the dam (see Figure 3-32). After the dam was installed, the suspended sediment discharge exiting the dam dropped to 2% of its original concentration at Otowi gage.

Bed Material – The median bed material at the Cochiti Dam gage was fine to medium sand in 1970, very coarse sand to coarse gravel in 1980, and coarse gravel to very coarse gravel in 1998 (refer to Table 3-11).

Coarsening of the bed sediments increased overall with distance downstream and with time. The median grain size was sand until the dam was built. Armoring clearly began with the

appearance of gravel as the median sediment size in the mid 1970s. Subreach 1 generally had bed sediment trends that were representative of the entire reach.

Channel pattern – From GIS analysis, the overall trend of the channel from 1918 to 2004 has been a narrowing of the width and a shift from a braided to meandering planform. According to the width measurements from the digitized aerial photos, the overall width of the reach increased from 1918 to 1949, drastically decreased after 1949 to 1973, and then decreased slightly from 1973 to 2004. This finding is supported by the HEC-RAS modeling results from 1973 to 2002. This suggests that the channelization efforts beginning in the 1930s may have had more of an impact on the river than the dam itself. Average sinuosity increased slightly from 1.20 in 1918 to 1962 and decreased from 1962 to 2004 from 1.21 to 1.13.

Channel Classification – The channel classification methods produced mixed results. From the 1962 planforms, Lane, Henderson, and van den Berg's methods were most accurate. They described the channel as braided, which can be verified by the aerial photos. Van den Berg's method also described the channel as low sinuosity, which can be verified by the sinuosity trends seen in Figure 3-10. After 1962, the channel appeared to be narrowing and becoming mostly single-thread. For these years, Ackers and Charlton, Rosgen, and Parker produced accurate results. They predicted meandering channels for each subreach and the total reach. Van den Berg also predicted that the channel would be single-thread. Overall, van den Berg's method produced the most complete and accurate representation of the Cochiti Dam reach from 1962 to 2004.

Vertical Movement – Thalweg analysis was done on CO-lines 2 through 8. The thalweg degraded over almost every CO-line in the reach between 1 and 3 feet from 1962 to 2002. Thalweg analysis from 1962 to 2002 demonstrated a degradation of almost 3 feet at CO-5 and an aggradation of almost 2 feet just upstream at CO-4. The aggradation here may be due to

an overbank area (Figure 3-24). With the exclusion of CO-4, the average reach degradation was 2.15 feet.

Based on mean bed elevations from Agg/Deg surveys, the mean bed elevation degraded slightly after 1962, but began aggrading in the 1970s. Total mean bed degradation from 1962 to 1972 averaged over the entire reach was approximately one third of a foot. Mean bed elevation increase in the reach from 1972 to 2002 totaled about one-half of a foot. Further analysis of the discrepancy between thalweg degradation and mean bed aggradation led to the conclusion that the "aggradation" seen in the agg/deg range-lines are most likely average mean bed elevation changes due to a channel geometry change, not of actual aggradation in the channel bed.

Channel Geometry – General trends in channel geometry are summarized in Table 5-1. The changes are summarized for each subreach and the total reach. Note that a plus (+) indicates an increase in parameter value, a negative (-) denotes a decrease, and an equality (=) indicates no change. Overall from 1962 to 2002, there was a decrease in width, area, width/depth ratio and wetted perimeter. There was an increase in energy grade slope, velocity, depth, Froude number, and water surface slope.

From GIS coverages, the width changes are similar to those modeled in HEC-RAS. From digitized aerial photos, the width increased from 1918 to 1949, decreased drastically from 1949 to 1972, increased slightly from 1972 to 1985, and finally decreased slightly from 1985 to 2004 (see Figure 3-26). From the analysis of width and depth trends, it appears that most narrowing of the channel occurred before the dam. The dam may act as a control, which may have kept the channel at the relatively the same width for the last few decades.

Overbank Flow/Channel Capacity – Based on the HEC-RAS modeling results at a discharge of 5,000 cfs, a small amount of overbank flow occurs in subreach 2 for all years (see Figure 3-24). This may explain the aggradational trend seen at CO-4 (see Figure 3-7).

Equilibrium Predictors – Several predictors were used to estimate equilibrium and stable conditions in the reach. Leon's (2003) modeling program predicted an equilibrium slope much shallower than the slopes observed in the reach (between 70% and 85% of the observed slopes). Both Williams and Wolman (1984) and Richard's (2001) models fit accurate decreasing trends to the historic width-discharge data. None of the hydraulic geometry equations accurately predict width; however, they accurately estimate unchanging width trends with time. Julien-Wargadalam's equations predict stable slope and width that are very close to those observed for 1998.

5.2 Conclusions

The hydraulic modeling of the Cochiti Dam reach on the Middle Rio Grande River, NM, produced a detailed characterization of the river over space and time. The highly controlled dam's reduced flows and clearwater discharge induced major changes to the channel and its flow regime.

The Middle Rio Grande Database was organized and updated for facilitation of this analysis. The discharge, sediment, and geometric data in this database, in addition to the numerous literature resources, were then compiled to analyze spatial and temporal trends in the Cochiti Dam reach of the Middle Rio Grande River.

After the dam closure in 1973, floods were nearly eliminated since peak annual flows did not exceed 10,000 cfs. The channel narrowed by 50 - 100 feet after the dam closure. Both average width-depth ratio and cross-sectional area were reduced by a third and thalweg degradation averaged 2 feet over the entire reach. Median bed sediment sizes jumped from an average of 0.1 mm in 1962 to an average of 24 mm in 1998, armoring the bed. This was due to the 98% decrease in suspended sediment after the dam construction. The changes in bed sediment sizes are more apparent in subreach 1 than subreach 3, indicating a decrease of dam effects with distance downstream. This is corroborated by outside analyses on downstream

reaches of the Middle Rio Grande. Overall, Cochiti dam had a much more noticeable effect on bed sediment than channel geometry.

Equilibrium analysis of the reach using sediment transport functions, equilibrium channel width and slope analysis, and regime equations suggested that the Cochiti Dam reach is moving towards stable channel conditions and the channel may begin experiencing lateral motion, which will begin eroding the banks.

References

Ackers, P. (1982). Meandering Channels and the Influence of Bed Material. *Gravel Bed Rivers. Fluvial Processes, Engineering and Management.* Edited by R.D. Hey, J.C. Bathurst and C.R.Thorne. John Wiley & Sons Ltd. 389-414

Albert, J., Sixta, M., Leon, C., and Julien, P.Y. (2003). Corrales Reach. Corrales Flood Channel to Montano Bridge. Hydraulic Modeling Analysis. 1962-2001. Middle Rio Grande, New Mexico. Prepared for U.S. Bureau of Reclamation. Albuquerque, New Mexico. Colorado State University, Fort Collins, CO.

Albert, J. (2004) Hydraulic Analysis and Double Mass Curves of the Middle Rio Grande from Cochiti to San Marcial, New Mexico. M.S. Thesis. Colorado State University, Fort Collins, CO. 207 pp.

Baird, D. C. (1996). River Mechanics Experience on the Middle Rio Grande. *6th Federal Interagency Sediment Conference.* March 11-14. 8 pp.

Bauer, T. R. (2000). Morphology of the Middle Rio Grande from Bernalillo Bridge to the San Acacia Diversion Dam, New Mexico. M.S. Thesis. Colorado State University, Fort Collins, CO. 308 pp.

Blench, T. (1957). *Regime Behaviour of Canals and Rivers.* London: Butterworths Scientific Publications. 138 pp.

Bullard, K.L. and Lane, W.L. (1993). Middle Rio Grande Peak Flow Frequency Study. U.S. Department of the Interior, Bureau of Reclamation, Albuquerque, NM. 36 pp.

Burkholder, J.L., Report of the Chief Engineer. Middle Rio Grande Conservancy District. Albuquerque, New Mexico. Dated March 19, 1929.

Chang, H.H. (1979). Minimum Stream Power and River Channel Patterns. *Journal of Hydrology*, 41, 303-327.

Crawford, C.S., Culley, A.C., Leutheuser, R., Sifuentes, M.S., White, L.H., Wilber, J.P. (1993). Middle Rio Grande Ecosystem: Bosque Biological Management Plan. U.S. Fish and Wildlife Service, Albuquerque, New Mexico.

Dewey, J.D., Roybal, F.E., Funderburg, D.E., (1979). Hydraulic Data on Channel Adjustments 1970 to 1975, on the Rio Grande Downstream from Cochiti Dam, New Mexico Before and After Closure. U.S. Geological Survey, Water Resources Investigations.

Graf, W.L. (1994). *Plutonium and the Rio Grande. Environmental Change and Contamination in the Nuclear Age.* New York : Oxford University Press.

Henderson, F.M. (1966). *Open Channel Flow*. New York, NY : Macmillan Publishing Co., Inc.

Hereford, R., (1984) Climate and ephemeral-stream processes: Twentieth-century geomorphology and alluvial stratigraphy of the Little Colorado River, Arizona. *Geological Society of America Bulletin*, v. 95, p. 654-668.

Holmquist-Johnson, C. (2005) Personal Communication. Hydraulic Engineer. Representing U.S. Bureau of Reclamation, Sedimentation and Hydraulics Group. Denver, CO.

Julien, P.Y. (1995) *Erosion and Sedimentation*. New York, NY: Cambridge University Press. 280 pp.

Julien, P.Y. (1998) *River Mechanics*. New York, NY: Cambridge University Press. 434 pp.

Julien, P.Y. and Wargadalam, J. (1995). Alluvial Channel Geometry: Theory and Applications. *Journal of Hydraulic Engineering,* 121(4), 312-325.

Klaassen, G.J. and Vermeer, K. (1988). Channel Characteristics of the Braiding Jamuna River, Bangladesh. *International Conference on River Regime*, 18-20 May 1988. W.R. White (ed.), Hydraulics Research Ltd., Wallingford, UK. pp 173-189.

Knighton, A.D. and Nanson, G.C. (1993). Anastomosis and the Continuum of Channel Pattern. *Earth Surface Processes and Landforms*, 18, 613-625.

Lagasse, P.F. (1980). An Assessment of the Response of the Rio Grande to Dam Construction – Cochiti to Isleta Reach. U.S. Army Corps of Engineers. Albuquerque, NM.

Lagasse, P. F. (1994). Variable Response of the Rio Grande to Dam Construction, The Variability of Large Alluvial Rivers. ASCE Press, New York, NY.

Lane, E.W., Borland, W.M., (1953), River Bed Scour During Floods. Transactions, ASCE, Paper No. 2712.

Lane, E.W. (1955). The importance of fluvial morphology in hydraulic engineering. *Proc. ASCE*, 81(745):1-17.

Leon, C. (1998). Morphology of the Middle Rio Grande from Cochiti Dam to Bernalillo Bridge, New Mexico. M.S. Thesis. Colorado State University, Fort Collins, CO. 210 pp.

Leon, C. and Julien, P.Y. (2001a). Hydraulic Modeling on the Middle Rio Grande, NM. Corrales Reach. Corrales Flood Channel to Montano Bridge. Prepared for U.S. Bureau of Reclamation. Albuquerque, New Mexico. Colorado State University, Fort Collins, CO. 83 pp.

Leon, C. and Julien, P.Y. (2001b). Bernalillo Bridge Reach. Highway 44 Bridge to Corrales Flood Channel Outfall. Hydraulic Modeling Analysis. 1962-1992. Middle Rio Grande, New Mexico. Prepared for the U.S. Bureau of Reclamation. Albuquerque, New Mexico. Colorado State University, Fort Collins, CO. 85 pp.

Leon, C. (2003). Analysis of Equivalent Widths of Alluvial Channels and Application for Instream Habitat in the Rio Grande. Ph.D. Dissertation. Colorado State University, Fort Collins, CO. 308 pp.

Leopold, L.B. and Maddock, T. Jr. (1953). The Hydraulic Geometry of Stream Channels and Some Physiographic Implications. USGS Professional Paper 252, 57 pp.

Leopold, L.B. and Wolman, M.G. (1957). River Channel Patterns: Braided, Meandering and Straight, USGS Professional Paper 282-B. 85 pp.

Mackin, J. H. (1948). Concept of the graded river. *Geol. Soc. Am. Bull.,* 59:463-512

Mosley, J. and Boelman, S. (1998). Santa Ana Reach. Geomorphic Report – Draft. U.S. Bureau of Reclamation, Albuquerque, NM.

Nanson, G.C. and Croke, J.C. (1992). A genetic classification of floodplains. *Geomorphology*. 4, 459-486.

New Mexico Culturenet. The science of the river. Available at: http://www.nmculturenet.org/heritage/river/pdf_files/science/day_nine_science.pdf. Accessed August 3, 2005.

Nordin, C.F. Jr., Beverage, J.P., (1965) Sediment Transport in the Rio Grande, New Mexico, USGS Professional Paper 462-F.

Nouh, M. (1988). Regime Channels of an Extremely Arid Zone. *International Conference on River Regime*, 18-20 May 1988. W.R. White (ed.). Hydraulics Research Ltd., Wallingford, UK. pp 55-66.

Novak, S.J., Julien, P.Y. (2005 draft). Cochiti Dam Reach. Cochiti Dam to Galisteo Creek. Hydraulic Modeling Analysis. 1962-2002. Middle Rio Grande, New Mexico. Prepared for U.S. Bureau of Reclamation. Albuquerque, New Mexico. Colorado State University, Fort Collins, CO.

Ortiz, R.M., Meyer, G.A. Downstream Effects of Cochiti Dam on the Middle Rio Grande and the Channel Transition Zone near Albuquerque, New Mexico. *2005 Salt Lake City Annual Meeting, Geological Society of America*, Paper No. 145-3.

Parker, G. (1976). On the Cause and Characteristic Scales of Meandering and Braiding in Rivers. *Journal of Fluid Mechanics*, vl. 76, part 3, pp 457-480.

Pueblo de Cochiti Farm Enterprise. The Official Web site of the Cochiti Pueblo. Available at: http://www.pueblodecochiti.org/farm.html. Accessed August 2, 2005.

Richard, G., Leon, C., and Julien, P.Y. (2001). Hydraulic Modeling on the Middle Rio Grande, New Mexico. Rio Puerco Reach. Prepared for U.S. Bureau of Reclamation. Albuquerque, New Mexico. Colorado State University, Fort Collins, CO.

Richard, G. (2001). Quantification and Prediction of Lateral Channel Adjustments Downstream from Cochiti Dam, Rio Grande, NM. Ph.D. Dissertation. Colorado State University, Fort Collins, CO. 244 pp.

Richard,G., Julien, P.Y., and Baird, D. (2005). Case Study: Modeling the Lateral Mobility of the Rio Grande below Cochiti Dam, New Mexico. *Journal of Hydraulic Engineering*. Vol. 131 No. 11. pp. 931-941.

Richardson, E.V., Simons, D. B. and Julien, P.Y. (1990). Highways in the River Environment. U.S. Department of Transportation. *Federal Highway Administration*. 610 pp.

Rosgen, D. (1996). *Applied River Morphology*, Pagosa Springs, CO: Wildland Hydrology. 360 pp.

Sanchez, V. and Baird, D. (1997). River Channel Changes Downstream of Cochiti Dam. Middle Rio Grande, New Mexico. *Proceedings of the Conference of Management of Landscapes Disturbed by Channel Incision.* University of Mississippi, Oxford, MS.

Schembera, R.E., (1963). Development of Hydraulics and Sediment Transport Relationships and Their Use for Channel Design of Middle Rio Grande Channelization. U.S. Bureau of Reclamation, Albuquerque, New Mexico.

Schumm, S.A. (1969). River Metamorphosis. *Journal of the Hydraulics Division.* Vol. 95, No. 1. pp 255-273.

Schumm, S. A. and Khan, H.R. (1972). Experimental Study of Channel Patterns. *Geological Society of America Bulletin*, 83, 1755-1770.

Scurlock, D. (1998). From the Rio to the Sierra. An Environmental History of the Middle Rio Grande Basin. General Technical Report RMRS-GTR5. USDA, Forest Service, Rocky Mountain Research Station, Fort Collins, CO. 440 pp.

Simons, D.B. and Albertson, M.L. (1963). Uniform Water Conveyance Channels in Alluvial Material. *Transactions of the American Society of Civil Engineers*. Paper No. 3399. Vol. 128, Part I. pp 65-107.

Sixta, M., Albert, J., Leon, C., and Julien, P.Y. (2003a). Bernalillo Bridge Reach. Highway 44 Bridge to Corrales Flood Channel Outfall. Hydraulic Modeling Analysis. 1962-2001. Middle Rio Grande, New Mexico. Prepared for U.S. Bureau of Reclamation. Albuquerque, New Mexico. Colorado State University, Fort Collins, CO. 87 pp.

Sixta, M., Albert, J., Leon, C., and Julien, P.Y. (2003b) San Felipe Reach. Arroyo Tonque to Angostura Diversion Dam. Hydraulic Modeling Analysis. 1962-1998. Middle Rio Grande, New Mexico. Prepared for U.S. Bureau of Reclamation. Albuquerque, New Mexico. Colorado State University, Fort Collins, CO. 85 pp.

Sixta, M. (2004). Hydraulic Modeling and Meander Migration of the Middle Rio Grande, New Mexico. M.S. Thesis. Colorado State University, Fort Collins, CO. 109 pp.

U.S. Army Corps of Engineers, USACE (2002). HEC-RAS River Analysis System. User's Manual. v. 3.1. U.S. Army Corps of Engineers Institute for Water Resources. Hydrologic Engineering Center, Davis, CA.

U.S. Army Corps of Engineers, USACE (2005). Upper Rio Grande Water Operations Model Physical Accounting Model Documentation. Retrieved September 15, 2005 from http://www.spa.usace.army.mil/urgwom/docintro.htm

U.S. Bureau of Reclamation, USBR. Middle Rio Grande Project Water Data. Available at http://www.usbr.gov/dataweb/html/ucmrgwatdata.html. Accessed September 1, 2005.

U.S. Geological Survey, USGS. Middle Rio Grande Basin Study. U.S. Department of the Interior, U.S. Geological Survey, Albuquerque, NM. Available at http://nm.water.usgs.gov/mrg/index.htm. Accessed August 20, 2005.

Van den Berg, J.H. (1995). Prediction of Alluvial Channel Pattern of Perennial Rivers. *Geomorphology*. 12, 259-279.

Williams, G. and Wolman, G. (1984). Downstream Effects of Dams on Alluvial Rivers. U.S. Geological Survey Professional Paper 1286, 83 pp.

Wargadalam, J. (1993). Hydraulic Geometry of Alluvial Channels. Ph.D. Dissertation. Colorado State University, Fort Collins, CO. 203 pp.

Watson, C., Biedenharn, D., Thorne, C. (2005) *Stream Rehabilitation*. Cottonwood Research LLC. Fort Collins, Colorado. 202pp.

Woodson, R.C. (1961). Stabilization of the Middle Rio Grande in New Mexico. *Proceedings of the American Society of Civil Engineers. Journal of the Waterways and Harbor Division*. 87:No. WW4: pp. 1-15

Woodson, R.C. and Martin, J.T. (1962). The Rio Grande Comprehensive Plan in New Mexico and its Effects on the River Regime Through the Middle Valley. Control of Alluvial Rivers by Steel Jetties. *Proceedings of the American Society of Civil Engineers. Journal of Waterways and Harbor Division.* Carlson, E. J. and Dodge E. A. eds. American Society of Civil Engineers, New York, NY, 53-81.

APPENDIX A – AERIAL PHOTO INFORMATION

			Mean Daily Discharge (cfs)			
Date	**Type**	**Scale**	**Otowi**	**Cochiti Dam**	**Albuquerque**	**Notes**
1918	topographic map	1:12,000	Mean = 1926 Max = 8410 Min = 375	No data	No data	Hand-drafted linens (39 sheets), USBR Albuquerque Office. Surveyed in 1918, published in 1922.
1935	aerial photo	1:8,000	Mean = 1520 Max = 7490 Min = 350	No data	No data	Black and white photography, USBR Albuquerque Area Office. Flown in 1935, published in 1936.
1949	aerial photo	1:5,000	Mean = 1833 Max = 10200 Min = 373	No data	Mean = 1690 Max = 10300 Min = 62	Photo-mosaic. J-Ammann Photogrammetric Engineers, San Antonio, TX. USBR Albuquerque Area Office.
March 15, 1962	aerial photo	1:4,800	824	No data	620	Photo-mosaic. Abram Aerial Survey Corp. Lansing, MI. USBR Albuquerque Area Office.
April, 1972	aerial photo	1:4,800	Mean = 741 Max = 1070 Min = 537	Mean = 632 Max = 870 Min = 464	Mean = 705 Max = 2540 Min = 116	Photo-mosaic. Limbaugh Engineers, Inc. Albuquerque, NM. USBR Albuquerque Area Office.
March 31, 1985	aerial photo	1:4,800	2310	650	491	Orthophoto. M&I Consulting Engineers, Fort Collins, CO. Aero-Metric Engineering, Sheboygan, MN. USBR Albuquerque Area Office.
February 24, 1992	aerial photo	1:4,800	1110	291	329	Ratio-rectified photo-mosaic. Koogle and Poules Engineering, Albuquerque, NM. USBR Albuquerque Area Office.
February 13, 2001	aerial photo	1:4,800	606	623	687	Ratio-rectified photo-mosaic. Pacific Western Technologies, Ltd., Albuquerque, NM. USBR Albuquerque Area Office.
March 2002	aerial photo	1:4,800	Mean = 703 Max = 902 Min = 497	Mean = 575 Max = 678 Min = 473	Mean = 501 Max = 603 Min = 404	Digital ortho-imagery. Pacific Western Technologies, Ltd. Albuquerque, NM. USBR Albuquerque Area Office.
Winter 2004	aerial photo	1:4,800	Mean = 737 Max = 2180 Min = 425	Mean = 649 Max = 1790 Min = 386	Mean = 657 Max = 1660 Min = 409	Photo-mosaic. USBR Albuqerque Area Office.

Table A-1 GIS coverage source, scale, and mean daily discharge statistics.
Source: Richard et al. (2000) and Oliver (2004)

APPENDIX B – CROSS-SECTION PLOTS

CO-2

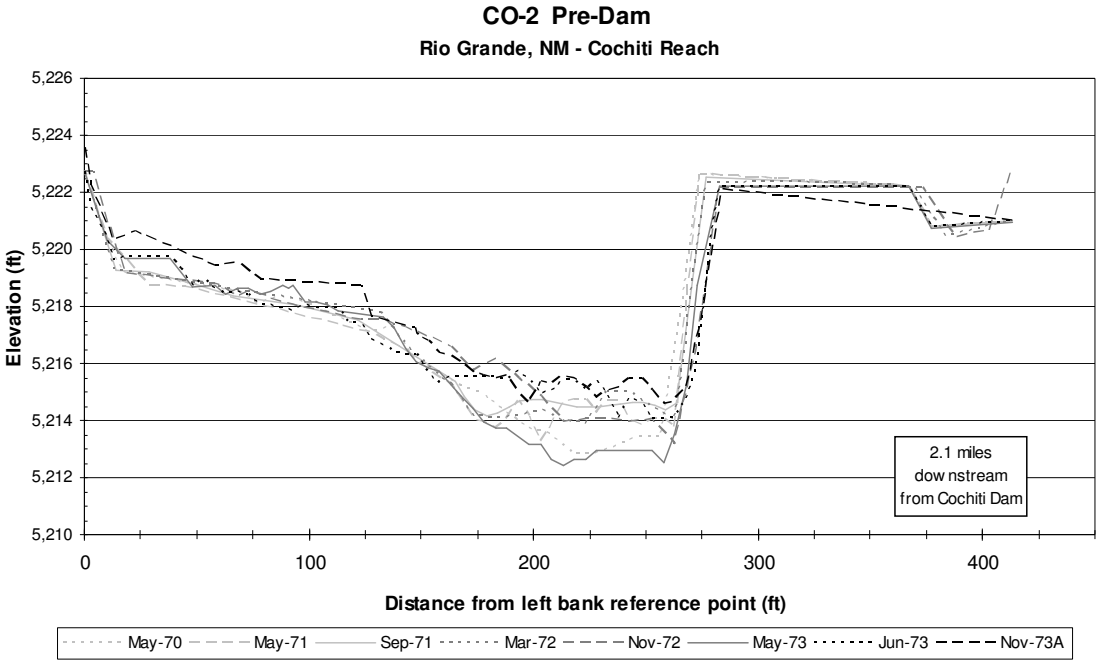

Figure B-1 Pre-dam conditions (all cross-sections up to Nov. 1973)

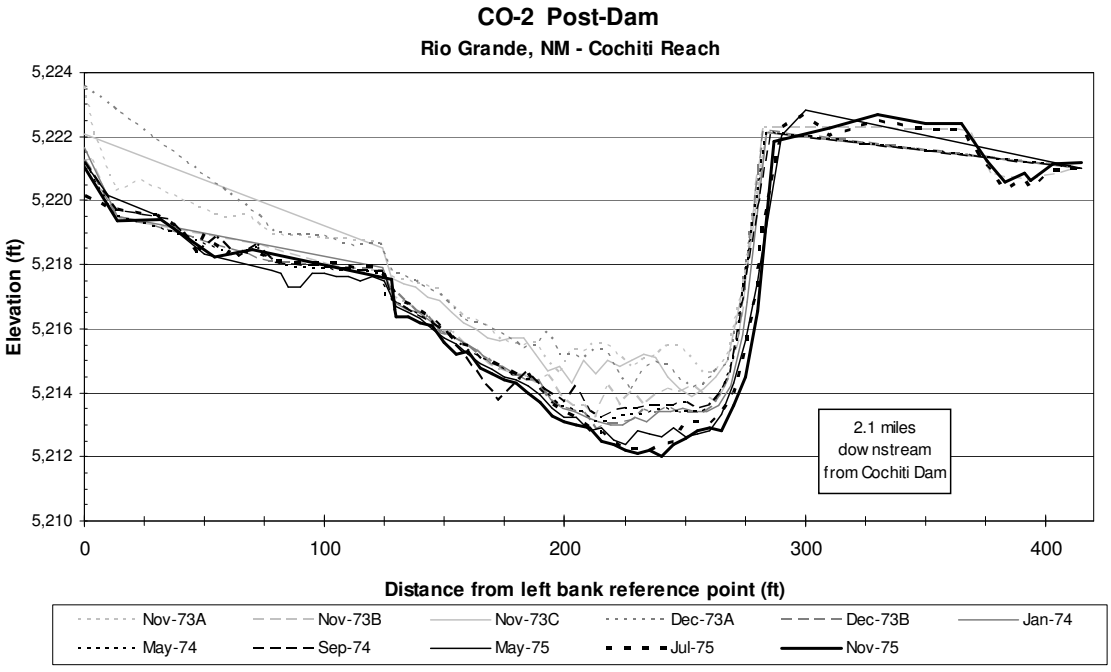

Figure B-2 Immediate post-dam conditions (after November 1973)

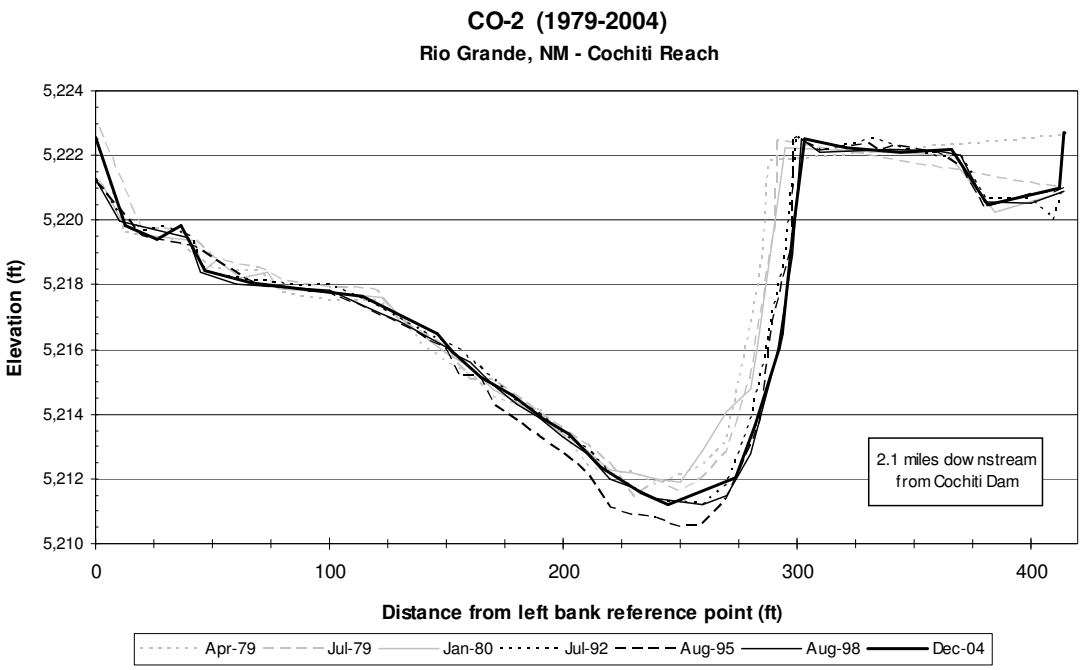

Figure B-3 Post-dam conditions (April 1979 to December 2004)

CO-3

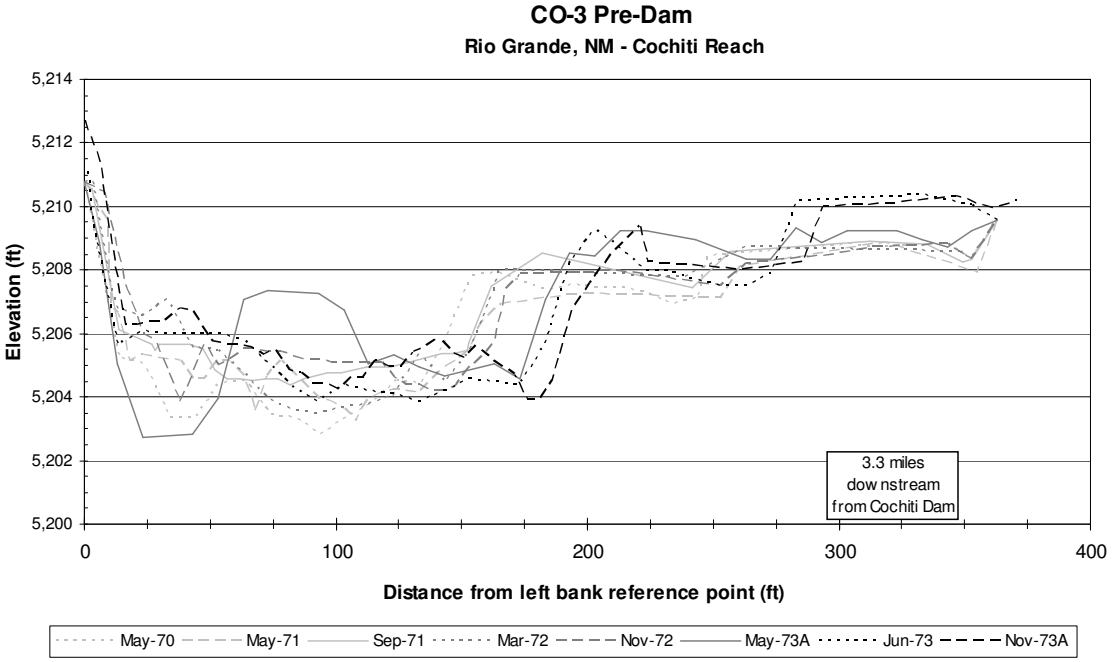

Figure B-4 Pre-dam conditions (all cross-sections up to Nov. 1973)

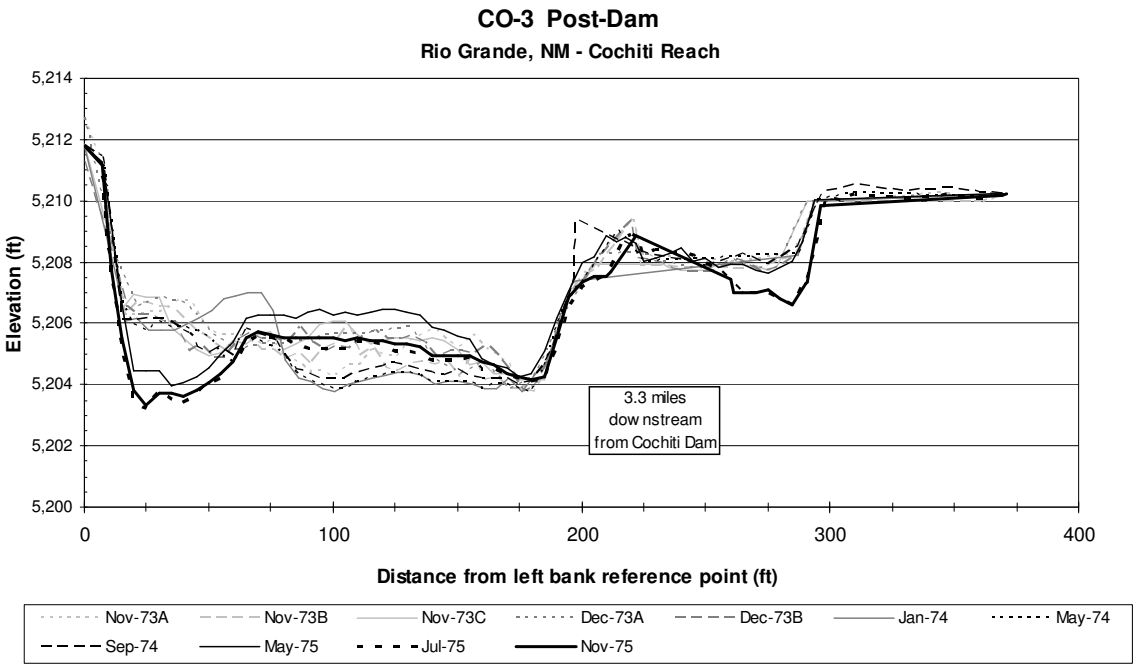

Figure B-5 Immediate post-dam conditions (after November 1973)

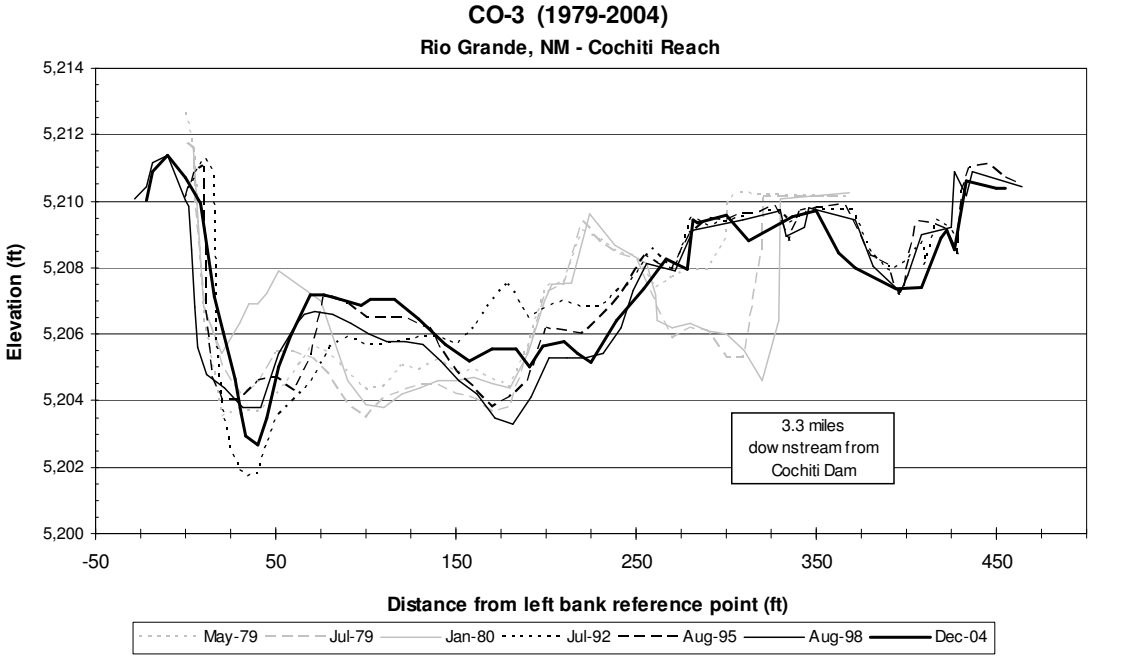

Figure B-6 Post-dam conditions (April 1979 to December 2004)

CO-4

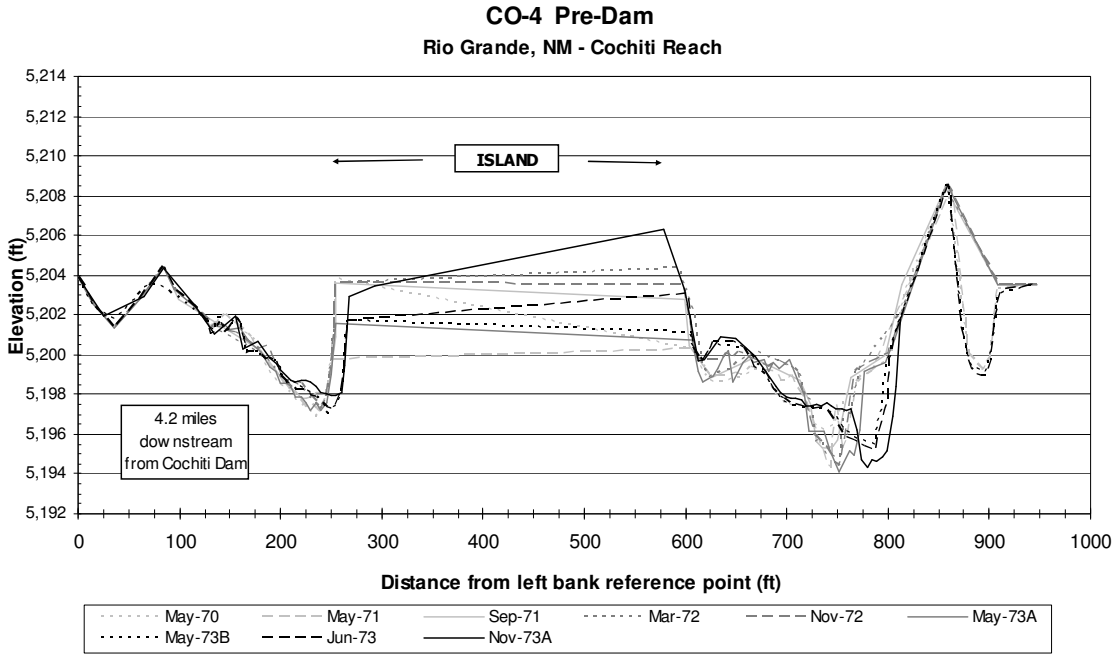

Figure B-7 Pre-dam conditions (all cross-sections up to Nov. 1973)

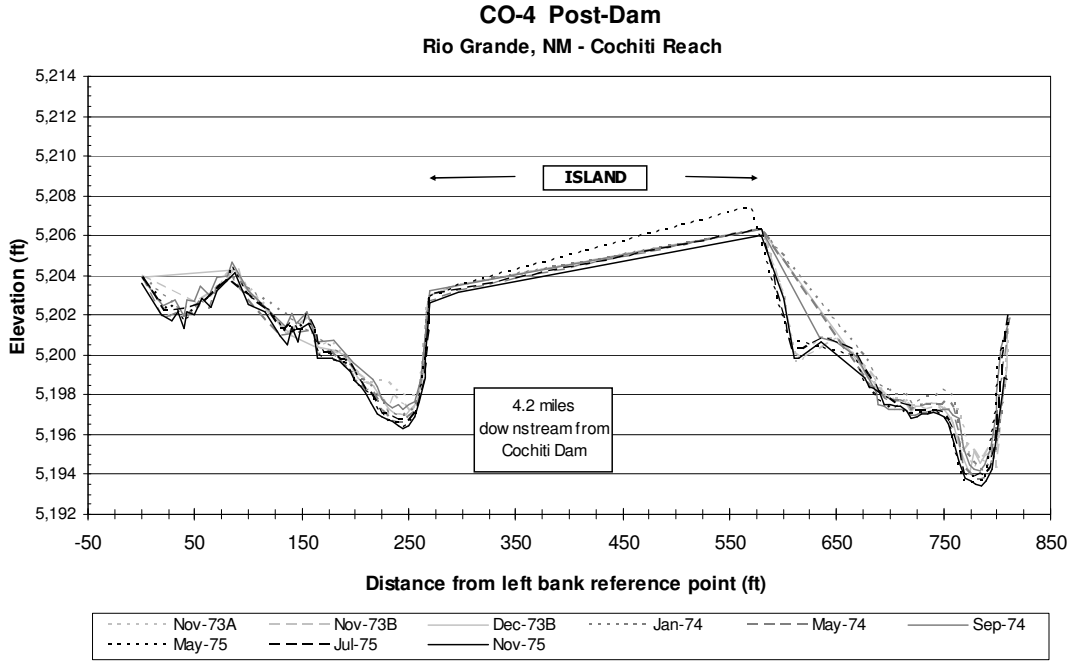

Figure B-8 Immediate post-dam conditions (after November 1973)

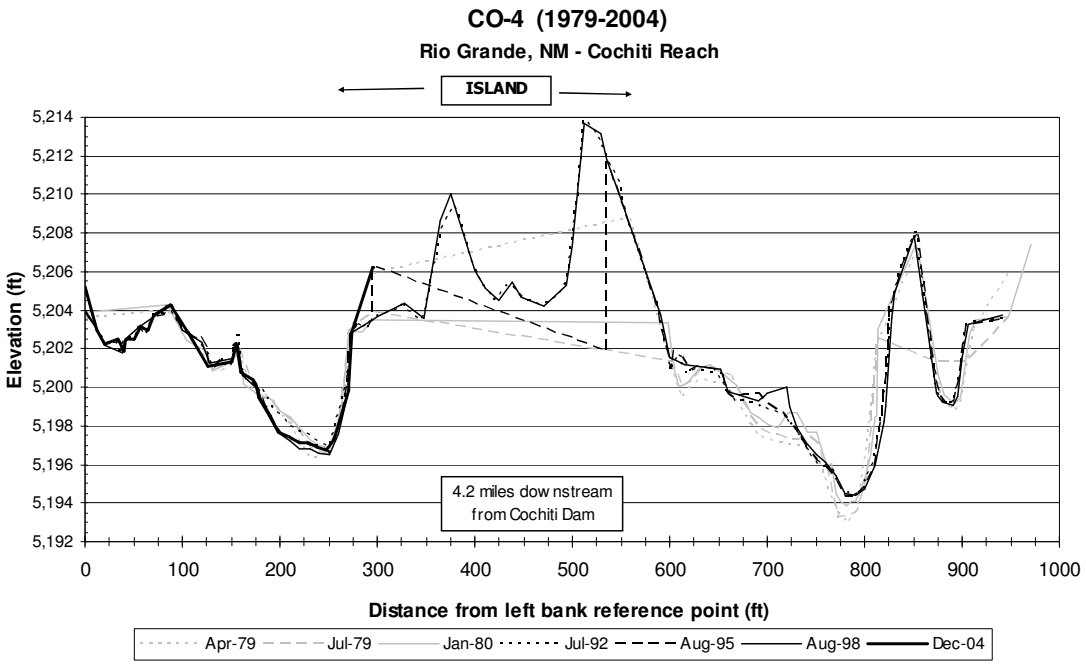

Figure B-9 Post-dam conditions (April 1979 to December 2004)

CO-5

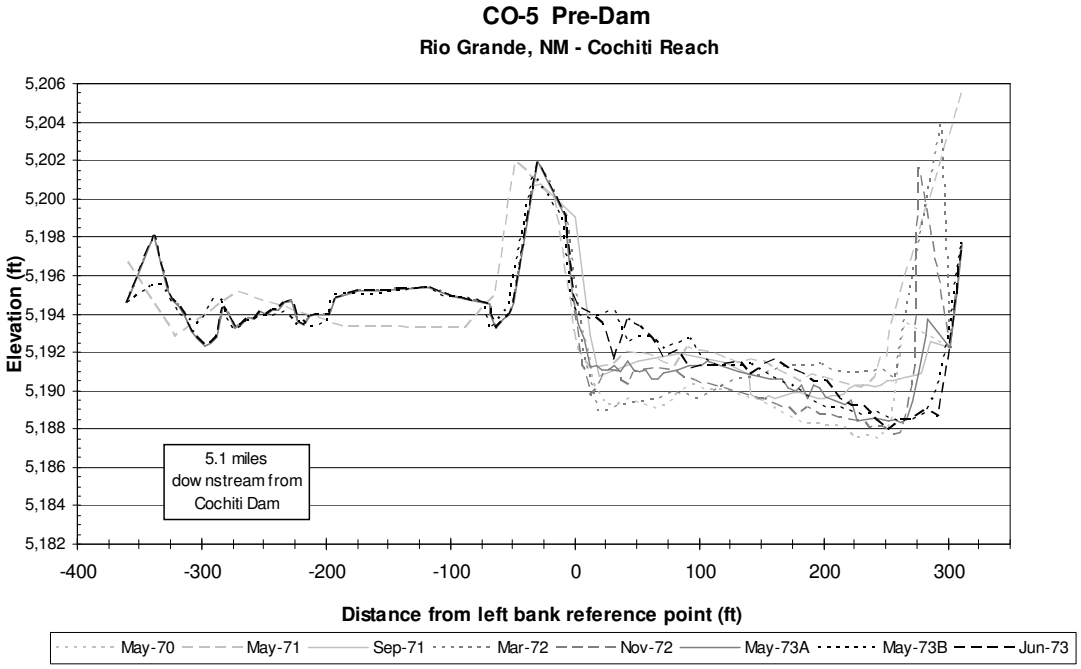

Figure B-10 Pre-dam conditions (all cross-sections up to Nov. 1973)

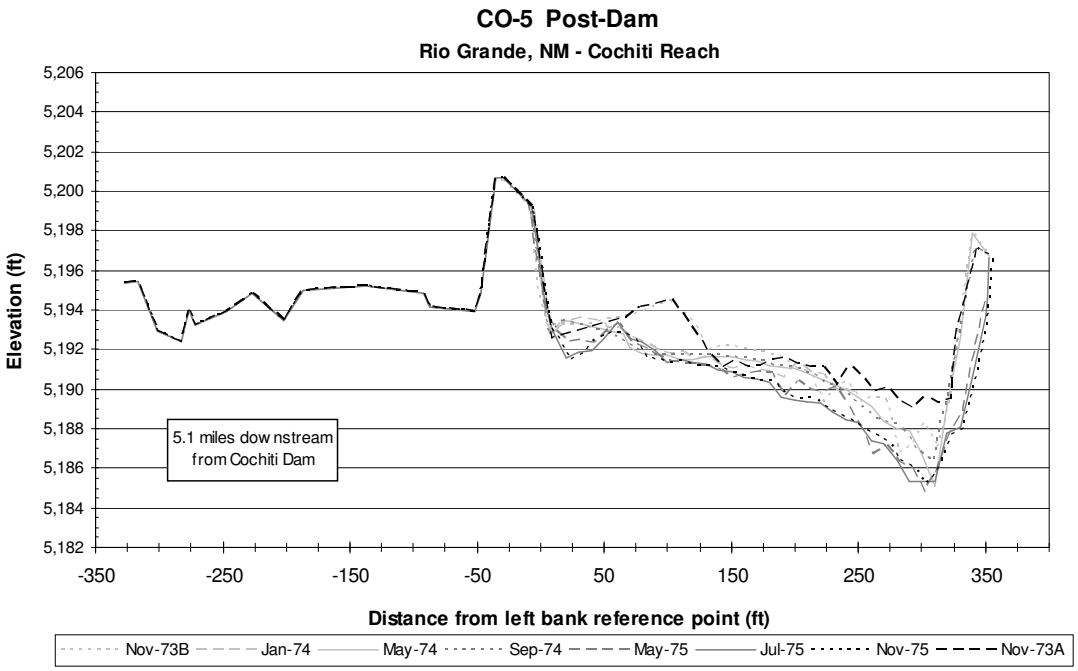

Figure B-11 Immediate post-dam conditions (after November 1973)

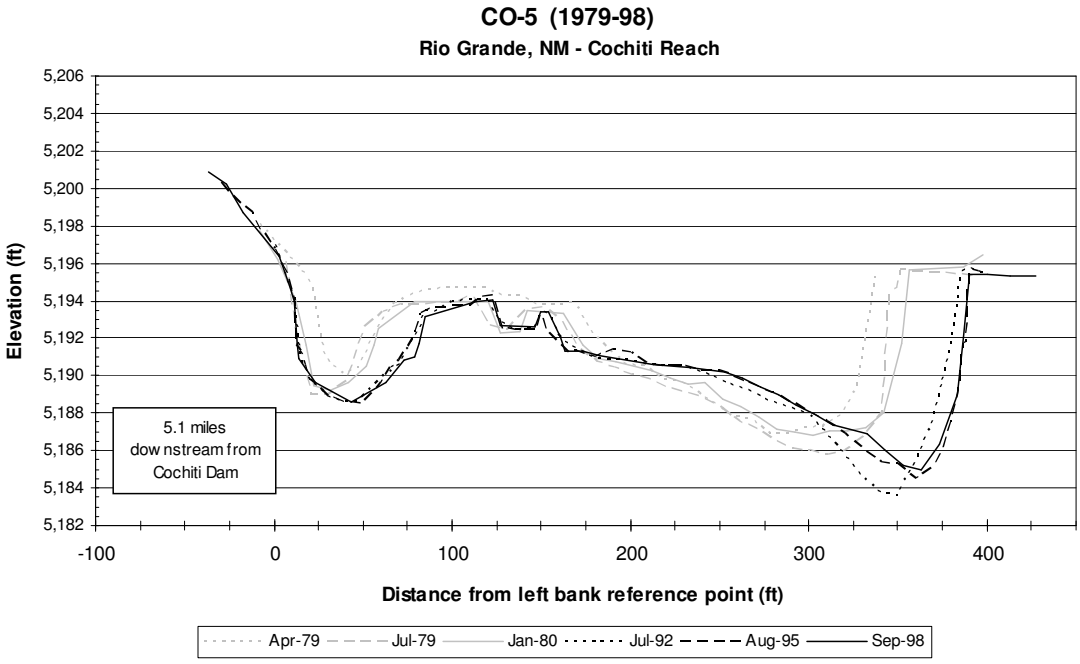

Figure B-12 Post-dam conditions (April 1979 to September 1998)

CO-6

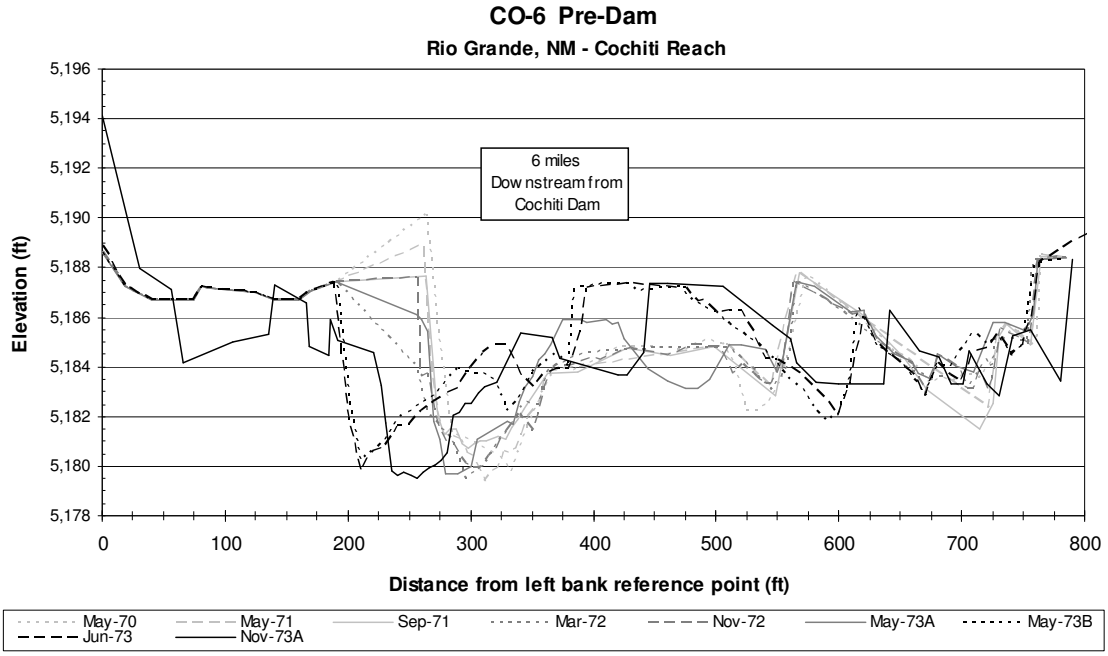

Figure B-13 Pre-dam conditions (all cross-sections up to Nov. 1973)

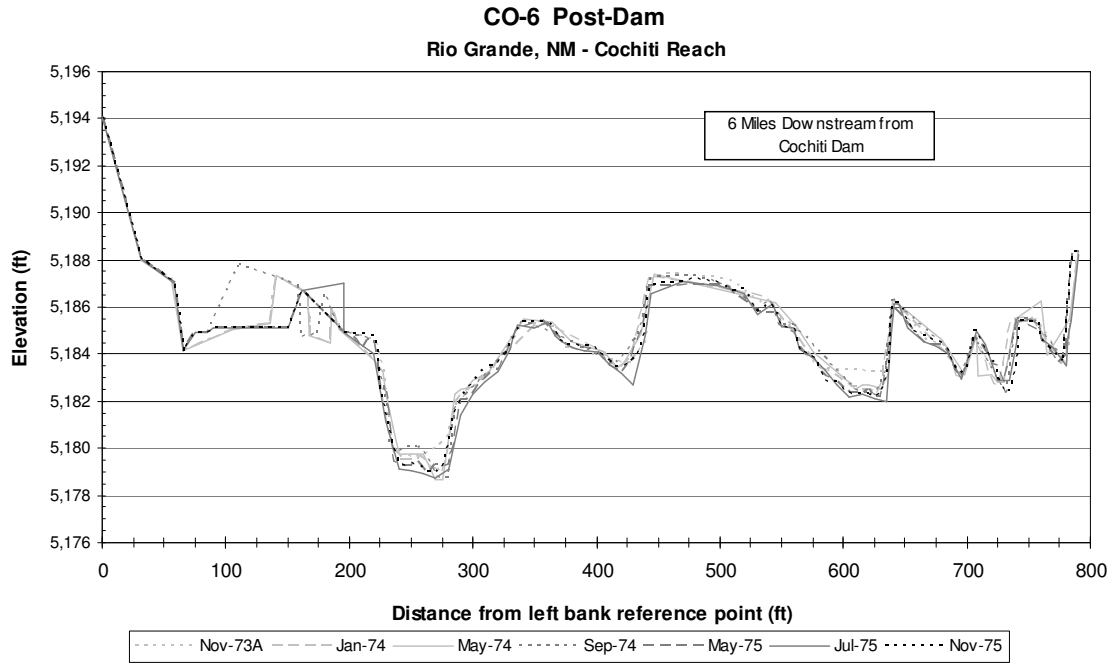

Figure B-14 Immediate post-dam conditions (after November 1973)

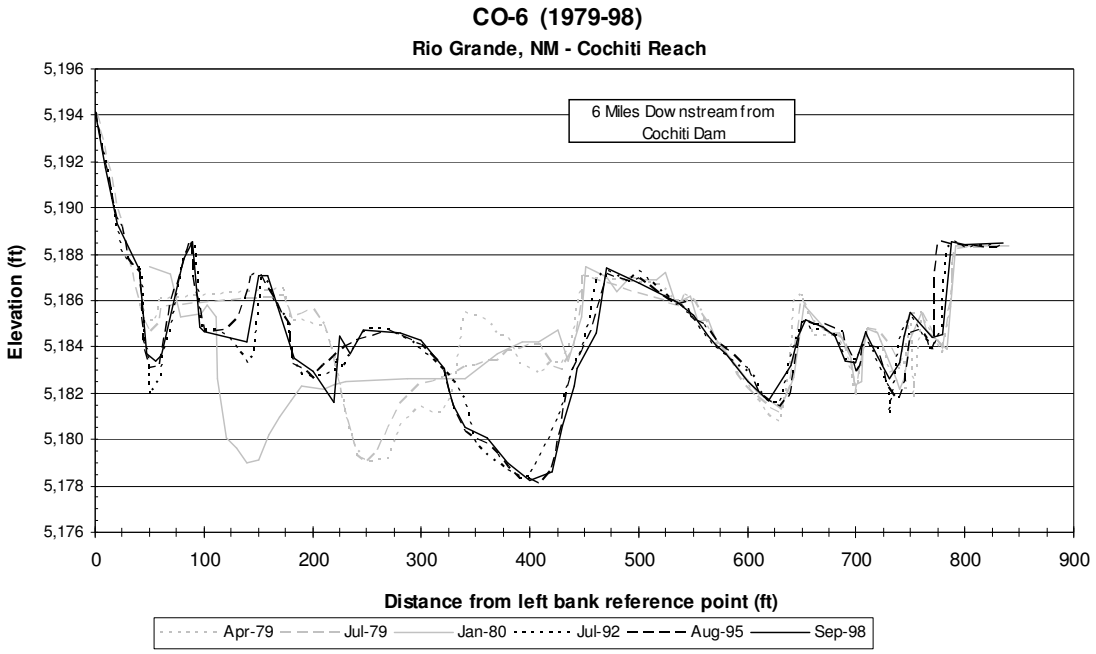

Figure B-15 Post-dam conditions (April 1979 to September 1998)

CO-7

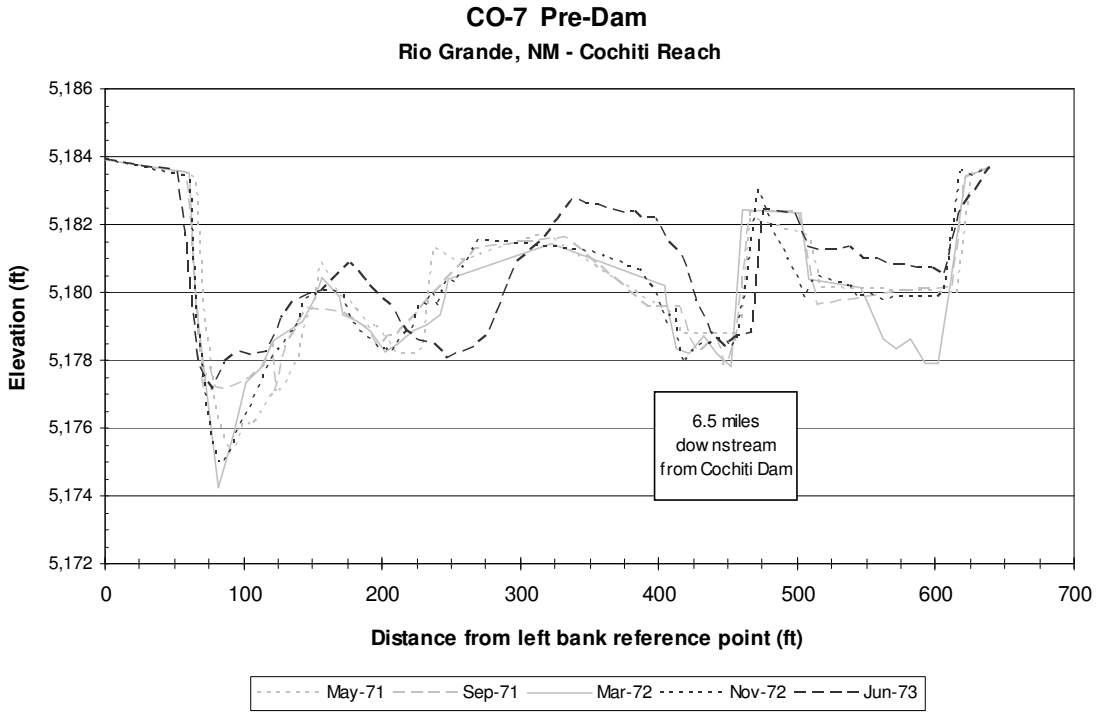

Figure B-16 Pre-dam conditions (all cross-sections up to Nov. 1973)

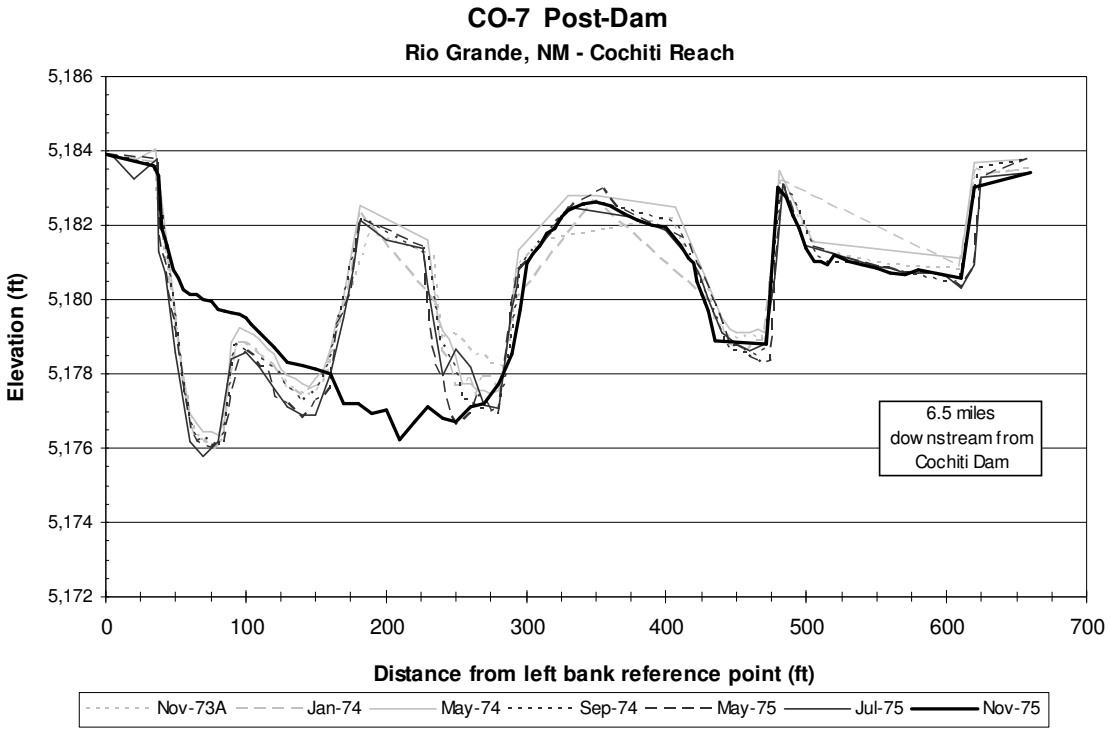

Figure B-17 Immediate post-dam conditions (after November 1973)

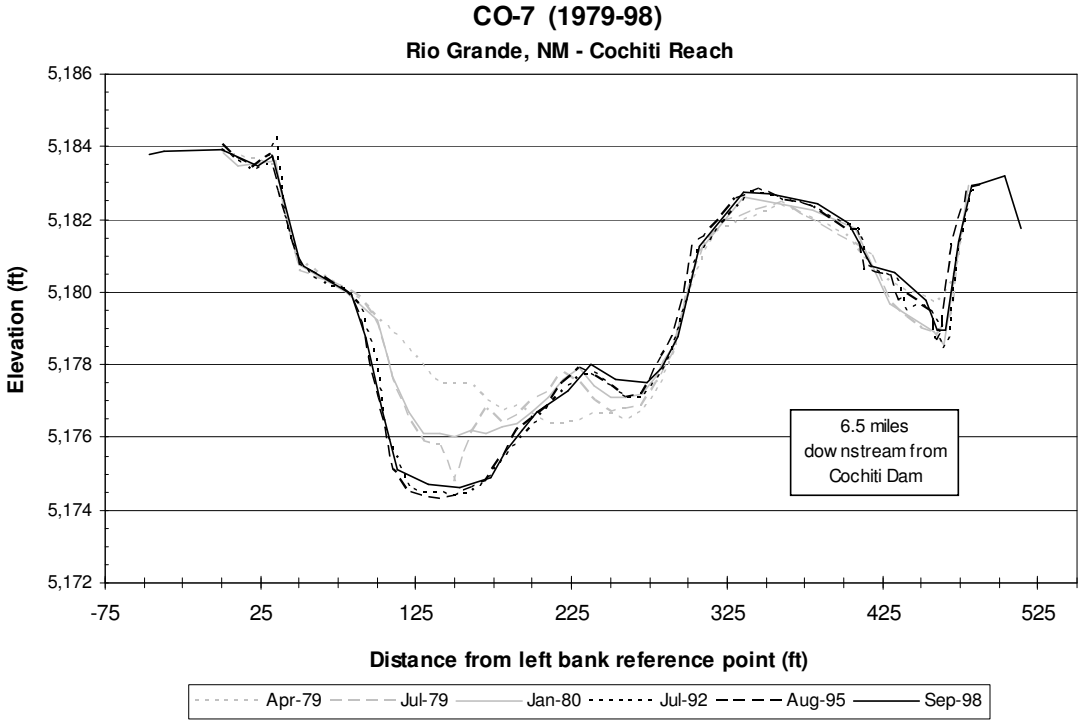

Figure B-18 Post-dam conditions (April 1979 to September 1998)

CO-8

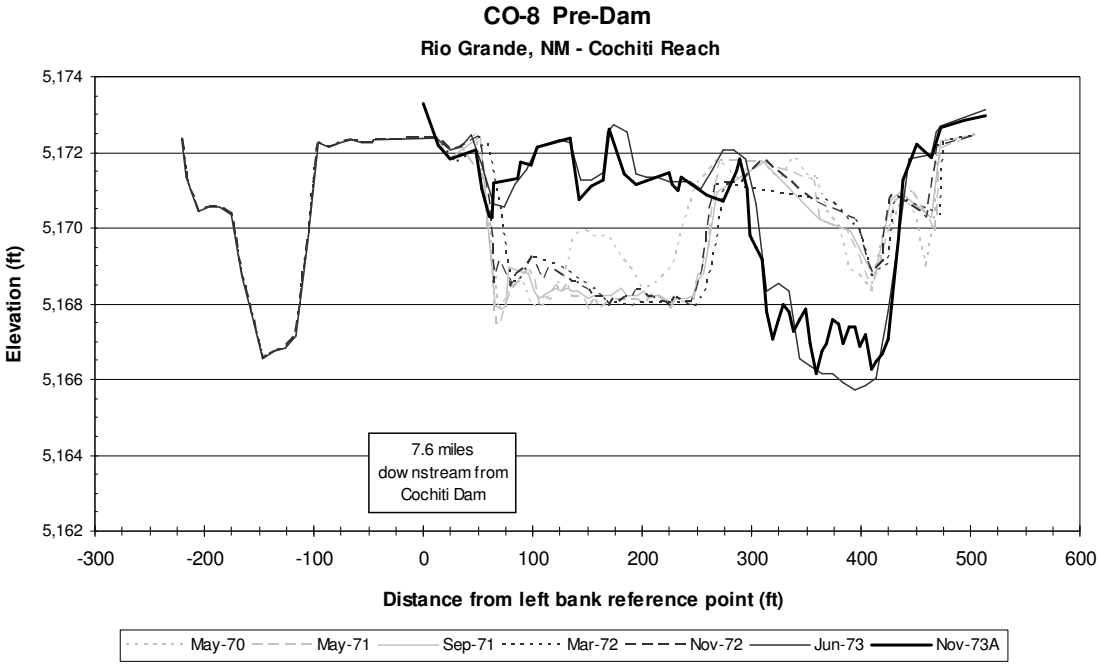

Figure B-19 Pre-dam conditions (all cross-sections up to Nov. 1973)

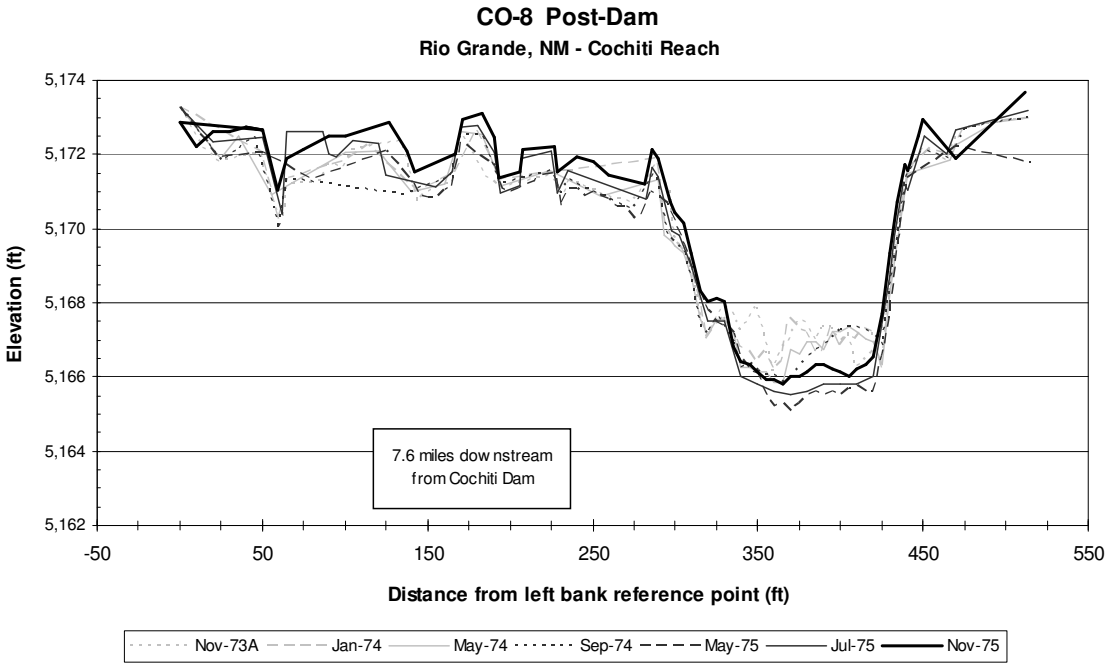

Figure B-20 Immediate post-dam conditions (after November 1973)

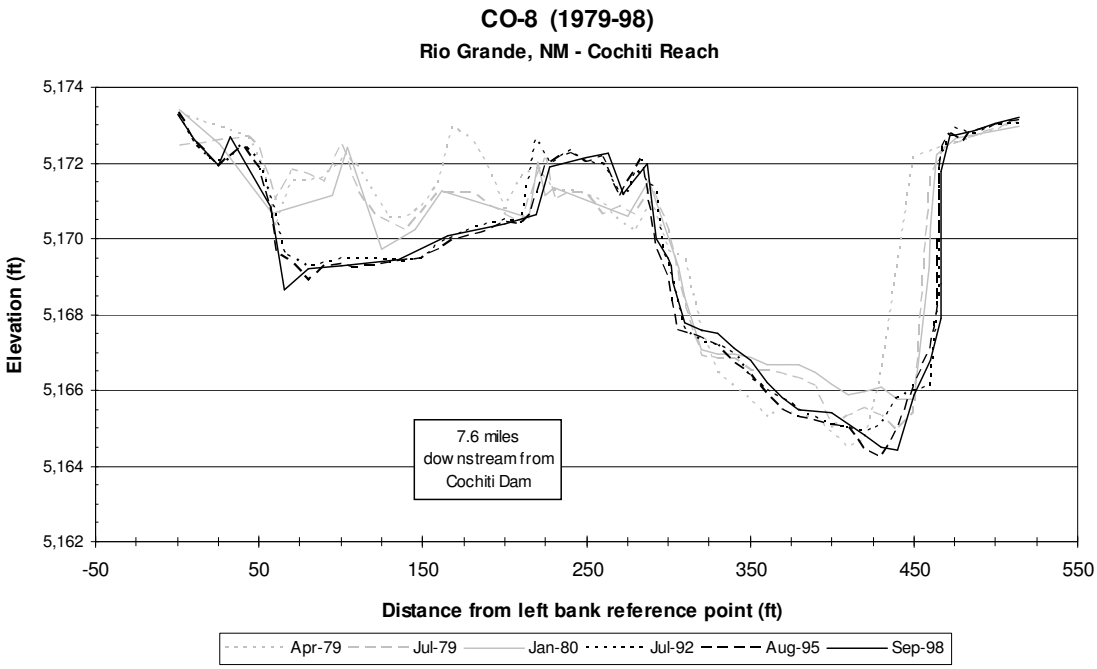

Figure B-21 Post-dam conditions (April 1979 to September 1998)

APPENDIX C – HEC-RAS HYDRAULIC GEOMETRY RESULTS

HEC-RAS Modeling Results for each agg/deg line at 5,000 cfs

HEC-RAS Plan: 1962aplan River: Middle Rio Grand Reach: Cochiti Dam Q = 5,000 cfs

Agg / Deg line	Min Ch El (ft)	W.S. Elev (ft)	E.G. Elev (ft)	E.G. Slope (ft/ft)	Velocity (ft/s)	Flow Area (sq ft)	Top Width (ft)	Froude #	Wetted P (ft)	WS Slope (ft/ft)
19	5225.6	5228.9	5229.74	0.002311	7.34	680.81	225.78	0.75	230.9	-0.00201
20	5224.8	5227.39	5228.52	0.003904	8.56	584.45	231.02	0.95	233.63	-0.00201
22	5221.8	5226.89	5227.28	0.001486	5	1000.31	426.41	0.58	433.93	-0.00133
23	5222.5	5226.06	5226.61	0.001989	5.94	842.2	344.55	0.67	351.17	-0.00131
24	5221.7	5225.58	5225.92	0.001165	4.63	1079.22	432.11	0.52	437.09	-0.00086
25	5220.7	5225.2	5225.45	0.000754	4.05	1247.94	436	0.42	442.14	-0.00053
26	5219.2	5225.05	5225.14	0.000372	2.43	2068.69	919.6	0.29	929.31	-0.00059
27	5220.6	5224.61	5224.85	0.000757	3.93	1271.46	472.6	0.42	476.71	-0.00188
28	5220.9	5223.17	5223.94	0.00456	7.05	709.08	422.81	0.96	425.57	-0.00177
29	5218.9	5222.84	5223.05	0.000901	3.66	1367.49	645.13	0.44	651.66	-0.00152
30	5217.7	5221.65	5222.1	0.00116	5.44	932.3	289.34	0.54	292.14	-0.00237
31	5216.3	5220.47	5221.31	0.00195	7.36	695.74	197.53	0.7	201.9	-0.00188
32	5215.8	5219.77	5220.38	0.001484	6.26	820.27	243.35	0.61	246.6	-0.00126
33	5215.6	5219.21	5219.69	0.001111	5.59	894.07	260.83	0.53	263.42	-0.00093
34	5214.7	5218.84	5219.18	0.000777	4.7	1099.4	304.82	0.44	310.54	-0.00122
35	5214.7	5217.99	5218.55	0.001864	6.06	851.12	312.69	0.66	316.88	-0.00127
36	5214.6	5217.57	5217.86	0.000887	4.3	1195.5	425.61	0.46	426.83	-0.0014
37	5212.3	5216.59	5217.24	0.001489	6.44	803.19	225.75	0.61	229.78	-0.00169
38	5212.1	5215.88	5216.47	0.001425	6.14	837.84	247.41	0.6	250.29	-0.0016
39	5211	5214.99	5215.63	0.002063	6.45	822.2	285.23	0.69	292.04	-0.00126
40	5210.8	5214.62	5214.92	0.000824	4.39	1161.82	381.92	0.45	385.95	-0.00134
41	5209.4	5213.65	5214.31	0.00179	6.52	785.92	252.9	0.66	256.21	-0.00163
42	5207.4	5212.99	5213.48	0.001347	5.62	907.86	295.1	0.57	300.41	-0.00162
43	5207.8	5212.03	5212.73	0.001594	6.71	758.43	215.21	0.64	219.23	-0.0018
44	5206.9	5211.19	5211.79	0.002224	6.21	805.62	338.05	0.71	341.75	-0.00139
45	5205.2	5210.64	5211.04	0.001565	5.06	988.36	430.93	0.59	436.75	-0.00094
46	5206.8	5210.25	5210.48	0.000668	3.86	1504.54	445.68	0.4	447.44	-0.00079
47	5204.7	5209.85	5210.1	0.000837	4.09	1382.51	451.75	0.44	458.43	-0.00117
48	5204.5	5209.08	5209.54	0.001193	5.5	1018.93	281.39	0.54	285.21	-0.00138
49	5203.4	5208.47	5208.88	0.00125	5.15	1010.78	348.01	0.54	352.73	-0.00137
50	5203.7	5207.71	5208.14	0.00164	5.38	1131.1	372	0.61	379.4	-0.00207
51	5203.8	5206.4	5206.83	0.001471	5.26	1007.97	374.56	0.58	375.84	-0.00189
52	5201.8	5205.82	5206.18	0.001434	4.77	1076.32	467.5	0.56	474.03	-0.00137
53	5202.3	5205.03	5205.39	0.001278	4.94	1446.16	375.13	0.54	379.04	-0.00136
54	5200.3	5204.46	5204.71	0.001263	4.2	1915.05	516.53	0.52	522.77	-0.00153
55	5200	5203.5	5203.82	0.001894	4.65	1310.24	587.75	0.62	598.16	-0.0019
56	5198.2	5202.56	5202.96	0.002062	5.37	1496.33	400.82	0.66	408.44	-0.00148
57	5197.4	5202.02	5202.25	0.001168	4.07	1820.97	535.66	0.5	544.13	-0.00105
58	5197.4	5201.51	5201.69	0.001266	3.62	2000.13	731.48	0.5	740.11	-0.00103
59	5197.1	5200.99	5201.14	0.00073	3.27	2192.82	667.43	0.4	671.4	-0.00183
60	5196.6	5199.68	5200.41	0.00251	6.97	918.31	267.36	0.76	270.47	-0.00226
61	5195.5	5198.73	5199.28	0.001621	6.05	995.95	278.32	0.62	282.49	-0.00266
62	5195.2	5197.02	5197.9	0.004794	7.57	685.07	368.1	1	369.13	-0.00161

63	5193.6	5197.12	5197.22	0.000341	2.59	2591.21	692.73	0.28	694.36	-0.00064
64	5191.3	5196.38	5196.82	0.001931	5.46	1190.17	392.42	0.65	397.63	-0.00156
65	5191.6	5195.56	5196.06	0.002058	5.74	1010.02	373.56	0.68	376.61	-0.00159
66	5191.3	5194.79	5195.39	0.002545	6.28	891.46	356.5	0.75	358.95	-0.00126
67	5190.1	5194.3	5194.52	0.000857	3.87	1663.77	503.88	0.44	512.44	-0.00176
68	5190.8	5193.03	5193.57	0.002834	6.01	990.95	422.38	0.77	424.76	-0.00238
69	5188.1	5191.92	5192.18	0.001264	4.07	1344.84	624.62	0.52	629.85	-0.00186
70	5187.2	5191.17	5191.36	0.001308	3.59	1427.17	893.91	0.51	898.83	-0.00169
71	5186.8	5190.23	5190.45	0.001614	3.79	1374.06	914.71	0.56	917.09	-0.0018
72	5185.5	5189.37	5189.62	0.001655	4.01	1246.44	808.55	0.57	815.03	-0.00195
73	5184	5188.28	5188.63	0.002032	4.79	1050.48	605.71	0.64	610.15	-0.00189
74	5183.4	5187.48	5187.74	0.001139	4.06	1404.56	587.86	0.5	592.11	-0.00138
75	5182.1	5186.9	5187.17	0.001051	4.12	1312	529.45	0.48	536.71	-0.00104
76	5181.1	5186.44	5186.67	0.000682	3.88	1557.27	440	0.4	446.24	-0.00114
77	5181.9	5185.76	5186.19	0.001307	5.46	1371.58	289.52	0.56	291.77	-0.00171
78	5181	5184.73	5185.3	0.002655	6.4	1239.29	318.78	0.76	321.99	-0.00157
79	5180.4	5184.19	5184.51	0.000813	4.64	1420.55	317.7	0.45	319.65	-0.0016
80	5177.8	5183.13	5183.71	0.002476	6.48	1144.75	290.18	0.74	296.36	-0.00225
81	5179.1	5181.94	5182.36	0.001848	5.19	964.37	463.8	0.63	465.95	-0.00256
82	5177.3	5180.57	5181.19	0.002381	6.3	796.15	343.26	0.73	346.56	-0.00237
83	5176.7	5179.57	5180.13	0.001915	6.03	829.35	325.55	0.67	328.48	-0.00166
84	5175.3	5178.91	5179.35	0.001325	5.33	943.15	334.67	0.56	338.29	-0.00144
85	5174.1	5178.13	5178.64	0.001652	5.74	871.23	323.63	0.62	332.52	-0.0013
86	5172.7	5177.61	5178.03	0.000887	5.19	962.82	261.12	0.48	267.85	-0.00078
87	5171	5177.35	5177.58	0.000613	3.81	1311.26	428.6	0.38	439.6	-0.00114
88	5171.9	5176.47	5177.12	0.001699	6.62	1015.36	219.07	0.64	226.39	-0.00164
89	5171.1	5175.71	5176.39	0.001777	6.78	954.35	213.46	0.66	219.59	-0.00048
90	5170.4	5175.99	5176.04	0.000147	1.78	2896.86	997.28	0.19	1005.62	0.00015
91	5169.4	5175.86	5175.96	0.000355	2.54	2014.01	793.15	0.28	803.25	-0.00032
92	5168.2	5175.67	5175.75	0.000394	2.31	2255.47	1092.91	0.29	1101.65	-0.00021
93	5167.9	5175.65	5175.68	0.000049	1.39	4354.38	800	0.12	806.89	-0.00008
94	5167.3	5175.59	5175.65	0.000101	1.96	4060.59	542.55	0.17	552.51	-0.00010
95	5167.5	5175.55	5175.6	0.000083	1.87	4381.14	530	0.15	533.1	

Table C-1 1962 HEC-RAS Modeling Results for agg/degs at 5,000 cfs

HEC-RAS Plan: 1972plan River: Middle Rio Grand Reach: Cochiti Dam Q = 5,000 cfs

Agg /Deg line	Min Ch El (ft)	W.S. Elev (ft)	E.G. Elev (ft)	E.G. Slope (ft/ft)	Velocity (ft/s)	Flow Area (sq ft)	Top Width (ft)	Froude #	Wetted P (ft)	WS Slope (ft/ft)
19	5224.3	5228.06	5228.65	0.001425	6.2	806.03	241.03	0.6	244.98	-0.00106
20	5223.8	5227.47	5228.09	0.001378	6.33	789.77	224.25	0.59	227.08	-0.00106
22	5223.1	5227	5227.39	0.001413	5.03	994.64	406	0.57	411.8	-0.00114
23	5221.7	5226.33	5226.8	0.001624	5.69	1101.23	307.48	0.61	315.2	-0.00147
24	5221.3	5225.53	5226.1	0.001654	6.27	984.94	245.23	0.63	251.44	-0.00145
25	5220.8	5224.88	5225.37	0.001308	5.75	1080.77	257.82	0.57	262.85	-0.00116
26	5220	5224.37	5224.76	0.001028	5.17	1204.49	284.35	0.5	289.52	-0.00067
27	5220	5224.21	5224.36	0.0004	3.08	1620.86	532.45	0.31	541.75	-0.00069
28	5218.9	5223.68	5224.02	0.000891	4.69	1065.26	335.91	0.46	346.06	-0.00086

29	5218.8	5223.35	5223.62	0.00089	4.18	1196.56	454.94	0.45	462.29	-0.00114
30	5218.3	5222.54	5222.89	0.000738	4.76	1060.4	287.87	0.44	290.42	-0.00223
31	5216.9	5221.12	5222.19	0.002458	8.29	612.34	174.3	0.79	178.69	-0.00213
32	5216.2	5220.41	5221.1	0.001543	6.67	754.59	213.25	0.63	217.03	-0.00101
33	5216	5220.11	5220.48	0.000722	4.86	1030.21	268.65	0.44	271.21	-0.00081
34	5215.1	5219.6	5220.02	0.001137	5.19	997.96	318.57	0.53	322.41	-0.0016
35	5214.1	5218.51	5219.23	0.001903	6.82	772.67	235.27	0.68	239.51	-0.00156
36	5214	5218.04	5218.45	0.001077	5.13	1012.74	314.19	0.51	317.58	-0.00165
37	5213.3	5216.86	5217.66	0.002008	7.17	700.73	216.91	0.71	220.41	-0.00181
38	5212.1	5216.23	5216.8	0.001221	6.05	843.65	228.51	0.56	231.67	-0.00125
39	5208.4	5215.61	5216.16	0.001351	5.96	851.76	252.17	0.58	260.46	-0.00182
40	5210.8	5214.41	5215.32	0.002057	7.65	655.44	187.33	0.72	191.13	-0.00174
41	5210	5213.87	5214.45	0.00124	6.09	832.41	227.33	0.57	230.64	-0.00119
42	5208.8	5213.22	5213.84	0.001175	6.29	807.72	199.86	0.56	204.32	-0.00137
43	5208.5	5212.5	5213.17	0.001471	6.6	778.54	210.29	0.61	214.14	-0.00129
44	5209.2	5211.93	5212.34	0.001622	5.14	972.55	428.85	0.6	431.92	-0.00181
45	5208.3	5210.69	5211.43	0.003809	6.9	724.51	388.54	0.89	392.4	-0.00199
46	5205.4	5209.94	5210.33	0.001141	5.01	998.76	350.73	0.52	354.6	-0.00119
47	5204.2	5209.5	5209.79	0.000911	4.35	1167.57	414.72	0.46	424.62	-0.00111
48	5205.4	5208.83	5209.25	0.001024	5.22	989.49	290.8	0.51	293.54	-0.00125
49	5204.3	5208.25	5208.64	0.00124	5.07	1032.61	357.93	0.54	364.23	-0.00109
50	5204.2	5207.74	5208.08	0.00094	4.65	1142.14	361.48	0.48	366.42	-0.00204
51	5203.8	5206.21	5206.81	0.002613	6.22	814.31	380.72	0.75	383.61	-0.00273
52	5202.1	5205.01	5205.65	0.002764	6.46	843.86	352.87	0.78	356.49	-0.00239
53	5200.6	5203.82	5204.34	0.001777	5.83	862.73	328.46	0.64	337.19	-0.00163
54	5199	5203.38	5203.65	0.000877	4.19	1317.5	444.38	0.45	450.35	-0.00136
55	5198.3	5202.46	5202.91	0.001931	5.36	988.51	433.47	0.65	440.27	-0.0015
56	5198.4	5201.88	5202.24	0.001182	4.91	1373.57	361.59	0.53	366.43	-0.00125
57	5197.3	5201.21	5201.67	0.001429	5.44	971.75	330.32	0.58	338.51	-0.00152
58	5196.3	5200.36	5200.86	0.002337	5.71	1020.25	421.46	0.7	429.31	-0.00192
59	5195.6	5199.29	5199.74	0.001632	5.38	1079.11	373.68	0.61	381.86	-0.00152
60	5194.5	5198.84	5199.11	0.000727	4.2	1389.75	381.79	0.42	384.93	-0.00153
61	5192.1	5197.76	5198.39	0.002725	6.4	861.65	358.12	0.77	363.83	-0.00229
62	5191.7	5196.55	5197.07	0.002261	5.79	890.55	404.11	0.7	409.21	-0.00228
63	5190.2	5195.48	5196.03	0.001806	5.98	896.43	311.13	0.65	317.47	-0.00198
64	5190	5194.57	5195.06	0.001672	5.64	983.09	338.81	0.62	343.89	-0.00139
65	5189.8	5194.09	5194.47	0.001293	5	1059.39	380.75	0.55	385.74	-0.00079
66	5189.7	5193.78	5194.1	0.001151	4.51	1151	455.2	0.51	459.99	-0.00086
67	5189	5193.23	5193.52	0.000934	4.32	1240.52	432.37	0.47	437.09	-0.00188
68	5188.8	5191.9	5192.51	0.002788	6.34	875.14	365.29	0.77	374.39	-0.00205
69	5186.1	5191.18	5191.42	0.000813	3.98	1460.59	467.92	0.43	476.25	-0.00156
70	5184.5	5190.34	5190.71	0.001657	4.95	1208.53	455.89	0.6	464.55	-0.00166
71	5184.6	5189.52	5189.81	0.001202	4.37	1348.94	488.31	0.51	496.18	-0.00142
72	5184.9	5188.92	5189.22	0.001126	4.53	1436.79	408.7	0.5	418.48	-0.00208
73	5184	5187.44	5188.22	0.003206	7.32	893.26	277.4	0.85	280.61	-0.00239
74	5181.8	5186.53	5186.9	0.001438	4.86	1029.14	445.49	0.56	454.46	-0.00165
75	5180.6	5185.79	5186.16	0.001393	4.92	1021.58	416.52	0.55	430.44	-0.00151
76	5181.3	5185.02	5185.42	0.001166	5.12	982.22	337.95	0.53	341.16	-0.00137
77	5180.1	5184.42	5184.89	0.000971	5.53	1163.95	235.74	0.5	239.13	-0.00104
78	5179.1	5183.98	5184.43	0.000886	5.47	1197.86	222.76	0.48	227.15	-0.00176

79	5179.1	5182.66	5183.57	0.003249	8.05	866.03	211.21	0.87	214.94	-0.00168
80	5178.4	5182.3	5182.57	0.000743	4.23	1356.7	375.8	0.43	378.85	-0.00124
81	5177	5181.42	5181.86	0.001886	5.35	933.85	429.45	0.64	436.83	-0.00199
82	5176.5	5180.31	5180.84	0.001801	5.94	1063.4	306.49	0.64	315.67	-0.00169
83	5174.6	5179.73	5180.1	0.001139	4.98	1271.61	339.18	0.52	347.38	-0.00116
84	5175.4	5179.15	5179.57	0.001081	5.35	1288.99	269.72	0.52	275.88	-0.00109
85	5173.5	5178.64	5179.02	0.001154	5.09	1320.47	317.36	0.53	322.31	-0.00097
86	5173	5178.18	5178.45	0.001041	4.31	1428.48	450.26	0.49	455.1	-0.00112
87	5172.6	5177.52	5177.84	0.001201	4.55	1098.59	460.27	0.52	467.42	-0.00176
88	5172	5176.42	5177.16	0.001895	7.02	870.14	207.65	0.68	214.53	-0.0019
89	5171.8	5175.62	5176.29	0.002136	6.69	892.99	259.1	0.71	264.55	-0.0012
90	5170.2	5175.22	5175.41	0.001404	3.53	1460.75	966.44	0.52	985.03	-0.00101
91	5170.8	5174.61	5174.91	0.001198	4.37	1145.04	512.62	0.52	516.79	-0.00127
92	5167.7	5173.95	5174.24	0.001327	4.31	1160.44	566.16	0.53	577.7	-0.00107
93	5169.2	5173.54	5173.72	0.000702	3.45	1447.64	616.25	0.4	623.16	-0.00107
94	5168.2	5172.88	5173.29	0.00118	5.12	976.02	332.61	0.53	343.26	-0.00119
95	5165.4	5172.35	5172.73	0.001024	4.97	1005.43	325.36	0.5	332.33	

Table C-2 1972 HEC-RAS Modeling Results for agg/degs at 5,000 cfs

HEC-RAS Plan: 1992plan River: Middle Rio Grand Reach: Cochiti Dam Q = 5,000 cfs

Agg /Deg line	Min Ch El (ft)	W.S. Elev (ft)	E.G. Elev (ft)	E.G. Slope (ft/ft)	Velocity (ft/s)	Flow Area (sq ft)	Top Width (ft)	Froude #	Wetted P (ft)	WS Slope (ft/ft)
19	5225.6	5228.24	5229	0.003036	7.57	1121.72	222.66	0.84	223.87	-0.00032
20	5223.9	5228.16	5228.36	0.000615	3.58	1397.13	514.24	0.38	516.03	-0.00032
22	5223.8	5227.92	5228.08	0.000602	3.13	1599.31	708.57	0.37	712.24	-0.00098
23	5224.2	5227.18	5227.63	0.002579	5.49	1097.09	485.66	0.73	486.36	-0.00145
24	5223	5226.47	5226.85	0.001313	5.12	1163.54	349.31	0.56	351.27	-0.00126
25	5221.9	5225.92	5226.3	0.001014	5.15	1255.87	280.3	0.5	282.93	-0.00227
26	5222.1	5224.2	5225.2	0.006258	8.54	768.39	291.77	1.13	293.12	-0.00192
27	5219.6	5224	5224.12	0.000395	2.79	1794.65	690	0.3	692.56	-0.00109
28	5219.6	5223.11	5223.66	0.001923	5.96	839.46	337.67	0.67	339.66	-0.00117
29	5219	5222.83	5223.09	0.000768	4.09	1222.12	434.16	0.43	436.4	-0.00086
30	5216.9	5222.25	5222.53	0.000505	4.25	1201.27	288.52	0.37	289.66	-0.00181
31	5216.8	5221.02	5222	0.002121	7.94	630.95	176.7	0.74	178.27	-0.00181
32	5216.5	5220.44	5221.02	0.001358	6.15	822.99	238.51	0.59	241.04	-0.00111
33	5216.2	5219.91	5220.37	0.001074	5.52	979.11	261.09	0.52	262.88	-0.00102
34	5214.5	5219.42	5219.82	0.001025	5.09	1091.59	308.2	0.51	309.51	-0.00116
35	5214.8	5218.75	5219.26	0.001068	5.7	908.39	241.65	0.53	242.85	-0.00119
36	5214.5	5218.23	5218.7	0.001173	5.51	923.54	282.89	0.54	284	-0.00238
37	5212.3	5216.37	5217.55	0.00457	8.73	573.1	247.22	1.01	249.93	-0.00243
38	5211.4	5215.8	5216.3	0.001113	5.7	877.64	250.36	0.54	251.93	-0.00132
39	5209.5	5215.05	5215.7	0.001316	6.46	800.09	205.32	0.59	208.2	-0.00082
40	5209.6	5214.98	5215.22	0.000446	3.98	1395.44	304.41	0.35	307.32	-0.0005
41	5209.6	5214.55	5214.93	0.00076	5	1113.49	254.85	0.45	258.35	-0.00089
42	5209.8	5214.09	5214.44	0.001217	5.03	1405.98	320.93	0.54	323.27	-0.00125
43	5208.9	5213.3	5213.86	0.001031	6	898.47	206.79	0.53	208.01	-0.00073
44	5208.6	5213.36	5213.5	0.000276	2.95	1753.31	454.83	0.27	458.34	-0.00044

45	5208.5	5212.86	5213.27	0.001417	5.15	1022.64	385.6	0.57	387.16	-0.00205
46	5208.3	5211.31	5212.09	0.003883	7.09	705.05	370.11	0.91	371.9	-0.00181
47	5206.7	5211.05	5211.24	0.00068	3.48	1525.09	590.58	0.39	593.12	-0.00121
48	5206.5	5210.1	5210.64	0.00169	5.9	846.79	312.36	0.63	315.09	-0.00235
49	5205.5	5208.7	5209.46	0.002914	7.04	743.01	302.46	0.81	304.19	-0.00179
50	5204.6	5208.31	5208.61	0.000816	4.41	1266.81	373.16	0.45	375.19	-0.00188
51	5204.6	5206.82	5207.38	0.003101	5.98	896.49	478.15	0.8	478.35	-0.00258
52	5201.8	5205.73	5206.18	0.002384	5.41	989.77	498.98	0.7	501.05	-0.00218
53	5200.7	5204.64	5205	0.001683	4.88	1025.01	502.84	0.6	506.27	-0.00159
54	5200.6	5204.14	5204.33	0.000925	3.49	1539.89	733.59	0.44	737.31	-0.00233
55	5199.5	5202.31	5203.23	0.004666	7.69	671.95	345	0.99	347.04	-0.00206
56	5197.9	5202.08	5202.31	0.000814	3.89	1524.29	502.44	0.43	506.94	-0.00106
57	5198.2	5201.25	5201.73	0.002377	5.65	1064.99	438.3	0.71	441.02	-0.00165
58	5196.6	5200.43	5200.79	0.001744	4.83	1144.41	523.79	0.61	526.87	-0.00195
59	5195.8	5199.3	5199.75	0.001873	5.37	1024.53	422.59	0.64	425.25	-0.00168
60	5194.2	5198.75	5199.06	0.000804	4.51	1160.34	353.55	0.45	354.33	-0.00149
61	5192.6	5197.81	5198.37	0.00211	6.05	930.54	342.31	0.69	343.79	-0.0012
62	5193	5197.55	5197.75	0.000574	3.55	1478.14	494.34	0.37	497.42	-0.00092
63	5192.6	5196.89	5197.3	0.001314	5.16	1058.29	360.08	0.56	361.3	-0.00112
64	5192	5196.43	5196.7	0.000806	4.41	1932.28	329.87	0.45	331.58	-0.00073
65	5190.9	5196.16	5196.42	0.000623	4.24	1811.65	316	0.4	318.83	-0.00065
66	5191.8	5195.78	5196.19	0.000878	5.33	1501.27	230.73	0.48	232.34	-0.00196
67	5191.3	5194.2	5195.22	0.00432	9.04	1109.23	174.7	1	176.33	-0.00305
68	5189.4	5192.73	5193.16	0.002149	5.35	1114.99	459.66	0.68	463.24	-0.00222
69	5188.3	5191.98	5192.18	0.000852	3.63	1678.78	611.78	0.43	616.19	-0.00239
70	5187.3	5190.34	5191.17	0.003445	7.38	744.5	301.38	0.87	303.73	-0.00231
71	5186.4	5189.67	5189.93	0.001018	4.15	1468.58	497.94	0.48	499.42	-0.00193
72	5186.1	5188.41	5189.04	0.003259	6.64	1031.34	354.26	0.84	354.83	-0.00204
73	5183.8	5187.63	5187.96	0.001187	4.6	1089.28	449.43	0.52	451.28	-0.00168
74	5182.3	5186.73	5187.13	0.001712	5.08	984.35	460.67	0.61	463.53	-0.00177
75	5182.1	5185.86	5186.23	0.001722	4.99	1134.62	465.55	0.61	467.72	-0.00144
76	5180	5185.29	5185.58	0.000736	4.35	1211.43	358.55	0.43	360.74	-0.00202
77	5180.3	5183.84	5184.85	0.003054	8.11	704.58	218.29	0.86	219.01	-0.00179
78	5179.1	5183.5	5183.9	0.000944	5.15	1068.6	281.06	0.49	282.46	-0.00076
79	5177.6	5183.08	5183.46	0.000729	4.93	1119.46	259.22	0.44	261.01	-0.00135
80	5178.4	5182.15	5182.76	0.001995	6.3	855.89	299.43	0.69	300.23	-0.0017
81	5177.6	5181.38	5181.73	0.00124	4.75	1051.58	427.57	0.53	429.18	-0.00124
82	5176	5180.91	5181.18	0.000766	4.25	1275.51	389.82	0.43	392.9	-0.0008
83	5175.8	5180.58	5180.85	0.000617	4.15	1254.21	356.05	0.4	357.72	-0.00182
84	5175.9	5179.09	5180.15	0.004478	8.27	613.99	280.32	0.99	281.31	-0.00262
85	5175	5177.96	5178.27	0.001098	4.49	1114.63	450.14	0.5	451.63	-0.00151
86	5174.4	5177.58	5177.79	0.000786	3.67	1489.81	572.84	0.42	575.27	-0.00116
87	5173.1	5176.8	5177.18	0.001626	4.94	1011.34	472.96	0.6	477	-0.00105
88	5171.7	5176.53	5176.78	0.00051	4.05	1415.76	318.3	0.37	320.27	-0.00108
89	5170.8	5175.72	5176.37	0.00187	6.58	878.84	247.99	0.68	249.36	-0.0026
90	5170.4	5173.93	5175.25	0.003293	9.38	662.2	156.73	0.91	158.2	-0.00174
91	5170.2	5173.98	5174.34	0.000972	4.86	1029.06	334.47	0.49	338.62	-0.00083
92	5169.2	5173.1	5173.67	0.001592	6.05	826.08	279.77	0.62	283.18	-0.00124
93	5168.2	5172.74	5172.98	0.000876	3.95	1264.49	518.53	0.45	524.51	-0.00175
94	5168.2	5171.35	5172.19	0.003657	7.35	680.49	323.76	0.89	325.39	-0.00197

95	5165.5	5170.77	5171.14	0.001087	4.9	1021.23	359.47	0.51	361.44

Table C-3 1992 HEC-RAS Modeling Results for agg/degs at 5,000 cfs

HEC-RAS Plan: 2002aplan River: Rio Grande Reach: Cochiti to EB Q = 5,000 cfs

Agg /Deg line	Min Ch El (ft)	W.S. Elev (ft)	E.G. Elev (ft)	E.G. Slope (ft/ft)	Velocity (ft/s)	Flow Area (sq ft)	Top Width (ft)	Froude #	Wetted P (ft)	WS Slope (ft/ft)
19	5224.8	5228.86	5229.11	0.000599	4.48	1631.98	223.41	0.4	225.8	-0.00112
20	5225.19	5228.33	5228.67	0.001153	5.28	1341.76	235.94	0.53	238.53	-0.00112
22	5224.19	5227.74	5228.04	0.000977	5.12	1499.34	204.65	0.5	206.83	-0.00129
23	5223.9	5227.04	5227.33	0.002148	4.33	1154.98	613.68	0.56	614.99	-0.00144
24	5222.18	5226.3	5226.61	0.001247	4.47	1118.98	391.75	0.47	397.57	-0.00135
25	5222.01	5225.69	5225.98	0.001153	4.31	1161.31	413.42	0.45	418.09	-0.00291
26	5220.86	5223.39	5224.33	0.024182	7.78	642.51	346.91	1.01	351.14	-0.0028
27	5219.88	5222.89	5223.07	0.000605	3.36	1489.52	595.54	0.37	599.76	-0.00108
28	5218.67	5222.31	5222.66	0.001401	4.74	1054.78	328.56	0.47	332.13	-0.00088
29	5217.81	5222.01	5222.26	0.0005	3.99	1252.04	334.19	0.36	337.99	-0.00088
30	5216.62	5221.43	5221.82	0.000883	5.04	991.42	286.23	0.48	287.13	-0.00164
31	5215.5	5220.37	5221.18	0.001583	7.23	691.89	176.98	0.64	181.02	-0.0018
32	5215.7	5219.63	5220.38	0.001536	6.94	720.62	194.11	0.63	195.91	-0.0012
33	5215.51	5219.17	5219.64	0.001142	5.53	904.75	274.5	0.54	277	-0.00172
34	5214.08	5217.91	5218.77	0.002989	7.44	671.99	270.12	0.83	271.04	-0.00169
35	5212.86	5217.48	5217.92	0.000866	5.41	998.08	233.01	0.48	234.36	-0.00072
36	5211.91	5217.19	5217.51	0.000647	4.57	1231.88	279.56	0.41	284.54	-0.00095
37	5211.87	5216.53	5217.06	0.001324	5.91	932.89	254.59	0.58	256.34	-0.00088
38	5210.02	5216.31	5216.61	0.000511	4.41	1269.72	254.65	0.37	261.51	-0.00205
39	5210.85	5214.48	5215.94	0.004056	9.94	633.32	156.72	1	157.75	-0.00188
40	5209.59	5214.43	5214.86	0.000818	5.43	1200.68	210.23	0.47	212.3	-0.00107
41	5209.38	5213.41	5214.26	0.002082	7.55	777.48	191.28	0.73	192.18	-0.00093
42	5207.92	5213.5	5213.68	0.000374	3.45	1534.17	200.25	0.27	203.29	-0.00074
43	5208.28	5212.67	5213.3	0.001236	6.4	781.54	202.82	0.57	203.83	-0.0009
44	5206.12	5212.6	5212.88	0.000364	4.39	1681.93	191.62	0.33	195.59	-0.0003
45	5206.32	5212.37	5212.7	0.000704	4.6	1114.42	300.57	0.43	304	-0.0016
46	5206.99	5211	5211.81	0.005115	7.22	692.73	436.36	1.01	437.58	-0.00249
47	5206.12	5209.88	5210.14	0.000822	4.11	1274.99	449.54	0.44	453.31	-0.00205
48	5204.71	5208.95	5209.5	0.001757	5.95	839.74	313.64	0.64	317.69	-0.00196
49	5203.3	5207.92	5208.57	0.001973	6.5	780.94	275.07	0.68	278.43	-0.0014
50	5202.84	5207.55	5207.86	0.000801	4.46	1123.9	359.54	0.44	363.65	-0.00128
51	5204.23	5206.64	5207.14	0.002225	5.67	882.8	428.35	0.7	428.59	-0.00186
52	5203.01	5205.69	5206.12	0.002438	5.26	1009.04	543.96	0.71	549.85	-0.00174
53	5202.2	5204.9	5205.18	0.001467	4.19	1237.59	645.51	0.54	647	-0.00236
54	5200.52	5203.33	5203.99	0.004067	6.55	815.96	557.59	0.99	559.2	-0.00284
55	5198.54	5202.06	5202.65	0.001877	6.19	828.5	313.6	0.68	317.72	-0.00151
56	5198.71	5201.82	5202.05	0.000796	3.94	1602.18	461.96	0.42	464.56	-0.00076
57	5196.95	5201.3	5201.69	0.000865	5.03	1201.85	340.19	0.52	346.27	-0.002
58	5197.2	5199.82	5200.67	0.013877	7.4	689.64	390.89	0.99	394.95	-0.00227
59	5194.84	5199.03	5199.36	0.000771	4.61	1083.83	347.41	0.46	351.04	-0.00133
60	5194.14	5198.49	5198.9	0.001067	5.09	991.36	322.82	0.51	324.05	-0.00144
61	5192.52	5197.59	5198.12	0.002447	5.88	854.87	416.95	0.73	420.58	-0.00137
62	5191.68	5197.12	5197.37	0.000788	3.96	1261.83	479.29	0.43	481.87	-0.00115

63	5191.56	5196.44	5196.85	0.001279	5.17	967.75	354.37	0.55	356.65	-0.00132
64	5190.54	5195.8	5196.22	0.000992	5.2	1140.27	368.69	0.57	372.22	-0.00218
65	5190.81	5194.26	5195.36	0.004357	8.47	629.59	257.25	0.99	258.73	-0.00136
66	5189.49	5194.44	5194.76	0.000461	4.51	1183.47	228.14	0.36	232.73	-0.0008
67	5190.03	5193.46	5194.22	0.002869	7.11	830.83	285.43	0.81	288.39	-0.00212
68	5189.51	5192.32	5192.79	0.002226	5.71	1173.79	390.74	0.7	393.51	-0.00236
69	5188.2	5191.1	5191.48	0.002062	5.05	1183.31	482.46	0.63	485.52	-0.00347
70	5186.3	5188.85	5189.89	0.004483	8.33	692.71	265.91	0.99	268.71	-0.003
71	5185.3	5188.1	5188.44	0.001539	4.82	1227.44	484.48	0.6	486.28	-0.00182
72	5183.82	5187.03	5187.46	0.00242	5.65	1388.85	393.33	0.72	394.93	-0.00164
73	5181.8	5186.46	5186.71	0.000854	3.97	1258.25	503.61	0.44	507.98	-0.00122
74	5181.15	5185.81	5186.24	0.00071	5.28	1053.72	218.64	0.45	220.46	-0.00126
75	5179.65	5185.2	5185.72	0.001404	5.84	954.94	274.31	0.59	278.49	-0.00143
76	5180.65	5184.38	5184.87	0.001497	5.57	897.07	330.72	0.6	332.26	-0.00207
77	5178.91	5183.13	5183.98	0.001905	7.42	699.66	192.63	0.7	194.26	-0.00183
78	5178.49	5182.55	5183.08	0.001556	5.84	861.06	302.19	0.61	304.57	-0.00125
79	5177.65	5181.88	5182.36	0.001265	5.54	902.54	295.64	0.56	297.27	-0.00132
80	5176.49	5181.23	5181.73	0.001212	5.7	943.69	264.25	0.55	265.64	-0.00103
81	5175.91	5180.85	5181.2	0.000669	4.78	1157.23	262.87	0.42	264.23	-0.0009
82	5175.6	5180.33	5180.79	0.000788	5.5	1085.38	206.24	0.47	208.37	-0.00092
83	5175.44	5179.93	5180.31	0.001058	4.95	1010.24	343.17	0.51	344.76	-0.00234
84	5174.77	5177.99	5179.32	0.004135	9.28	538.91	197.45	0.99	199.12	-0.00196
85	5175.02	5177.97	5178.23	0.000819	4.06	1231.47	464.49	0.44	466.8	-0.00045
86	5174.88	5177.54	5177.8	0.001169	4.12	1357.78	572.5	0.5	575.65	-0.00213
87	5172.39	5175.84	5176.73	0.005155	7.74	761.35	349.72	1.03	352.15	-0.00176
88	5170.36	5175.78	5175.99	0.000414	3.75	1487.3	330.93	0.33	335.36	-0.00106
89	5169.94	5174.78	5175.58	0.002564	7.32	806.29	241.5	0.78	243.12	-0.00178
90	5168.98	5174	5174.68	0.00108	6.62	854.71	164.96	0.55	167.48	-0.00091
91	5168.9	5173.87	5174.17	0.000588	4.46	1311.38	277.23	0.4	280.21	-0.00136
92	5169.19	5172.64	5173.61	0.002453	8.04	741.21	184.93	0.78	186.76	-0.00213
93	5167.75	5171.74	5172.61	0.00199	7.59	847.97	180.65	0.71	183	-0.0017
94	5167.13	5170.94	5171.6	0.002117	6.55	763.08	285.19	0.71	287.55	-0.00164
95	5165.55	5170.1	5170.65	0.001615	5.93	843.19	364.6	0.69	367.8	

Table C-4 2002 HEC-RAS Modeling Results for agg/degs at 5,000 cfs

Reach-averaged HEC-RAS results

1962 Averages

Subreach	E.G. Slope (ft/ft)	Velocity (ft/ft)	Flow Area (ft^2)	Top Width (ft)	Froude #	WS Slope (ft/ft)	Depth (ft)	W/D ratio	Wetted Perimeter (ft)
1	0.0015	5.47	1008.35	360.50	0.58	-0.0014	2.80	128.89	365.06
2	0.0017	4.77	1393.15	537.95	0.59	-0.0016	2.59	207.73	542.96
3	0.0012	4.47	1745.52	469.27	0.47	-0.0013	3.72	126.16	475.28
all	0.0015	4.98	1328.49	444.26	0.55	-0.0015	2.99	148.56	461.10

1972 Averages

Subreach	E.G. Slope (ft/ft)	Velocity (ft/ft)	Flow Area (ft2)	Top Width (ft)	Froude #	WS Slope (ft/ft)	Depth (ft)	W/D ratio	Wetted Perimeter (ft)
1	0.0014	5.70	949.93	299.93	0.57	-0.0014	3.17	94.70	304.81
2	0.0017	5.28	1094.87	392.07	0.60	-0.0017	2.79	140.40	398.59
3	0.0014	5.16	1140.58	388.52	0.55	-0.0014	2.94	132.34	395.70
all	0.0015	5.43	1046.47	352.29	0.58	-0.0015	2.97	118.60	366.36

1992 Averages

Subreach	E.G. Slope (ft/ft)	Velocity (ft/ft)	Flow Area (ft2)	Top Width (ft)	Froude #	WS Slope (ft/ft)	Depth (ft)	W/D ratio	Wetted Perimeter (ft)
1	0.0016	5.45	1082.52	349.03	0.58	-0.0014	3.10	112.54	351.03
2	0.0018	5.23	1220.80	421.92	0.61	-0.0017	2.89	145.82	424.34
3	0.0016	5.50	1032.56	350.99	0.59	-0.0015	2.94	119.31	353.20
all	0.0017	5.40	1110.56	371.63	0.59	-0.0015	2.99	124.36	376.19

2002 Averages

Subreach	E.G. Slope (ft/ft)	Velocity (ft/ft)	Flow Area (ft2)	Top Width (ft)	Froude #	WS Slope (ft/ft)	Depth (ft)	W/D ratio	Wetted Perimeter (ft)
1	0.0021	5.50	1064.97	300.87	0.56	-0.0014	3.54	85.00	303.75
2	0.0024	5.54	1056.81	393.62	0.64	-0.0018	2.68	146.61	396.66
3	0.0017	6.03	955.07	289.82	0.62	-0.0015	3.30	87.95	292.14
all	0.0021	5.66	1032.13	325.88	0.60	-0.0016	3.17	102.89	330.85

Table C-5 Reach-averaged HEC-RAS modeling results for Cochiti Dam Reach 1962, 1972, 1992, and 2002.

APPENDIX D – BED MATERIAL PLOTS

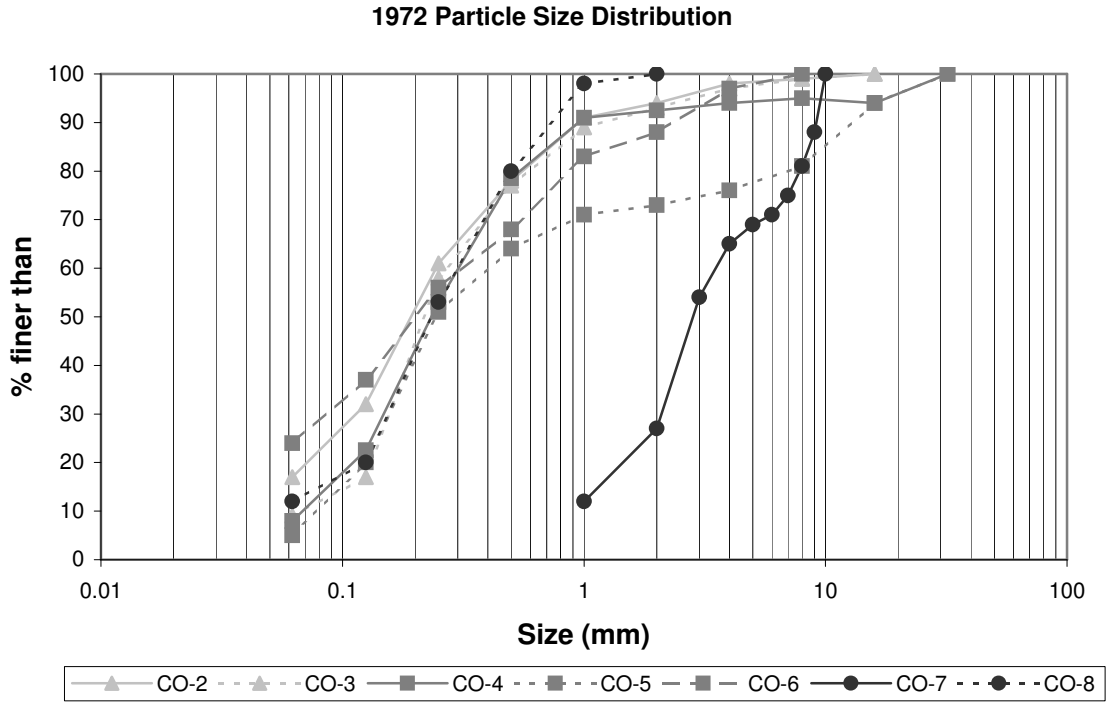

Figure D-1 Particle Size Distribution in the Cochiti Dam reach for 1972. Triangles denote subreach 1, squares denote subreach 2, and circles denote subreach 3.

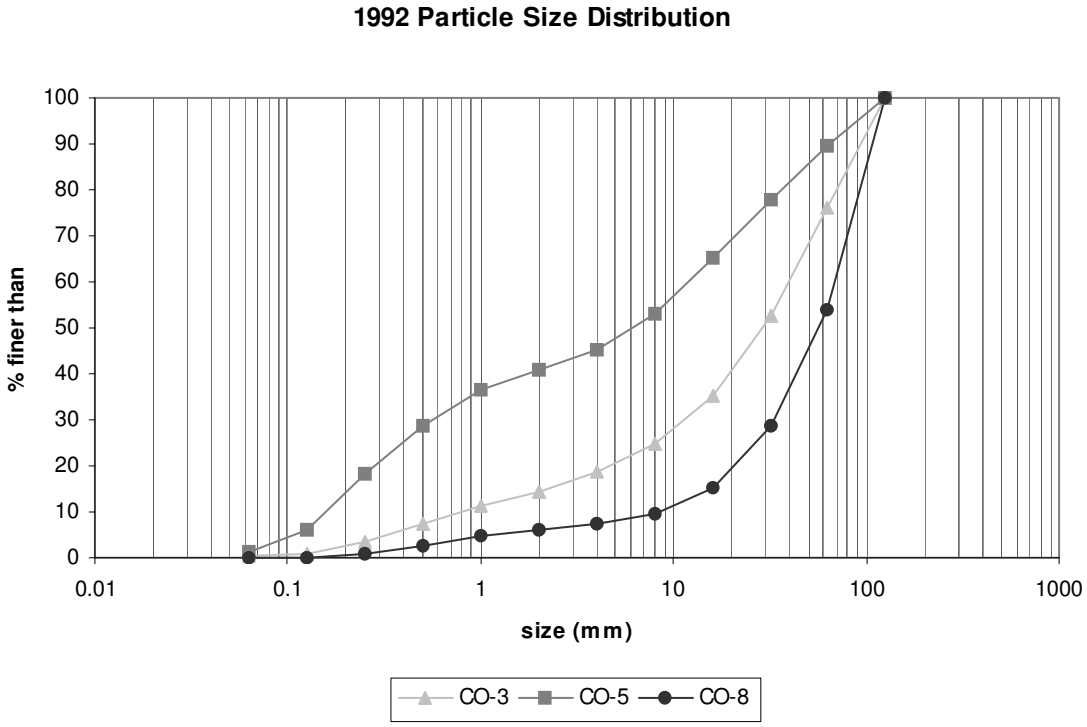

Figure D-2 Particle Size Distribution in the Cochiti Dam reach for 1992. Triangles denote subreach 1, squares denote subreach 2, and circles denote subreach 3.

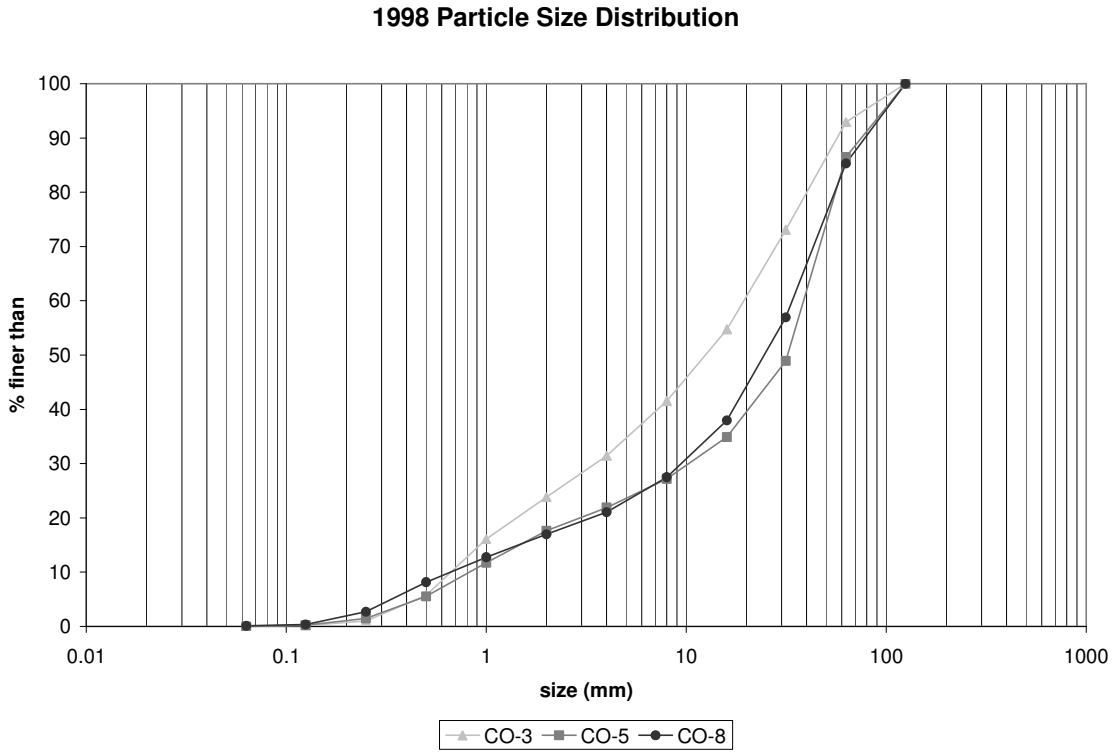

Figure D-3 Particle Size Distribution in the Cochiti Dam reach for 1998. Triangles denote subreach 1, squares denote subreach 2, and circles denote subreach 3.

APPENDIX E – SEDIMENT TRANSPORT CAPACITY

Assumptions (From HEC-RAS 3.1.3)

Ackers-White (flume):

0.04 < d < 7 mm	1.0 < s < 2.7
0.07 < V < 7.1 fps	0.01 < D < 1.4 ft
0.00006 < S < 0.037	0.23 < W < 4.0 ft
46 < T < 89 degrees F	

A total load function developed under the assumption that fine sediment transport is best related to the turbulent fluctuations in the water column and coarse sediment transport is best related to the net grain shear with the mean velocity used as the representative variable. The transport function was developed in terms of particle size, mobility and transport. A dimensionless size parameter is used to distinguish between the fine, transitionary, and coarse sediment sizes. Under typical conditions, fine sediments are silts less than 0.04 mm, and coarse sediments are sands greater than 2.5 mm. Since the relationships developed by Ackers-White are applicable only to non-cohesive sands, greater than 0.04 mm, only transitionary and coarse sediments apply. Experiments were conducted with coarse grains up to 4 mm. This function is based on over 1000 flume experiments using uniform or near-uniform sediments with flume depths of up to 1.4 m. A range of bed configurations was used, including plane, rippled, and dune forms, however the equations do not apply to upper phase transport (e.g. anti-dunes) with Froude numbers in excess of 0.8. A hiding adjustment factor was developed for the Ackers-White method by Profitt and Sutherland (1983), and is included in RAS as an option. The hiding factor is an adjustment to include the effects of a masking of the fluid properties felt by smaller particles due to shielding by larger particles. This is typically a factor when the gradation has a relatively large range of particle sizes and would tend to reduce the rate of sediment transport in the smaller grade classes.

Engelund-Hansen (flume):

0.19 < dm < 0.93 mm	0.65 < V < 6.34
0.19 < D < 1.33 fps	0.000055 < S < 0.019 ft
45 < T < 93 degrees F	

A total load predictor, which gives adequate results for sandy rivers with substantial suspended load. It is based on flume data with sediment sizes between 0.19 and 0.93 mm. It has been extensively tested, and found to be fairly consistent with field data.

Laursen (Copeland) (field):

0.08 < dm < 0.7 mm	0.068 < V < 7.8 fps
0.67 < D < 54 ft	0.0000021 < S < 0.0018
63 < W < 3640 ft	32 < T < 93 degrees F

Laursen (Copeland) (flume):

0.011 < dm < 29 mm	0.7 < V < 9.4 fps
0.03 < D < 3.6 ft	0.00025 < S < 0.025
0.25 < W < 6.6 ft	46 < T < 83 degrees F

A total sediment load predictor, derived from a combination of qualitative analysis, original experiments and supplementary data. Transport of sediments is primarily defined based on the hydraulic characteristics of mean channel velocity, depth of flow and energy gradient, and on the

sediment characteristics of gradation and fall velocity. Contributions by Copeland (Copeland, 1989) extend the range of applicability to gravel-sized sediments. The overall range of applicability is 0.011 to 29 mm.

MPM. Meyer-Peter Muller (flume):

0.4 < d < 29 mm	1.25 < s < 4.0
1.2 < V < 9.4 fps	0.03 < D < 3.9 ft
0.0004 < S < 0.02	0.5 < W < 6.6 ft

BED LOAD ONLY! A bed load transport function based primarily on experimental data. It has been extensively tested and used for rivers with relatively coarse sediment. The transport rate is proportional to the difference between the mean shear stress acting on the grain and the critical shear stress. Applicable particle sizes range from 0.4 to 29 mm with a sediment specific gravity range of 1.25 to in excess of 4.0. This method can be used for well-graded sediments and flow conditions that produce other-than-plane bed forms. The Darcy-Weisbach friction factor is used to define bed resistance. Results may be questionable near the threshold of incipient motion for sand bed channels as demonstrated by Amin and Murphy (1981).

Toffaleti (field):

0.062 < d < 4 mm	0.095 < dm < 0.76 mm
0.7 < V < 7.8 fps	0.07 < R < 56.7 ft
0.000002 < S < 0.0011	63 < W < 3640 ft
40 < T < 93 degrees F	

Toffaleti (flume):

0.062 < d < 4 mm	0.45 < dm < 0.91 mm
0.7 < V < 6.3 fps	0.07 < R < 1.1 ft
0.00014 < S < 0.019	0.8 < W < 8 ft
32 < T < 94 degrees F	

A modified-Einstein total load function that breaks the suspended load distribution into vertical zones, replicating two-dimensional sediment movement. Four zones are used to define the sediment distribution. They are the upper zone, the middle zone, the lower zone and the bed zone. Sediment transport is calculated independently for each zone and the summed to arrive at total sediment transport. This method was developed using an exhaustive collection of both flume and field data. The flume experiments used sediment particles with mean diameters ranging from 0.45 to 0.91 mm, however successful applications of the Toffaleti method suggests that mean particle diameters as low as 0.095 mm are acceptable.

Yang (field, sand):

0.15 < d < 1.7 mm	0.8 < V < 6.4 fps
0.04 < D < 50 ft	0.00004 < S < 0.028
0.44 < W < 1750	32 < T < 94 degrees F

Yang (field, gravel):

2.5 < d < 7.0 mm	1.4 < V < 5.1 fps
0.08 < D < 0.72 ft	0.0012 < S < 0.029
0.44 < W < 1750	32 < T < 94 degrees F

A total load function developed under the premise that unit stream power is the dominant factor in the determination of total sediment concentration. The research is supported by data obtained in both flume experiments and field data under a wide range conditions found in alluvial channels. Principally, the sediment size range is between 0.062 and 7.0 mm with total sediment concentration ranging from 10 ppm to 585,000 ppm. Yang (1984) expanded the applicability of his function to include gravel-sized sediments.

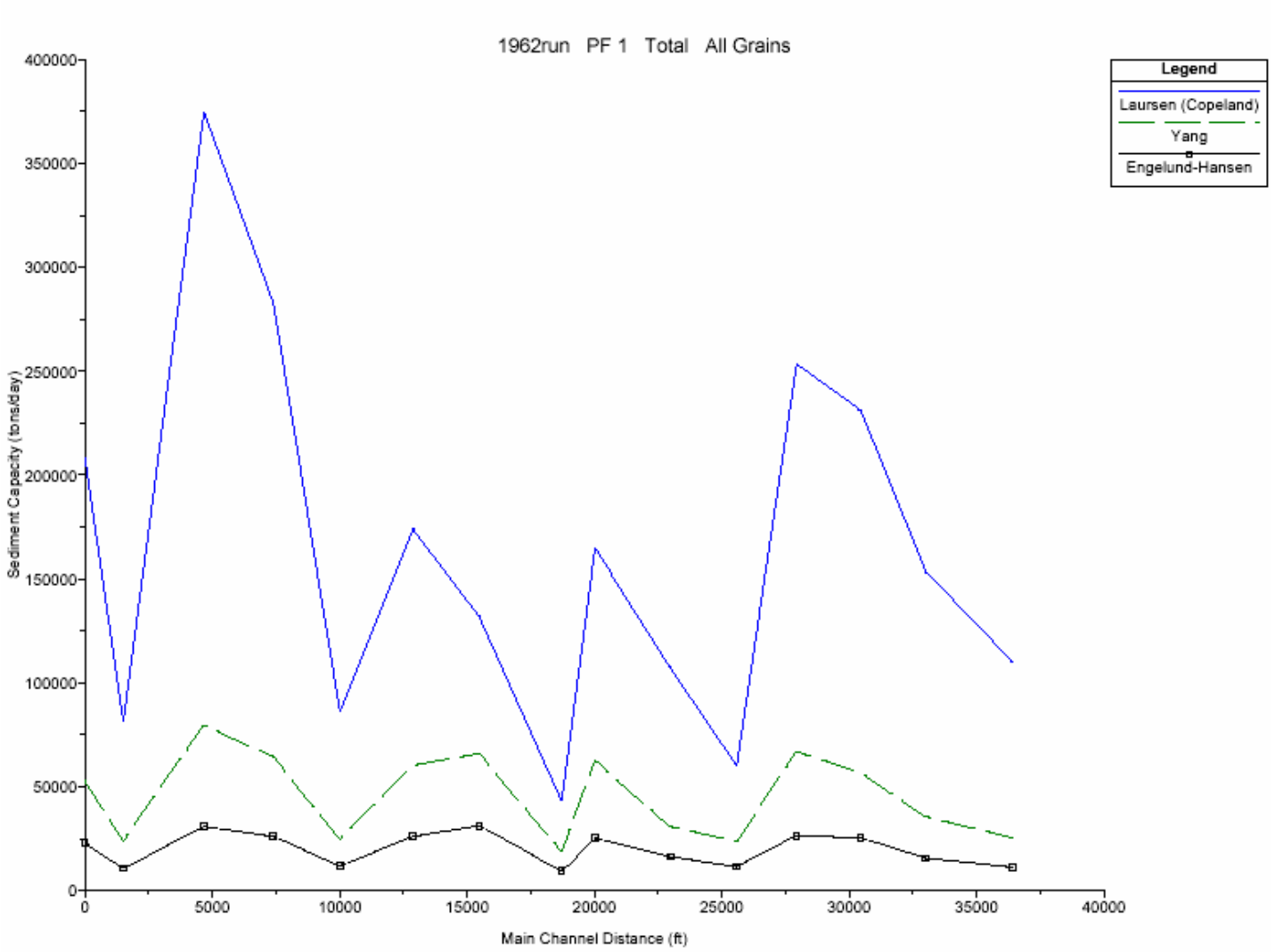

Figure E-1 1962 Sediment Transport Capacity run using HEC-RAS 3.1.3

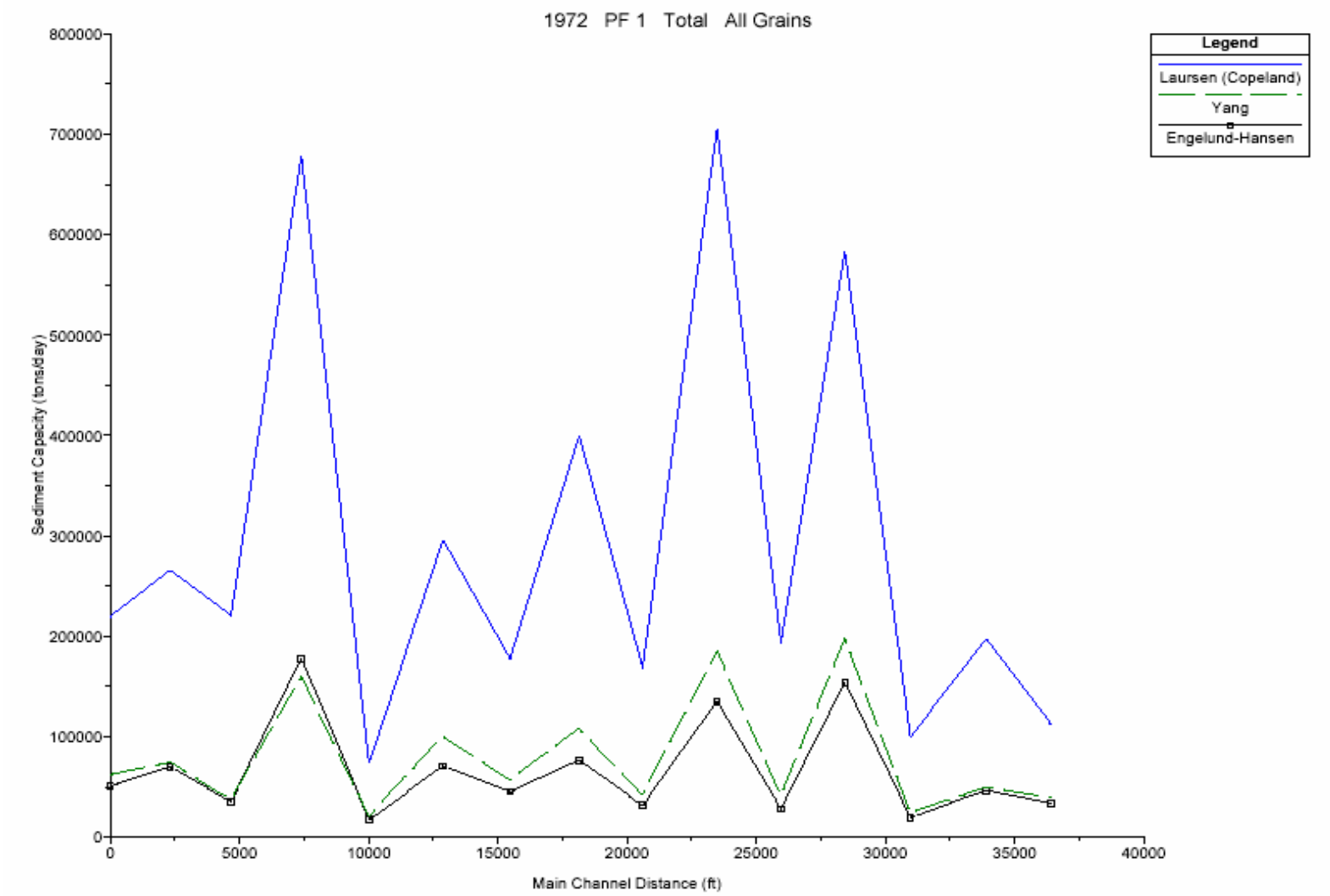

Figure E-2 1972 Sediment Transport Capacity run using HEC-RAS 3.1.

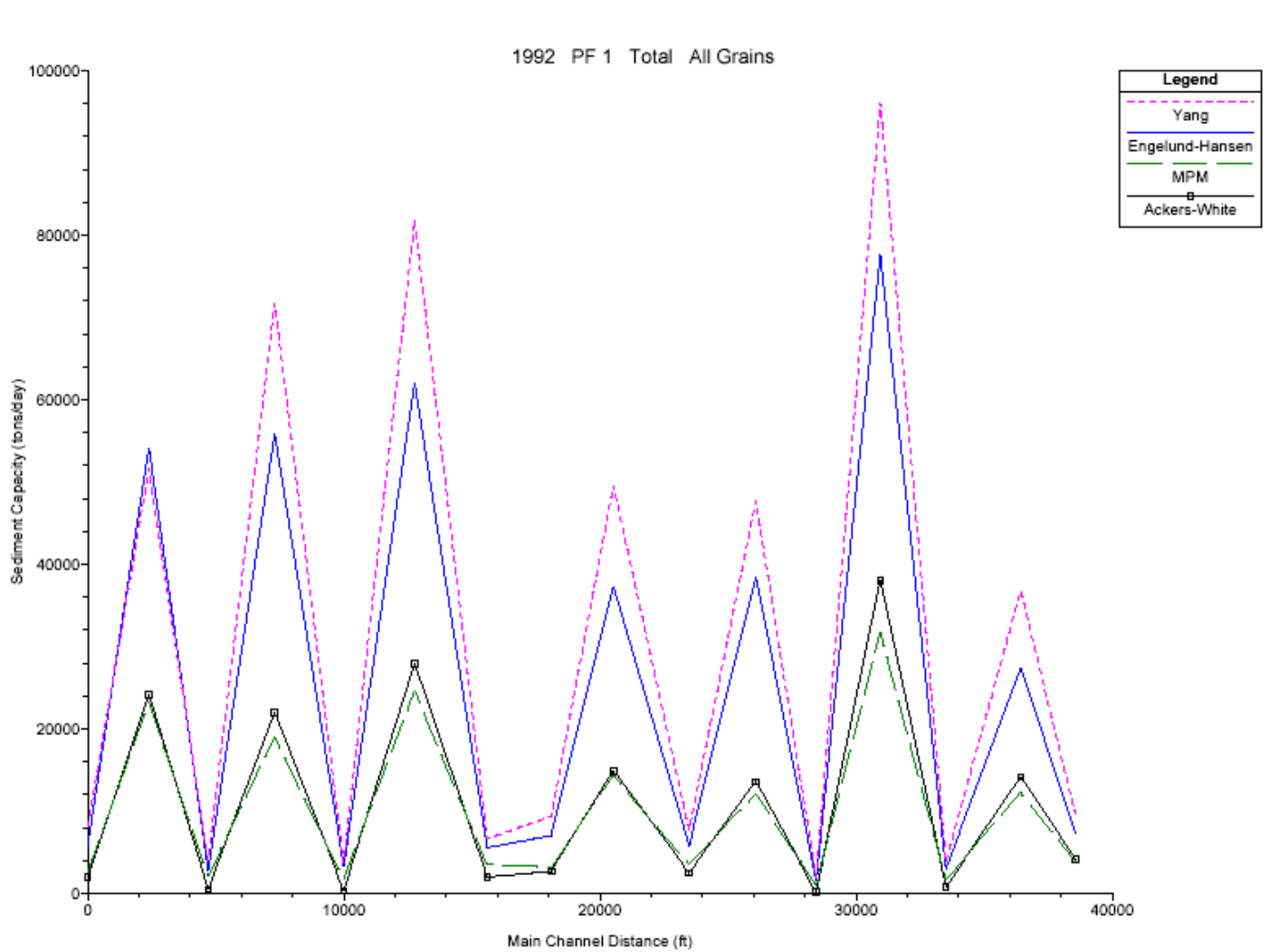

Figure E-3 1992 Sediment Transport Capacity run using HEC-RAS 3.1.3.

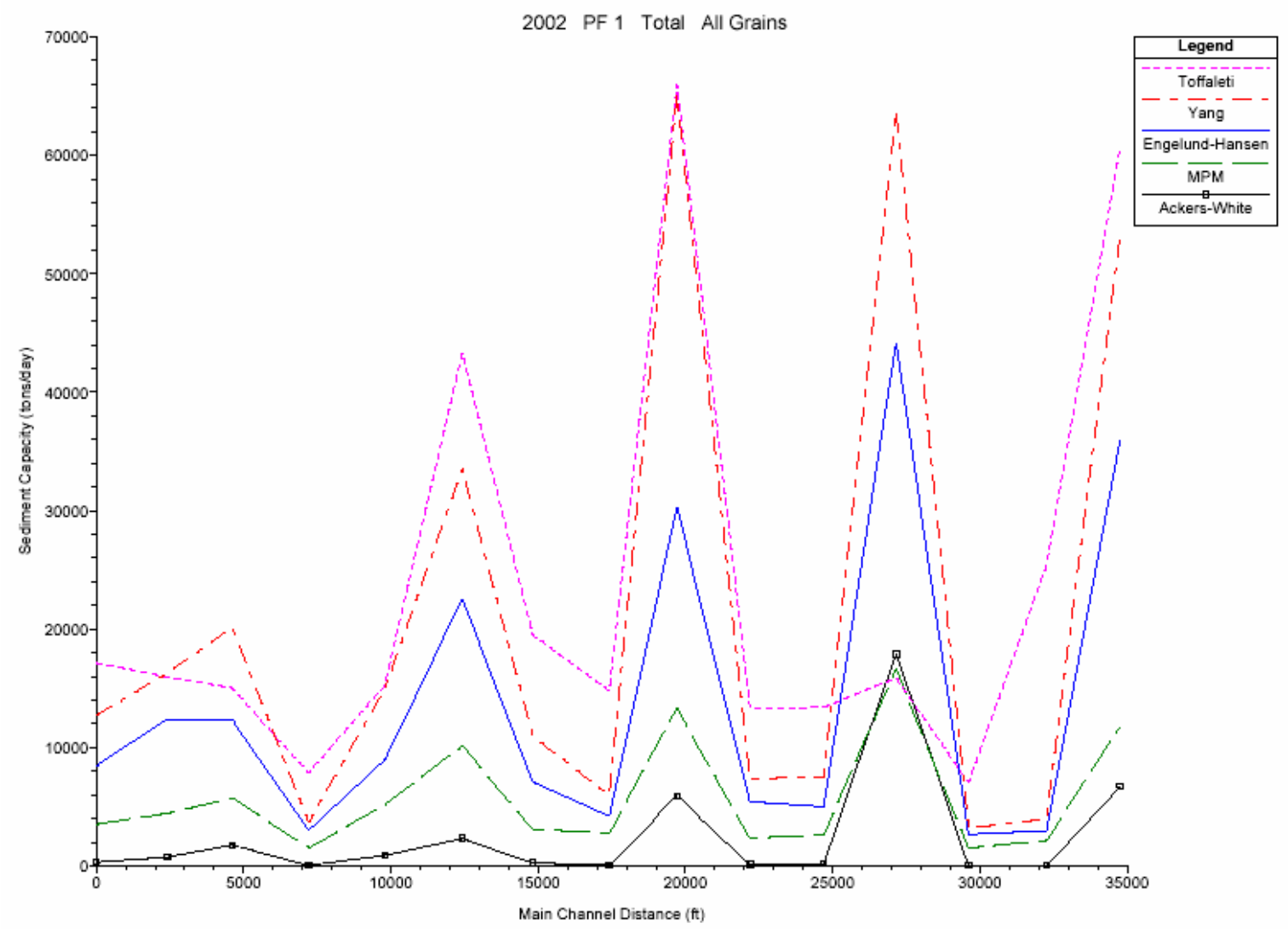

Figure E-4 2002 Sediment Transport Capacity run using HEC-RAS 3.1.3.

APPENDIX F – STABLE CHANNEL ANALYSIS

F.1 Methods

Two stable channel design programs were available for use: the USACE's HEC-RAS 3.1.3 and SE-CAP (unpublished by Shih, Watson, and Yang). HEC-RAS's hydraulic stable channel design function, based on the SAM Hydraulic Design Package for Flood Control Channels, was not used for the Cochiti Dam reach. The package uses Brownlie's flow resistance and sediment transport equations to produce multiple solutions for the width and slope given at the input values. Brownlie's method is for sand-sized bed material, with a maximum d_{50} of 2 mm. In the Cochiti Dam reach, the d_{50} is 24 for the total reach, putting it well outside the bounds of reasonable results.

Instead of SAM, the Visual Basic program SE-CAP was utilized. The program uses Yang-Copeland's procedure, which balances sediment transport and capacity by means of the user's choice of regime equations. For the Cochiti Dam reach, Ackers and White (1973) and Meyer-Peter and Muller (1948) were used for stable channel calculations. The program also has the capacity to use Yang's gravel (1984), Yang's sand (1979) (for both low and high concentrations), Engelund and Hansen (1967), and Bagnold (1966).

Ackers and White's total load function was chosen because of the higher degree of compatibility with the channel characteristics. This method has limitations, including the applicability of the equations to only non-cohesive sands, and a median grain size maximum of 7 mm. The Middle Rio Grande has fairly non-cohesive banks, so this assumption was acceptable. It was also developed for channel widths much smaller than the study reach. Meyer-Peter and Muller's bed load function can handle a median grain size up to 29 mm, making it a better fit for the bed material in the Cochiti Dam reach. However, this function was also developed for channel widths much smaller than the Middle Rio Grande.

The program was run for each subreach and the entire reach using 1998 data. Input parameters for the program are shown in Table F-1. The inputs were converted to metrics for input into the program. The bank slopes were computed from the CO-line cross-section plots.

Bank Slopes		Grain Size Diameter (mm)		
Left Bank	Right Bank	d16	d50	d84
16.4	9.1	1.3	24	60

Table F-1 Input parameters for equilibrium channel design runs for Cochiti Dam Reach in 1998

The model was run for a channel forming discharge of 5,000 cfs and incoming sediment concentrations of 38 mg/L. These values are for the post-dam conditions of the Cochiti Dam reach. The suspended sediment discharge entering the reach is assumed to be entirely consisting of washload. The bed material curve for the entire reach was obtained by averaging the bed material size distribution curves of the three subreaches in Appendix D.

F.2 Results

As mentioned in the methods section, Acker's and White (AW) total load equations and Meyer-Peter and Muller's (MPM) bed load transport equations were used in the stable channel design. The program SE-CAP was used to calculate Yang's stream power and slope as a function of width. A line of stable channel conditions was developed for widths between 3 and 700 feet. In this methodology, a "stable" channel refers to one in which sediment transport balances capacity. An "equilibrium" channel refers to the stable channel with the smallest stream power (the product of velocity and slope). The HEC-RAS-modeled channel widths at 5,000 cfs with corresponding friction slope for 2002 at all subreaches and the total reach were plotted against the predictions in Figure F-1.

The observed slopes are nearly half of the stable channel slopes predicted by both Meyer-Peter and Muller and Ackers and White. The stable line predicted by each method indicates

equality between sediment transport and sediment capacity. For the given concentration, the line predicts a slope for every width that will carry the sediment through the reach. If the input data is assumed correct, then the channel must increase in slope in order to become stable. However, since the observed slopes are lower, and are still carrying the required average 38 mg/L through the channel, two errors are possible. The input data (discharge, grain size distribution, slope, or concentration) may contain errors, or the Meyer-Peter and Muller equation and the Ackers and White equation may not be accurate for this reach. As shown in Figure F-1, the observed friction slopes for 2002 are too shallow to even pass 0 mg/L, according to both MPM and AW.

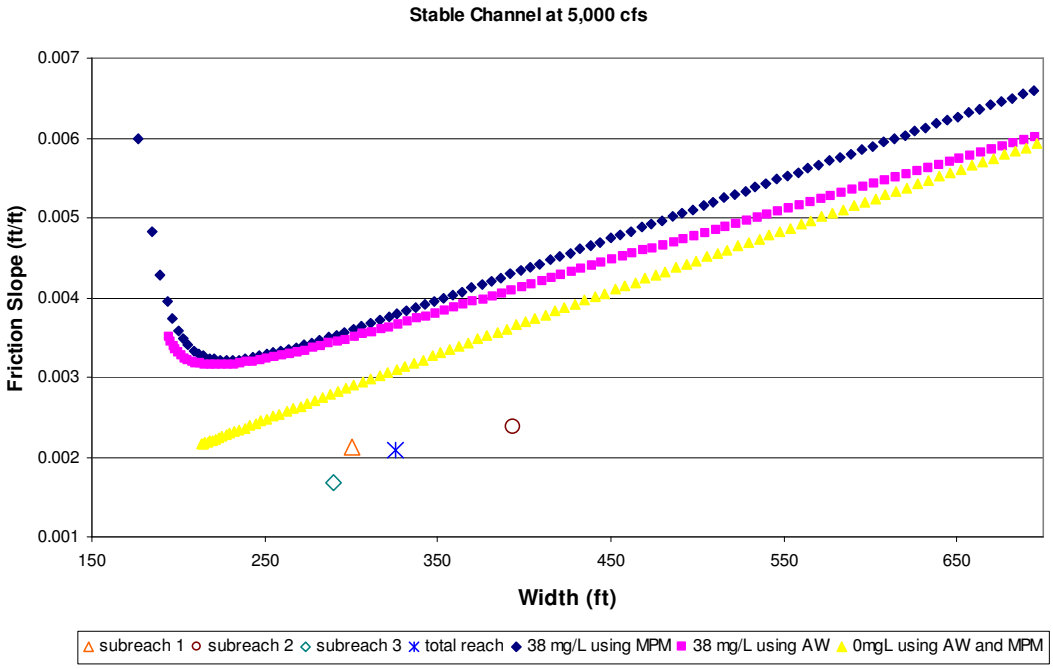

Figure F-1 Results from stable channel analysis using SE-CAP with Meyer-Peter and Muller (MPM) and Ackers and White (AW) equations for 1998. Observed values taken from HEC-RAS runs at 5,000 cfs.

According to the findings in Chapter 3, the overall trend of the reach since 1972 has been a slow decrease in width and an increase in slope. Thus, assuming the MPM and AW methods are correct, the Cochiti Dam reach has been moving towards stability. However, because the bed

of the Cochiti Dam reach is armored, little degradation is expected in the future. This leaves the channel little choice but to begin moving laterally, eroding the banks and increasing sinuosity.

APPENDIX G – MIDDLE RIO GRANDE DATABASE UPDATES

G.1 Introduction

The Rio Grande Database was a project for the US Bureau of Reclamation started in the late 1990s. The original database was compiled and discussed by Colorado State University's Claudia Leon in her thesis and dissertation. The database included cross-sectional plots, discharge data, and sediment data for both USGS gaging stations and range-lines along the Rio Grande. The reach in question stretched from Cochiti Dam to the San Acacia Diversion Dam. This area is still under study for biological, hydrological, and geological changes.

The MRG Database was compiled in order to facilitate analyses performed to better understand the changes that are affecting the Middle Rio Grande River. Studies have been done on meander migration patterns, lateral migration, and general morphology of the river. As more research is done, the database must be continually added to, organized, and updated.

G.2 The Existing Database

The existing data consisted of several different computer disks, text files, and spreadsheets, as well as hard-copy data compiled from research projects on several reaches of the Middle Rio Grande. The existing formal database contained some data analyses done for research. Some data was raw, and was not yet manipulated.

There were several types of data collected for the MRG Database. Discharge data was measured along the river at several USGS gaging stations. Instantaneous discharge measurements were taken at some range-line cross-sections and were available in part from the USBR.

Cross-sectional measurements of bed elevation, water surface elevation, and thalweg were taken at several range-lines. Many different cross-sections were collected. The Cochiti Range-Lines (CO) are the most frequently used by MRG researchers. In addition, Aggredation/Deggredation (Agg/Deg), Abeyta's Heading (AH), Bernardo Jack (BJ), Bernalillo Island (BI), Calabacillas (CA), and Casa Colorada (CC) lines were included.

Sediment data was collected at both USGS Gaging Stations as well as at Range-Lines. Bed Material and Suspended Sediment data were collected from the USGS and the USBR. Hydraulic Summaries and Total Load Summaries were also collected from the USBR. The sediment database was expanded with analyses of sediment continuity and sediment transport. FLO Engineering also contributed sediment data for the early to mid 1990's. Some sedimentary and water quality data was received from the EPA as well.

Claudia Leon's 1998 thesis, "*Morphology of the Middle Rio Grande from Cochiti Dam to Bernalillo Bridge, New Mexico"* contains more detailed information about the exact dates and sources of available data. This thesis is available in the database.

G.3 Database Updates

G.3.1 New Data

New updated information was added through the USGS, the USBR, the EPA, and from hardcopy reports and files.

The USGS website provided updated discharge data for USGS gaging stations up through water-year 2002. It also provided some of the needed suspended sediment data for USGS gaging stations. Particle-size distributions were readily available for each USGS Gaging Station in service for up to 2004. These were available from the "Water Quality" section of the USGS website. Suspended Sediment Discharge data was also available through this website; however, the most recent of this data was 1996.

Cross-sectional data was provided at all available range-lines through spreadsheets and Auto-CAD drawing files from the USBR-Albuquerque office. Water-surface elevations, bed elevations, and thalweg depths were also provided by the USBR.

Not every range-line was surveyed each year. The available range-lines varied from year-to-year, and also varied between discharge, sediment, and cross-sections. CO-lines were the

most commonly surveyed and the most widely available; however, even they were not surveyed each year. These cross-sections were available up to 2002 in a few cases, and at least to 2001 in most cases.

The EPA's STORET database was used to obtain a small amount of Albuquerque-area sediment data as well. Data retrieved from this data-storage facility was sparse and non-uniform. It was for the most part unusable, however, in the future, more data may become available from this source.

As recent USBR Hydraulic Modeling Analysis reports been produced, and as recent theses and dissertations by CSU graduate students have been published, more data has become available in hard-copy form. The data available in hard-copy form included sediment, discharge, and cross-sectional figures for the mid to late 90's. These reports were combed for new data that was added to the database.

Some data could not be updated. Certain USGS gages have been discontinued or removed. In addition, the USBR's Albuquerque office has been missing certain files since their system upgrade. New discharge and velocity measurements at range-lines below Bernalillo Bridge were unavailable. In addition, suspended sediment data was sparse and had several gaps in the records. The Albuquerque office staff was unaware of the missing recent data until this updating project brought their attention to it. As they find the missing data, it will be sent to be added to the updates.

G.3.2 Database Organization

New information was added into the existing data files. Any duplicate data was checked for consistency of numbers. In some older files, the data was based on estimates or on "real-time" data instead of official daily values. These values were used because the official values were unavailable. During the updates, the estimates or "real-time" data was replaced with the

official values if they were available. This kept the database from having too many unnecessary duplicate entries.

Some data files overlap dates. It was necessary to keep these duplicate files because different analyses were performed on each set of data. In some cases, an original, raw data set was kept for further or new analyses.

After the new information was obtained, it was organized into the database by reach and then by sub reach. The entire database was then reorganized for clarity and ease of use. A webpage interface was created to tie the folders together.

In the case that a researcher needed all discharge data for the Corrales reach, she could simply go directly to that folder. Any HEC-RAS data and analyses for the Bernardo reach could be easily accessed in the same way. The overall organization is shown in Figures G-1 through G-5. Finally, a "Readme" file was added to each subfolder to describe the contents of each section.

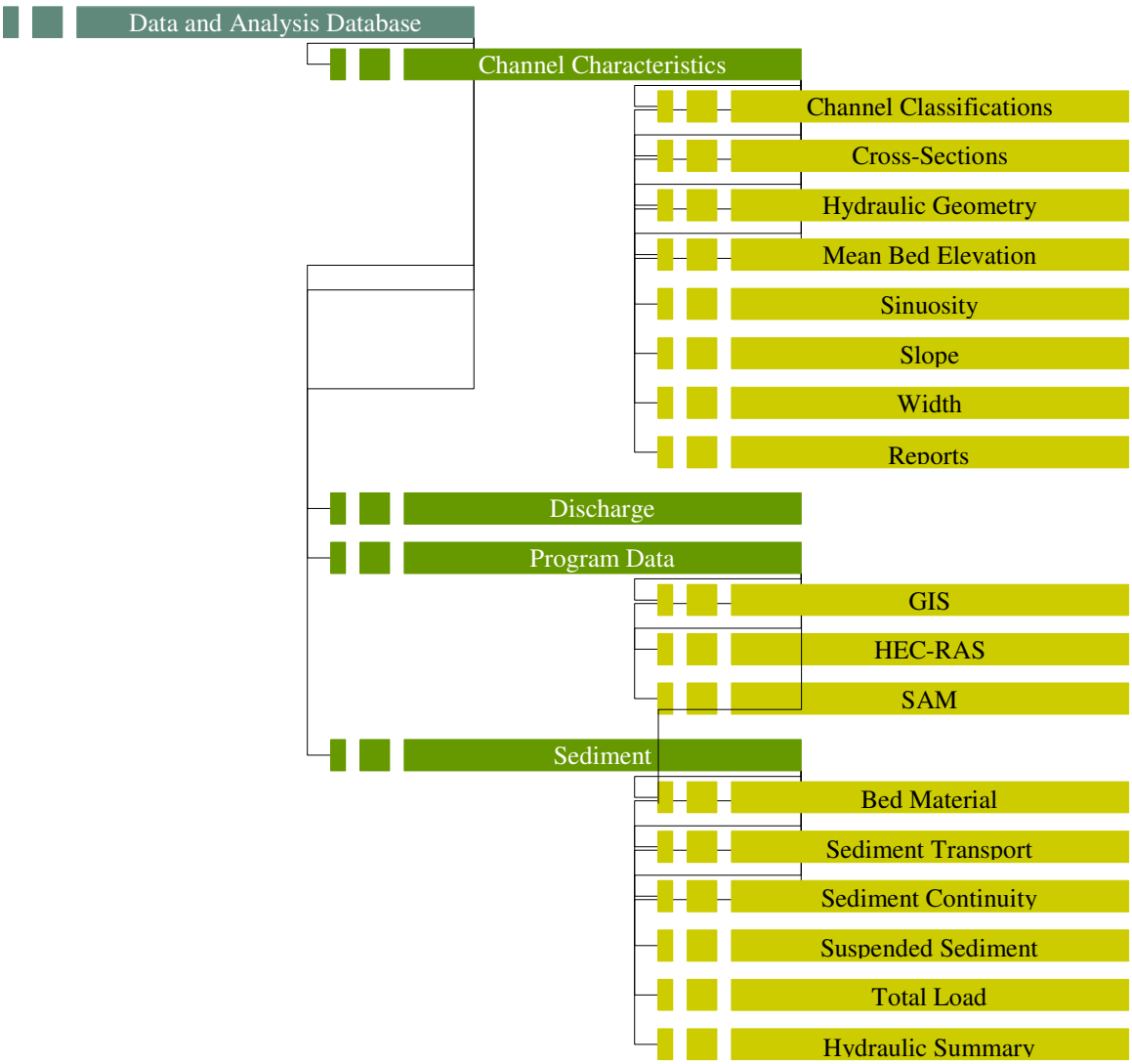

Figure G-1 Section 1 – Data and Analysis

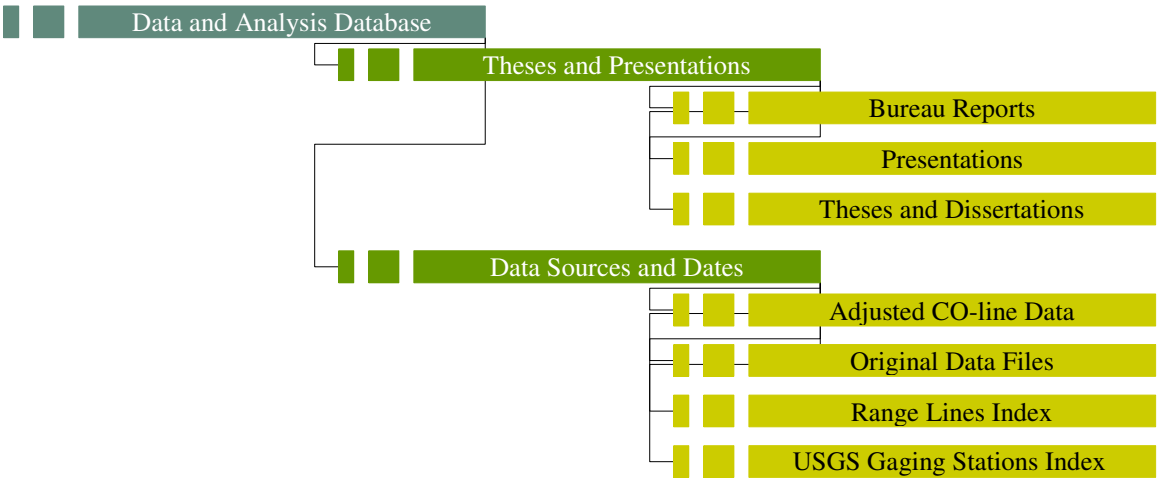

Figure G-2 Section 2 - Papers and Presentations

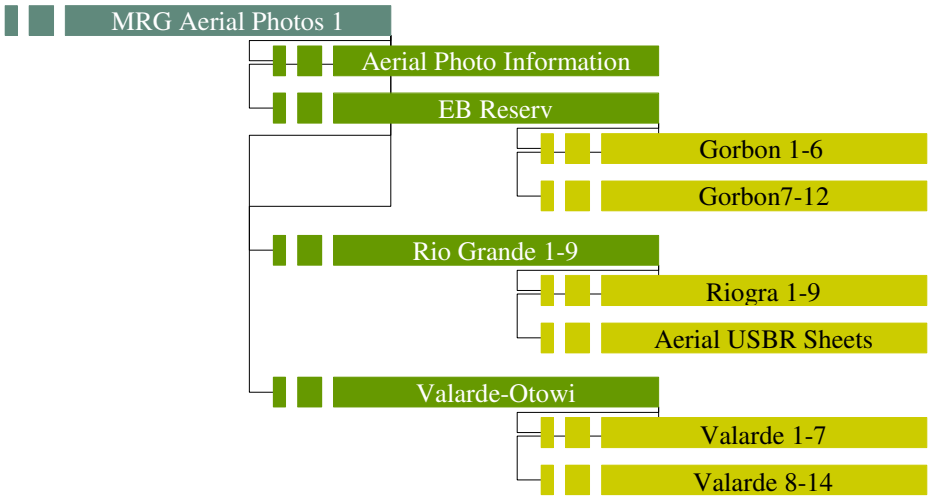

Figure G-3 Section 3 - MRG Aerial Photos 1

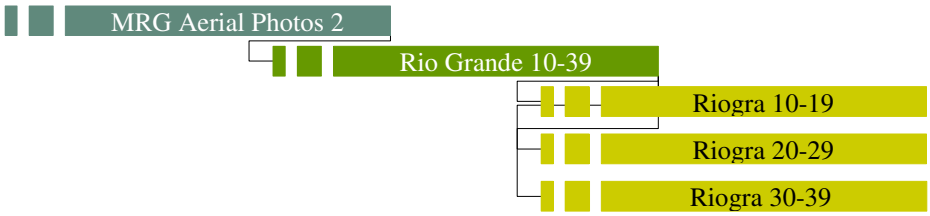

Figure G-4 Section 4 - MRG Aerial Photos 2

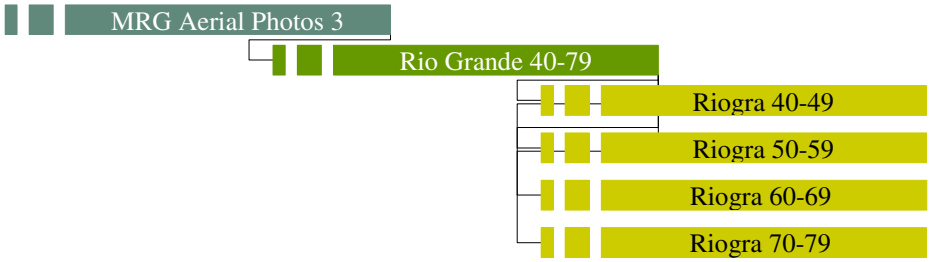

Figure G-5 Section 5 - MRG Aerial Photos 3

G.3.3 Database Layout

A DVD was created for the database, consisting of five sections. The first three sections consist of large, digital, aerial photos of the area. The fourth section contains the data and analyses for each reach. The fifth section contains all literature written on the reach, including any theses, dissertations, reports, and power-point presentations.

Sections 1, 2, and 3 contain the full, large versions of the aerial photos taken of the Rio Grande River in the 90's by the USBR. Some older, smaller resolution USBR photos are in this folder as well. Also included on this section are Valerde, Otowi, and Elephant Butte Reservoir photos. While they have been zipped to save space on the disks, the pictures themselves have not been reduced. Their large sizes have been preserved for detail. Several spreadsheets containing dates and sources of each photo were created and are in section 1.

The data and analysis section, section 4, is organized according to the type of data. Sediment, Discharge, Channel Characteristics, and various Program Data are available here. The Sediment folder is divided into Bed Material, Sediment Transport, Sediment Continuity, Suspended Sediment, and Total Load. Channel Characteristics is divided into Channel Classification, Cross-Sectional Surveys, Hydraulic Summaries, Mean Bed Elevation, Slope, Sinuosity, and Width. The analyses included in Program Data were done with the use of ArcGIS, HEC-RAS, or SAM.

Section 5 contains all literature written with the use of the database. Included are theses written by Travis Bauer, Claudia Leon, and Mike Sixta. Also included are Claudia Leon and Gigi Richard's dissertations. Hydraulic Modeling Analyses of several sub reaches were written for the USBR and are also included. Lastly, several power point presentations on the Middle Rio Grande, created by Gigi Richards, Claudia Leon, and Mike Sixta were collected and added.

The last two sections have their own webpage interfaces for navigation. The webpage may be used, or the database may be navigated manually. The Aerial Photos sections have a "Readme" file, but do not have a webpage interface because of their simplicity.

G.4 MRG Database DVD

The database DVD is the final product of this project. The DVD can be navigated using the webpage interfaces included, or it can be explored manually through each folder. A "Readme" file is included in each folder to facilitate use of the database for those who have not read this report.